Engineering of surfaces and interfaces using low energy ions

Engineering of Surfaces and Interfaces using Low Energy Ions

Improving the optical quality of multilayered systems
for x-ray reflection

The cover represents the main chamber of the deposition system that was used to study the process of layer growth and the effects of low energy ion bombardment.

Engineering of Surfaces and Interfaces using Low Energy Ions

PROEFSCHRIFT

ter verkrijging van de graad van doctor aan de Technische
Universiteit Eindhoven, op gezag van de Rector Magnificus,
prof.dr.ir. C.J. van Duijn, voor een commissie aangewezen
door het College voor Promoties in het openbaar te verdedigen
op woensdag 4 mei 2005 om 16.00 uur

door

Jan Verhoeven

geboren te Den Haag

Dit proefschrift is goedgekeurd door de promotoren:

prof.dr. M.J. van der Wiel
en
prof.dr.ir. R. de Gryse

Onderzoek is een proces van steegjes in gaan om te zien of ze doodlopen.
Wet van Bates

This thesis is based on the following publications representing experiments from my own group:

Chapters 2, 3, 4, and 5 appeared for a part as a chapter in:

J. Verhoeven, Chapter: "Application of low energy ions to modify multilayer systems for improved X-ray reflectivity" in book with title: Ion Beam analysis of Surfaces and Interfaces of Condensed Matter Systems, Editor: Prof Purushottam Chakraborty, NOVA SCIENCE PUBLISHERS, INC. (2002) ISBN 1-59033-538-4

Chapter 4 is based on:

1)   M.P. Bruijn and J. Verhoeven, unpublished results (1985).
2)   J. Verhoeven, unpublished results (1998)
3)   J. Verhoeven, unpublished results (1986)
4)   J. Verhoeven, H. Zeijlemaker, E.J. Puik and M.J. van der Wiel, Vacuum 41, 1327 – 1329 (1990)
5)   J. Verhoeven, unpublished results (1994)
6)   E.J. Puik, M.J. van der Wiel, J. Verhoeven and H. Zeijlemaker, Thin Solid Films, 193/194, 782-787 (1990)
7)   E.J. Puik, M.J. van der Wiel, H. Zeijlemaker and J. Verhoeven, Appl. Surf. Sci., 47, 251-260 (1991),
8)   E.J. Puik, M.J. van der Wiel, H. Zeijlemaker and J. Verhoeven, Appl. Surf. Sci., 47, 63 (1991),
9)   E..J. Puik, M.J. van der Wiel, H. Zeijlemaker and J. Verhoeven, Rev. Sci. Instr. 63, 1415 (1992)
10)   M.P. Bruijn, P. Chakraborty, H. van Essen, J. Verhoeven, M.J. van der Wiel and W.J. Bartels, Proc. SPIE, 563, 183 (1985)
11)   J. Verhoeven, Lu Chunguang, E.J. Puik, M.J. van der Wiel and T.P. Huijgen, Appl. Surf. Sci., 55, 97 (1992)
12)   Schlatmann, C. Lu, J. Verhoeven, E.J. Puik and M.J. van der Wiel, Appl. Surf. Sci., 78, 147 (1994)
13)   R. Schlatmann, A. Keppel, Y. Xue ad J. Verhoeven, Appl. Phys.   Lett., 63, 3297 (1993)
14)   R. Schlatmann, J.D. Schindler and J. Verhoeven, Phys. Rev. B, 51, 5345 (1995)
15)   R. Schlatmann, J.D. Schindler and J. Verhoeven, Phys. Rev. B, 54, 10880 (1996)
16)   M.J.H. Kessels, J. Verhoeven and F. Bijkerk, Appl. Optics to be published
17)   M.J.H. Kessels, J. Verhoeven, F.D. Tichelaar and F. Bijkerk Surface Science to be published
18)   M.H.J. Kessels, F.D. Tichelaar, J. Verhoeven and F. Bijkerk, J. Appl. Phys. To be published

Chapter 5 is based on:

1) J. Verhoeven, A. Keppel, R. Schlatmann, Y. Xue and I.V. Katerdjiev, Nucl. Instr. Methods, B94, 395 (1994)
2) R. Schlatmann, A. Keppel, S. Bultman, T. Weber and J. Verhoeven, Appl. Phys. Lett., 68, 2948 (1996)
3) M.J.H. Kessels, J. Verhoeven, A. Yakshin, F.D. Tichelaar, F. Bijkerk NIM B Vol 222/3-4 484-490 (2004)
4) R. Schlatman, A. Keppel, Y. Xue, J. Verhoeven and M.J. van der Wiel, Appl. Phys. Lett., 63, 3297 (1993),
5) R. Schlatmann, A. Keppel, J. Verhoeven, C.H.M. Marée and F.H.P.M. Habraken, J. Appl. Phys., 80, 2121 (1996)
6) M.J.H. Kessels, J. Verhoeven, F.D. Tichelaar and F. Bijkerk, J..Appl. Phys. to be published
7) L.G.A.M. Alink, R.W.E. van de Kruijs, E. Louis, F. Bijkerk and J. Verhoeven, Solid Thin Films to be published (Section 5.5)
8) R. Schlatmann, C. Lu, J. Verhoeven, E.J. Puik and M.J. van der Wiel
9) M. Cilia and J. Verhoeven, J. Appl. Phys., 82, 4137 (1997)
10) R. Schlatmann, C. Lu, J. Verhoeven, E.J. Puik and M.J. van der Wiel, Appl. Surf. Sci., 78, 147 (1994

Chapter 6 represents:

S. Dobrovolski, A.E. Yakshin, M. Kessels and J. Verhoeven, to be published (The application of energetic CH_x^+ ions   to   form Si/SiC multilayer systems for the reflection of   radiation between 20 and 80 nm)

Contents

1   Survey

1.1 Introduction

Thin films or coatings are used in a broad range of applications and can be divided into the following basic categories: optical, electronical, magnetic, chemical, mechanical and thermal. Many applications can be seen in daily life. Multilayered antireflective coatings have reduced the loss of light passing optical systems. Reflecting aluminium coatings form the basis of the well-known compact disk as well as of optical based memory disks. Aluminium thin films are also a major component for semiconductor devices. Magnetic thin films are applied in memory disks. Thin films are used as barriers to prevent alloying of a top layer and the substrate or to prevent oxidation. Important applications are tribological coatings and hard coatings. Also decorative coatings should not be forgotten. Often multiple properties are combined in one coating. Chromium coatings are used on plastic parts for automobiles to impart a metallic lustre at lower cost and weight than when produced from bulk material. An additional achievement is an improved hardness and a protection of plastic against ultraviolet. Titanium nitride layers on cutting tools reduce wear, increasing the maintenance periodicity of a production process. An increased hardness and a low friction cause this. Moreover these layers form a diffusion barrier against alloying of the tool with the work piece. Another application of titanium nitride is as a gold-colour decorative coating.

Evaporation and sputter deposition, both known as physical vapour deposition are the most widely applied techniques to produce thin films. Faraday probably deposited the first thin films by evaporation in 1857, by exploding metal wires in vacuum [1]. Nahrwold [2] discovered deposition of thin films by Joule heating in vacuum. Grove [3,4] was the first to mention the sputter process in 1852. Wright [5] reported in 1877 on the production of transparent metallic films by the electrical

discharge in evacuated tubes. The application of these techniques on industrial scale was boosted by the development of industrial-scale vacuum equipment dating from 1946 and onwards.

In general the quality of a thin layer is determined by the density, morphology, chemical composition, surface roughness and adhesion to the substrate. When the chemical composition of an optical coating is not stoichiometric, the refractive index will be different from the required value. Moreover when the density is not equal to the bulk density of the layer material due to pores, the refractive index will change as a function of time due to absorption of water vapour. Absorption of water vapour can even cause stress in the layer due to which detachment from the substrate underneath can occur. Initially adhesion of a thin film to the substrate depends on the mutual chemical reactivity. It can therefore be important to remove all contaminants from the substrate before starting the deposition process. For a decorative titanium nitride gold colour coating it is not important if the exact stoichiometric composition of the layer is obtained. More important are the reproducibility of the chemical composition and the homogeneity and hence the colour over the whole substrate. As an example, the gold colour should be the same for a whole coated door handle. For the application of titanium nitride as a hard coating on cutting tools, a reproducible warranty for wear is to be met. This is a crucial requirement for a production process using cutting tools.

Deposition processes that fulfil all before mentioned requirements are still developed empirically by variation of deposition parameters like deposition rate, substrate temperature and process pressure.

Theoretical models [6, 7] for layer growth at atomic scale were already available in the sixties and the first Molecular Dynamics [8] based computer models were developed in the eighties. However these models require the knowledge of atomic interaction potentials.

1.2 Multilayer systems and thin film requirements

At the end of the seventies a new application for thin films emerged. This concerned multilayer systems at nanometre scale as spectroscopic elements for wavelengths > 1 nm where crystals cannot be used any more. The reflection of radiation with a specific wavelength λ by a multilayer with period thickness d is given by the Bragg relation

$\lambda=2d\sin\theta$, where θ is the reflection angle with the surface. For the wavelength region considered, the periodicity (d) of the multilayer will be 1 nm or higher. The resolving power ($\lambda/\Delta\lambda$) is proportional to the number of interfaces that contribute to the reflection. Therefore multilayer systems to be applied in spectroscopy require the contribution of as many interfaces as possible. In that case contrast between the two materials should be low combined with a low absorption of the components.

In the beginning of the nineties a new application appeared for multilayers as optical reflection systems in the short wavelength region, to be used in the lithographic production of electronic components. Structures in micro electronic components are achieved by a combination of optical projection and printing, usually referred to as projection lithography. The wish to reduce the size of the structures and hence to increase the number of components per surface area has pushed the search for improvement of the resolution of the imaging optics. The resolution is limited by the wavelength of the light. While the development continued from visible light to UV light for which transmission optics still can be applied continued, the need for a next step to a shorter wavelength became obvious. However, the major problem for radiation with a wavelength shorter than 100 nm is its weak interaction with matter, which can be described by the classical Fresnel equations using the complex index of refraction n. This refractive index is related to the complex atomic polarizability alpha (α), via the complex dielectric constant epsilon (ε) and is written as $n=1-\delta + i\beta$ [9]. The real part $(1-\delta)$ of the refractive index represents the contrast between different materials and has a value slightly below 1, except around some absorption edges. The imaginary part (β) of the refractive index represents absorption and has values $< 10^{-3}$ in the XUV wavelength range. From this one can conclude that dispersion as well as reflection of radiation in the before-mentioned wavelength region can be neglected at near normal incident. That means that lenses are not available as optical elements and that total reflection only occurs for very small reflection angles. The only useful solution for a reflection optical element for large angles is coherent summation of radiation reflected at a series of interfaces formed by a multilayer. The optical requirements that a multilayer has to fulfil depends on the wavelength that has to be reflected and on the application. When applied as an optical element a maximum total reflection is required and a high

contrast at the interfaces should be preferred. However, a high absorption should be avoided, as it will reduce the number of interfaces that contribute to the total reflection. Reflection optics that has been developed over the last decennium for EUV lithography forms a good example for the choice of multilayer components. The wavelength of a promising radiation source for this process was 13.5 nm. That wavelength requires optics for perpendicular reflection with a periodicity of 6.7 nm. The combination of 50 periods of molybdenum and silicon has turned out to be a proper match, resulting in a theoretical reflectivity of $\approx 74\%$.

In practice the theoretical performance of multilayer systems is reduced by the occurrence of roughness at the interfaces. An important source of interface roughness is the surface roughness that is an inevitable result of the deposition process. This may lead to an accumulated interface roughness over the whole multilayer stack. The effect of roughness on the reflectivity is usually described by a Debye-Waller factor, given by $e^{-q^2 \sigma^2}$, where σ is the root mean square (r.m.s.) value of the roughness and $q = 4\pi\sin\theta / \lambda$. Note that $q = 2\pi/d$ when the Bragg condition is fulfilled and that for that case the Debye-Waller factor is independent of the wavelength. This factor expresses the decrease in the reflected intensity of an interface with roughness σ, compared to that of a perfectly smooth interface, at an angle of incidence θ and wavelength λ. As an example, the influence of a 0.5 nm r.m.s. roughness on the Debye-Waller factor is calculated for multilayers with a period of 10, 5 and 2.5 nm. For the reflectivity of the first Bragg peak this results in a Debye-Waller factor of respectively 0.91, 0.67 and 0.21. From this calculation it is quite clear that especially for short multilayer periods a small roughness causes a considerable loss of reflectivity for the first Bragg peak independent of the wavelength.

Another cause for reduction of the theoretical performance of a multilayer system is intermixing, which can also be described by a Debye-Waller factor. In that case σ represents the intermixed interlayer thickness. Intermixing can be a result from interdiffusion due to chemical reactivity of the multilayer components. Therefore components cannot be freely chosen even if they are optically favourable. Finally energetic particle bombardment during the deposition process may induce intermixing at deeper interfaces. Fraerman et al.[10] showed that a graded distribution of the materials within each period in the multilayer structure due to intermixing can

improve the wavelength selectivity of a multilayer system. Kessels et al [11] calculated the optical performances for multilayer systems with arbitrary density profiles of the components within each period. A decrease of the absorbing component within each period resulted in an improved selectivity due to the contribution of more and deeper interfaces to the reflected intensity. Nevertheless a density profile with sharp layer interfaces in all cases resulted in a multilayer structure with the highest reflectivity for any required selectivity.

In conclusion, the main challenges for the production of near-ideal multilayers are:

a) The formation of closed layers with a thickness of several nanometres and a surface roughness in the order of tenths of a nanometre.

b) A layer thickness for each multilayer component reproducible and accurate within 1%.

c) No interlayer formation due to intermixing.

1.3 This thesis

In this thesis an overview is given of the possibilities to apply energetic ions in order to meet the requirements for an optimum optical performance of multilayer systems. This was achieved by a decrease of the interface roughness, a reduction of interlayer formation and an improvement of the optical contrast.

Most of the work presented in this overview represents experiments performed in my own group as part of various projects.

The content of the following chapters specifically emphasizes the materials science problems playing a role by energetic ions.

Chapter 2 starts with the basics of layer growth, followed by a description of fundamental processes of the interaction of energetic ions with solid materials.

In Chapter 3 the different techniques applied for physical vapour deposition as used for multilayer production are treated.

Chapter 4 gives an overview of the application of energetic ions to improve the smoothness of the surface of thin films by treatment with noble gas ions during or after deposition. The following multilayer systems are discussed: Ni-C, W-C, Mo-Si, WRe-Si, W-Si, Cr-Sc and Ni-Ti.

In Chapter 5 the modification of the metal/silicon system is extensively discussed. Ion-bombardment induced layer-densification, intermixing or

implantation into one of the multilayer components, can achieve modification in order to improve the optical contrast or the thermal stability. All these applications are demonstrated for the Mo-Si, W-Si and Ni-Si combinations.

In Chapter 6 the formation of a Si-SiC$_X$ multilayer system produced by subsequent deposition of silicon followed by implantation with CH$_X^+$ ions is discussed.

References

1) M. Faraday, Phil. Trans. 147, 145 (1857)

2) R. Nahrwold, Ann. Phisik 31, 467 (1887)

3) W.R. Grove, Phil. Trans. Roy. Soc. London, 5, 87 ((1852)

4) W.R. Grove, Phil. Mag., 5, 203 (1853)

5) A.W. Wright, Amer. J. Science, 3, 49 (1877)

6) R.L. Schwoebel and E.J. Shipsey, J. Appl. Phys., 37, 3628 (1966),

7) G. Ehrlich and F.G. Hudda, J.Chem. Phys., 44, 1039 (1966)

8) K.H. Muller, Phys. Rev. B, 35, 7906-7913 (1987)

9) R.W. James, The Optical Principles of the Diffraction of X-rays (Bell, London 1948)

10) A. A. Fraerman, S. V. Gaponov, V. M. Genkin, and N. N. Salashchenko, Nuclear Instruments and Methods in Physics Research Section A: Accelerators, Spectrometers, Detectors and Associated Equipment **261,** 91-98 (1987).

11) M.J. H. Kessels, J. Verhoeven and F. Bijkerk, to be published

2   Layer growth and interaction with energetic ions.

Abstract

The formation of layers, based on physical vapour deposition is discussed. The process of layer growth depends on the activation energy of the arriving atoms related to the surface of the substrate as well as the growing layer. Depending on the activation energy and the external input of energy during or after the deposition process a displacement of the atoms is possible. Displacement in the bulk and at the surface of the layer is responsible for the layer density, layer morphology and the roughness of the surface. External energy is provided by the kinetic energy of the arriving atoms, heating of the substrate and the impact of energetic particles. Energetic ions hitting a material can penetrate to a certain depth and stay in the bulk after loosing all energy. The penetration depth depends on their initial energy. During this process energy is transferred to the environment of the track, resulting in displacement of atoms. Displacement causes damage in the bulk and sputtering at the surface.

2.1 Layer growth

Before discussing the different techniques of deposition, a basic knowledge of layer growth is required. In principle all deposition techniques applied to produce multilayer systems have been based on physical vapour deposition. That means that material is vaporised in some way and the vapour condenses at a surface. Atoms arriving at a substrate can chemically react with the substrate and can even diffuse into the substrate, which is temperature dependent. It is also possible

that atoms migrate over the substrate surface until they meet each other, forming a two dimensional island. Other atoms arriving at the residual substrate surface may cause a lateral growth of the initial two-dimensional islands. Also a lateral shrinking can occur due to detachment of atoms from the islands. All these atoms migrating over the surface can be considered as a two dimensional gas. There is an equilibrium between the size of the islands and the two dimensional pressure of the surrounding gas. The equilibrium atom density around a large island is lower than for a small island. As a result small islands evaporate while larger islands continue growing. This process is known as Ostwald Ripening [1,2,3]. Atoms arriving on top of the islands also tend to migrate over the island surface. There is a chance that atoms fall from the island and are trapped at the edge contributing to its lateral growth. It is possible that a third layer is growing on top of the second layer while the lateral extension of the first layer has not yet resulted in a closed layer. Random diffusion of ad-atoms on the surface of an island can result in a small shift in the centre of mass of this island. This results in the displacement of a whole island. When one island meets another they can merge and form a larger island. This process of island growth is known as coalescence. A good example of coalescence is the growth of palladium particles on a TiO_2 (110) surface as studied by Jak et al [4], using high speed Scanning Tunnelling Microscopy. Based on the particle size distribution they concluded that cluster diffusion and coalescence form the dominant growth mechanism. This conclusion was also supported by direct observation of mobile clusters at room temperature.

All these processes depend intrinsically on activation energies responsible for migration and attachment, and Ehrlich- Schwoebel barriers responsible for atoms falling from an island [5,6]. Kodambaka et all [7] used Scanning Tunnelling Microscopy to investigate Ostwald ripening and decay kinetics of two-dimensional TiN islands on atomically flat TiN(001) and TiN(111) terraces at elevated temperature. Ad-atom surface diffusion on the (001) surface and attachment/detachment at steps on the (111) surface turned out to be the rate-limiting mechanism for island decay.

Macroscopically there are three different growth models: layer-by-layer growth (Frank-van der Merwe), three-dimensional island growth

(Volmer-Weber) and a combination in which layer growth changes into island growth after several monolayers (Stranski-Krastanov) [8]. All growth processes can be considerably influenced by additional energy input during deposition. This can result in enhanced layer-by-layer growth and hence flat surfaces. However alternatively also enhanced nucleation can occur, resulting in surface waviness. Takenaka et al [9] observed a clear reduction of the interface waviness of their Ni/C multilayers when the substrate temperature was reduced from 80^0 C down to -20^0 C. Additional energy can be obtained from an increase of the substrate temperature, from energetic particles bombarding the substrate and from the energy contained in the arriving vapour. It should be emphasized that additional energy input also contains a risk of interdiffusion or intermixing at the interface with the substrate.
It can be concluded that energy input during as well as after deposition of a layer can be applied to control the layer quality.

2.2 Interaction of energetic ions with materials

Ions striking a material can penetrate to a certain depth and end up as implanted within a depth distribution. This depth distribution depends on the energy and angle of incidence of the ions and the atomic mass of these ions related to the atomic mass of target atoms. During their travel through the material energy is transferred to the near environment. Ions can transfer energy in a pure mechanical way by nuclear interaction (nuclear stopping power) but can also lose energy to electrons (electronic stopping power). Both mechanisms will cause displacement of the neighbouring bulk atoms, initiating an atomic collision cascade [10]. As a result target atoms will be relocated from their original position, causing damage to the crystal structure, destruction of an interface with a material underneath, densification or viscous flow [11]. The energy that is transferred back to the surface can result in the release of atoms located within a few monolayers from the surface, the so-called sputter process [12]. It should be noted that an interface with a high mass underneath a low mass over layer can cause an increase of the energy that is transferred back to the surface of the over layer. This
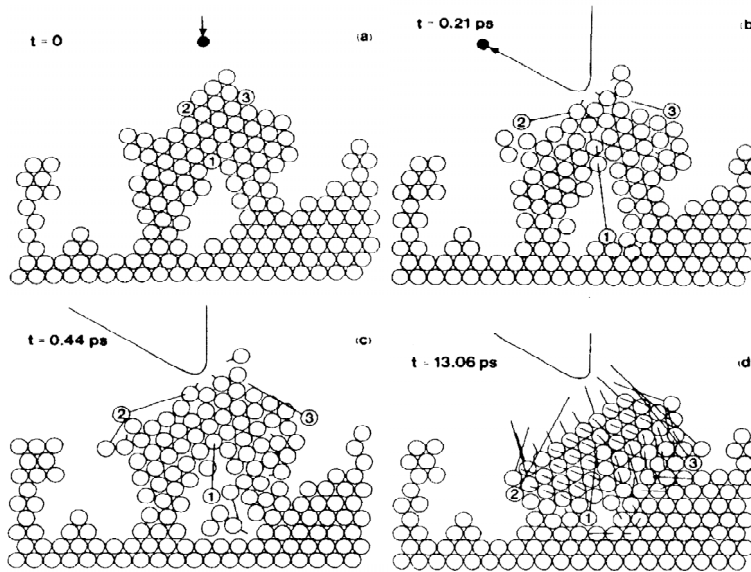
Figure 1. (a)-(d) Collision sequence resulting from impact of a 100 eV Ar ion hitting a porous Ni film

effect can be ascribed to an increased stopping power from the high mass interface. As a consequence an increased preferential sputtering of the low mass over layer can be expected. From a dynamic Monte Carlo code TRIDYN [13] to simulate sputtering yields Berg et al [14] as well as Harper et al [15] demonstrated that this effect is to be taken into consideration for over-layer thicknesses < 2 nm. A similar effect has experimentally been observed for a mixture of a high mass and a low mass material by Verhoeven et al [16]. They reported on an increased sputter yield of 31% for silicon intermixed with molybdenum.

For low-energy ion bombardment (low–keV or sub-keV), with decreasing ion energy, collision cascades become less fully developed [17]. This can continue up to a stage that only a few isolated collisions between the projectile or energetic recoil and the target atoms will dissipate the available energy.

As stated in the paragraph before, the impact of energetic particles during deposition will influence the growth process of a thin layer. A
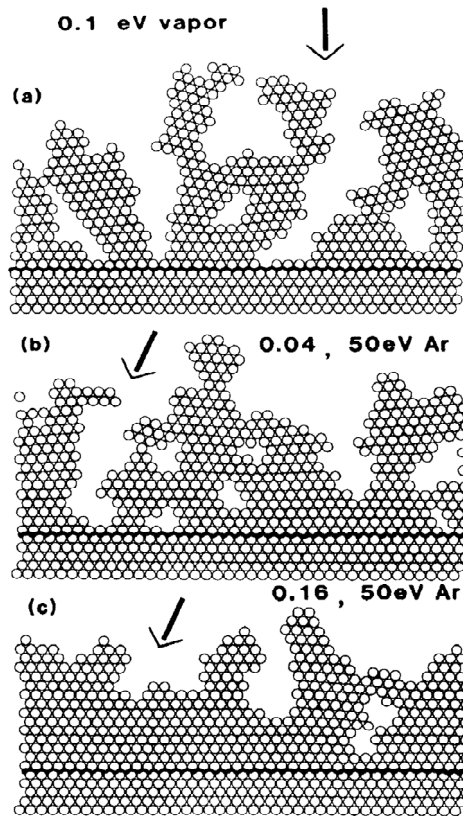
Figure 2. (a)-(c) Typical microstructure obtained for condensing vapour atoms of 0.1 eV kinetic energy, arriving under normal incidence (a) without ion bombardment. (b) with Ar ion bombardment under an angle of 30^0 with normal, E=50 eV and j_i/j_v = 0.04, with Ar bombardment of E = 50 eV and j_i/j_v = 0.16.

most instructive contribution in understanding this process was given by Müller [18]. He was the first to use a 2D Molecular Dynamics computer simulation to describe ion induced epitaxial vapour-phase growth. Two figures obtained from this simulation are representative for ion-induced processes. Figure 1 shows a collision sequence resulting from the

impact of a 100 eV argon ion hitting a porous nickel film. This picture clearly demonstrates that even a few isolated recoils cause surface diffusion, local heating and recrystallization. The initial ion-surface collision and the formation of knock-on atoms require only 0.2 ps. The freezing process, to establish the final atomic configuration, takes about 10 ps. In Figure 2a can be seen that condensing Ni vapour atoms arriving with a kinetic energy of 0.1 eV forms a porous layer with an initial columnar microstructure. Figure 2b and c show the influence of the ion-to-vapour flux ratio on the densification process and crystallization for a constant ion energy. The sputtering yield is found to be about 0.35. No argon entrapment in the film could be observed.

From these MD simulations Müller [18] concluded that: (i) atoms accumulated to form a void structure are dislodged and forward sputtered by incoming ions causing the void region to remain open until filled by new depositing atoms; (ii) ion impacts induce surface diffusion as well as local heating such that recrystallization takes place during growth and the underlying crystal structure is adopted.

Klaver et al [19] more recently conducted 3D MD simulations on the effect of bombardment of a Mo layer by energetic Kr^+ ions after deposition. They made their simulations for ion energies of 50, 100 and 300 eV and an angle of incidence of 30^0, 45^0 and 60^0 of normal. A fully crystallized film was used as a substrate. It became clear that 300 eV ions displace atoms they hit, regardless whether these were loosely bound atoms at the surface or strongly bound bulk atoms. This resulted in an increased surface roughness. More selective displacement of more loosely bound atoms was achieved by lower energy ions and slight decrease of the surface roughness was found.

As mentioned at the end of the section before, depending on the ion energy, ion mass, mass of the atoms forming a layer and the thickness of this layer, intermixing or interdiffusion with the layer underneath can occur. Also implantation cannot be ignored. Especially bombardment with ions that easily react chemically with the substrate cause the formation of compounds.

References

1) I.M. Lifshitz, V.V. Slyozov, J. Phys. Chem. Solids, 19, 35 (1961),

2) B.K. Shakraverti, J. Phys. Chem. Solids, 28, 2401 (1967),

3) M. Zinke-Allmang, Thin Solid Films, 346, 1 (1999)

4) M.J.J. Jak, C. Konstapel, A. van Kreuningen, J. Verhoeven and J.W.M. Frenken, Surf. Sci.,457, 295 (2000)

5) R.L. Schwoebel and E.J. Shipsey, J. Appl. Phys., 37, 3628 (1966),

6) G. Ehrlich and F.G. Hudda, J.Chem. Phys., 44, 1039 (1966)

7) S. Kodambaka, V. Petrova, A. Vailionis, I. Petrov and J.E. Greene, Surface-Science. 20 526(1-2) 85-96 (2003)

8) Donald L. Smith, Thin Film Deposition; Principles and Practice McGraw-Hill, (1995)

9) H. Takenaka, T. Kawamura and H. Kinoshita,Thin Solid Films, 288, 99 (1996)

10) P. Sigmund in: Radiation Damage Processes in Materials, ed. C.H.S. Dupuis (Noordhof, Leiden, 1975) p3

11) C. Volkert and A. Polman, in "Phase Formation and Modification by Beam-Solid Interactions", Edited by G.S. Was, L.E. Rehn and D. Follstaedt, Symposia Proceedings No.235 (Materials Research Society, Pittsburg, 1992) p3

12) P. Sigmund, ed., Fundamental Processes in Sputtering of Atoms and Molecules, K. Dan. Vidensk. Mat. Fys. Medd. 43 (1993)

13) J.P. Biersack, S. Berg and C. Nender, Nucl. Instr. Meth. B59/60 (1991) 21

14) S. Berg, A.M. Barklund, C. Nender, I.V. Katerdjiev and H. Barankova, Surface and Coating technology 54-55, 131 (1992)

15) J.M.E. Harper, S. Berg, C. Nender, I.V. Katardjiev and S. Motakef, J. Vac. Sci. Technol., 10, 1765 (1992)

16) J. Verhoeven, A. Keppel, R. Schlatmann, Y. Xue and I.V. Katerdjiev, Nucl. Instr. Methods, B94, 395 (1994)

17) Hubert Gnaser, Appl. Surf. Sci., 100-101, 316 (1996)

18) K.H. Muller, Phys. Rev. B, 35, 7906-7913 (1987)

19) P. Klaver, W. Goedheer, F. Bijkerk and B.J. Thijsse, Mat. Res. Soc. Ptoc., 585, 305 (2000)

3   Deposition techniques

Abstract

Three techniques for physical vapour deposition applied in the formation of multilayers are discussed: thermal evaporation, sputter deposition and pulsed laser deposition. During deposition the substrate is subject to the impact of energy, which differs for the three techniques. Energy can be provided by the kinetic energy of the atoms or molecules deposited at the substrate, by additional energetic particles and by heating of the substrate. An important part of the process is the accurate control of the layer thickness.

3.1. Introduction

Three major physical vapour deposition techniques have successfully been used for the production of multilayer systems: Evaporation, Sputter Deposition and Pulsed Laser Deposition. Evaporation is a classical technique based on heating of material that is to be deposited. Evaporation of refractive metals is generally achieved by electron beam heating. The vapour (mainly atoms some dimers and trimers) arrives with thermal kinetic energy at the substrate and additional energy is only provided by heat radiation from the evaporation source or heating of the substrate.

Sputtering of a solid by energetic ion impact forms the base for sputter deposition. The initial kinetic energy of atoms released from the target due to ion impact can be as high as tens of eV. The energy with which these atoms arrive at the substrate depends on the distance to the target in combination with the working pressure during the process.

Additional energy is provided by heat radiation as well as by energetic particles arriving at the substrate.

Pulsed laser deposition is a technique in which local heating with a laser causes evaporation. The main difference with classical evaporation is the formation of clusters, ions and the high initial energy of these ions.
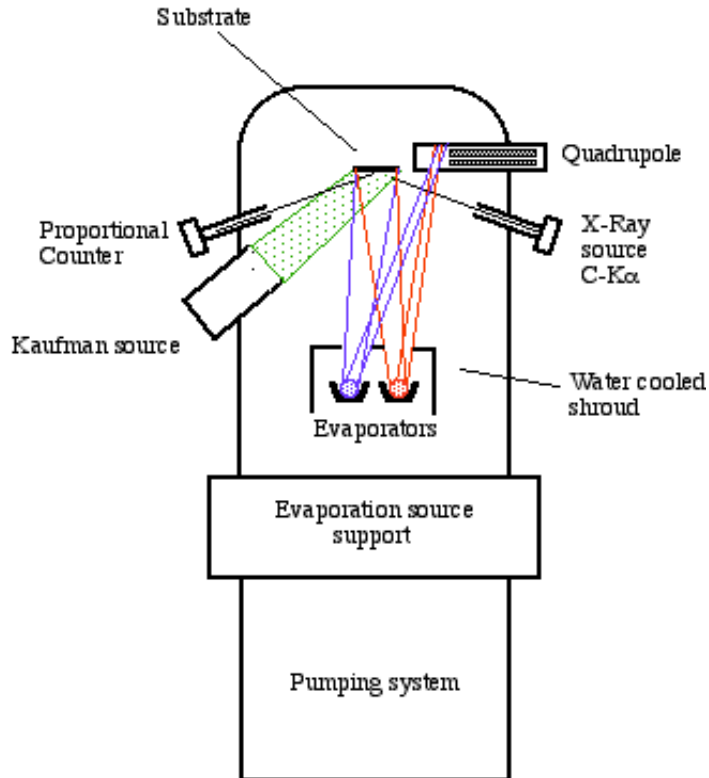
Figure 3 A deposition system for multilayers, based on e-beam evaporation. The layer thickness is monitored during growth as well as during etching by x-ray reflectometry. C-Kα or N-Kα radiation is reflected at a grazing angle of 35^0 and monitored by a gas filled proportional counter. According to the Bragg relation: $\lambda = 2d \sin\theta$, constructive interference will occur for a layer thickness of respectively n x 3.84 nm and n x 2.7 nm. A Kaufman source provides ions with energies > 150 eV. A quadrupole mass spectrometer monitors the amount of vapour during the deposition process.

For the reproducibility of the quality of the layers like density and smoothness, reproducible deposition parameters like deposition rate, substrate temperature and working pressure are required. For the production of multilayers with a periodicity in the order of several nanometres the thickness should be monitored with an accuracy better than 1%.

3.2 Evaporation

Spiller [1] has been the pioneer in evaporation, using in-situ reflectometry to accurately monitor the layer thickness of the multilayer components (Figure 3).
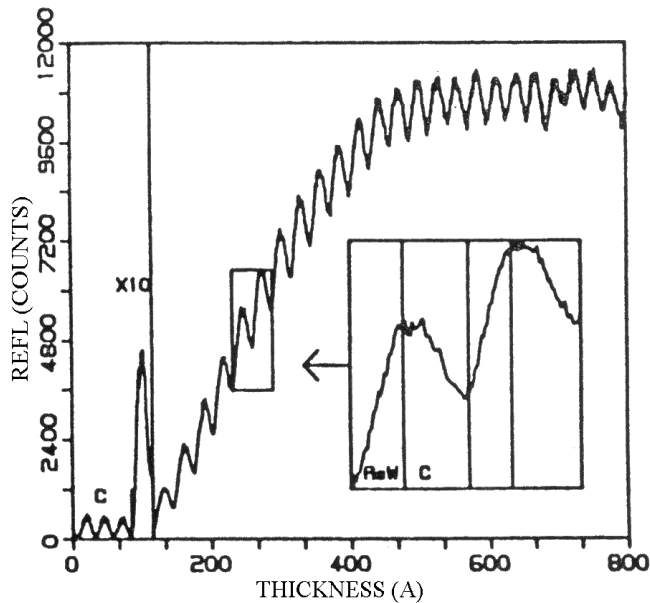
Figure 4 Reflectivity of N-Kα radiation versus thickness during deposition of a ReW-C coating (d=2.7 nm). First three oscillations represent the deposition of C only. The following sharp rise is due to the growth of a ReW layer. After reaching a maximum the process is continued by C deposition, resulting in a decrease of the reflectivity. This process, as shown in detail in the inset, is repeated 26 times.
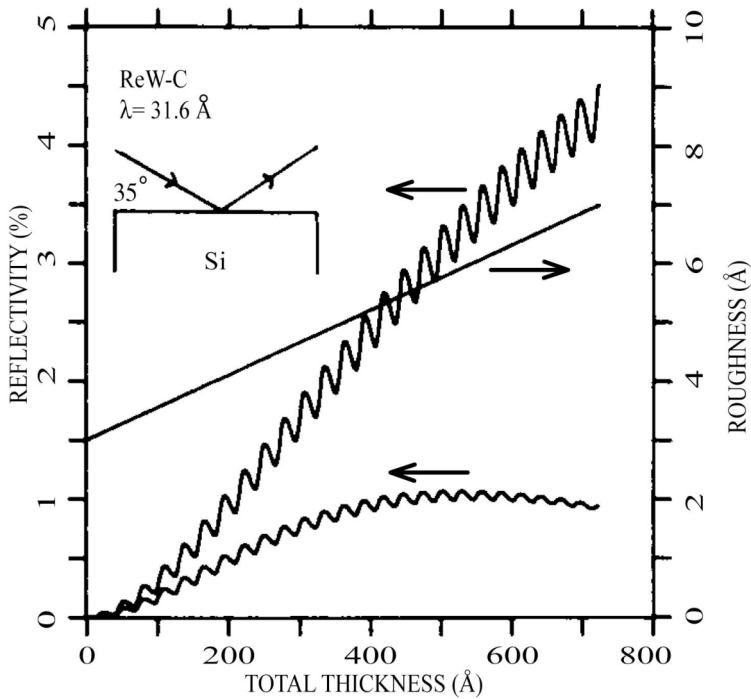
Figure 5 Simulation of the reflected intensity of N-Kα radiation during the growth of a 2.7 nm W-C multilayer system. The upper oscillating curve is calculated for theoretically smooth interfaces. In the lower curve the roughness is assumed to change according to the straight line from 0.3 to 0.7 nm (right scale).

This technique is based on interference of soft x-rays of a chosen wavelength reflected under a fixed angle from a substrate during layer growth. In first approximation maximum reflection occurs when the well-known Bragg relation $n\lambda = 2d\sin\theta$ is satisfied. The so-called spacer element is grown until a minimum reflection is reached, followed by the deposition of the reflective component to a constructive interference maximum (Figure 3). An advantage of this technique is that from the interference amplitude, observed during deposition, the change of the surface roughness of the growing layer can be retrieved [2]. This is achieved by simulating the theoretical reflectivity behaviour during

growth, modified by a proper Debye-Waller factor. An example can be seen in .Figure 5. representing the deposition of a W/C system [3]. From this simulation it becomes clear that a change in roughness from 0.3 - 0.7 nm during the deposition process results in a factor of 4 lower final in-situ reflectivity, compared to the theoretically possible reflectivity. Deposition by evaporation easily enables the installation an ion source for layer modification during or after deposition (Figure 3). Moreover the whole process of additional ion beam modification can be monitored by x-ray reflectometry [4].

3.3 Sputter deposition

Sputter deposition, pioneered by Barbee [5], has demonstrated to be another successful technique for the production of multilayer systems. The classical technique is based on a noble gas discharge between two electrodes. Ions hitting the cathode remove material that is deposited on the substrate that is mounted to the anode. For a discharge a DC or an RF voltage can be applied. The discharge can be boosted by a combination of the electric field with a magnetic field by adding magnets at a proper position (Penning Discharge), known as magnetron sputter sources. Basically the substrates, forming the anode, are mounted on a rotating support. (Figure 6) The cathodes are mounted on the opposite side of the support. The layer thickness of the components is a function the time the substrates spend in front of the targets. For an accurate thickness a stable discharge is required. This technique has demonstrated to be particularly suitable for mass production.

During the sputter deposition process the substrate is subjected to all kinds of impact of energetic particles. Ions hitting the cathode (target) can be reflected as energetic neutrals [6] and hit the substrate. Energetic electrons from the discharge reach the substrate and cause heating. Ions from an RF discharge or an unbalanced magnetron will also arrive at the substrate. The sputtered atoms have an initial energy of tens of eV. Their arrival energy depends on their mean free path before arriving at the substrate and hence the gas-pressure in the discharge. Actually the sputter deposition process can be considered as an "energetic particle assisted deposition" technique with its advantages and disadvantages.

Sputter Source A.B,C

Shutter
Assembly

A·

·B

C·

Top Plate

A'

Substrates

·B'

·C'

Vacuum
Chamber

Substrate
Mounting
Table

Vacuum
Pumping
Port

Rotating
Vacuum
Seal

Bottom
Plate

Substrate motion drive
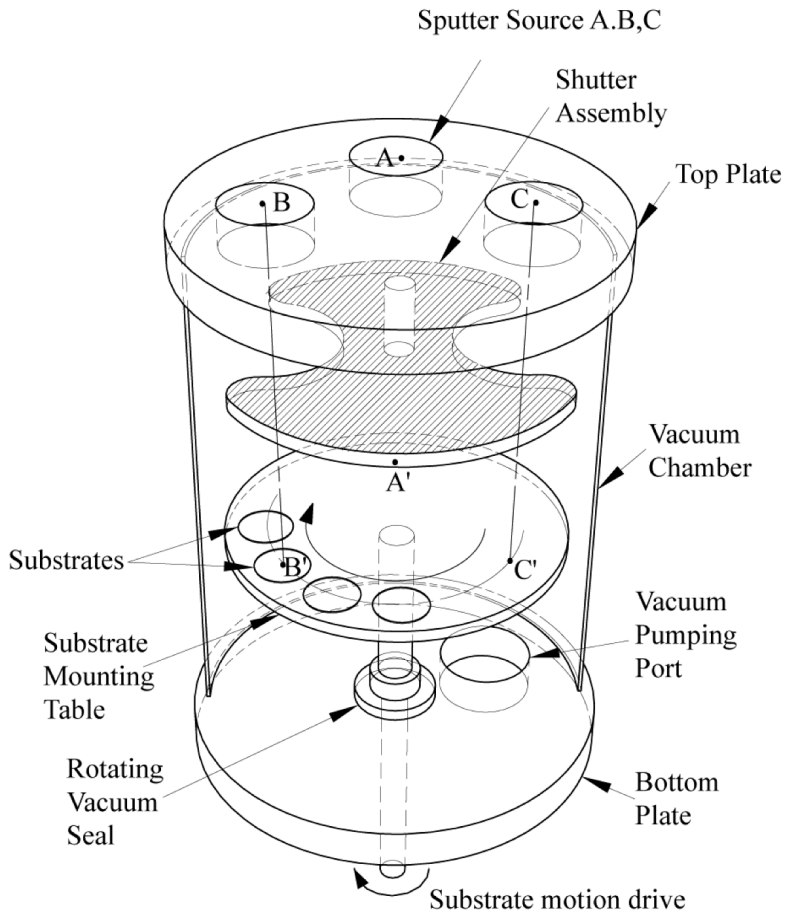
Figure 6 Schematic of a typical multi-source sputter deposition system used to
deposit super lattice films. A, B and C are sputter source positions. Substrates
are mounted on a rotating table, the layer being deposited as the substrate pass
by each source. The individual layer thicknesses are determined by the
deposition rate of the sputtered material, the rotation speed of the table and the
source-to substrate spacing.
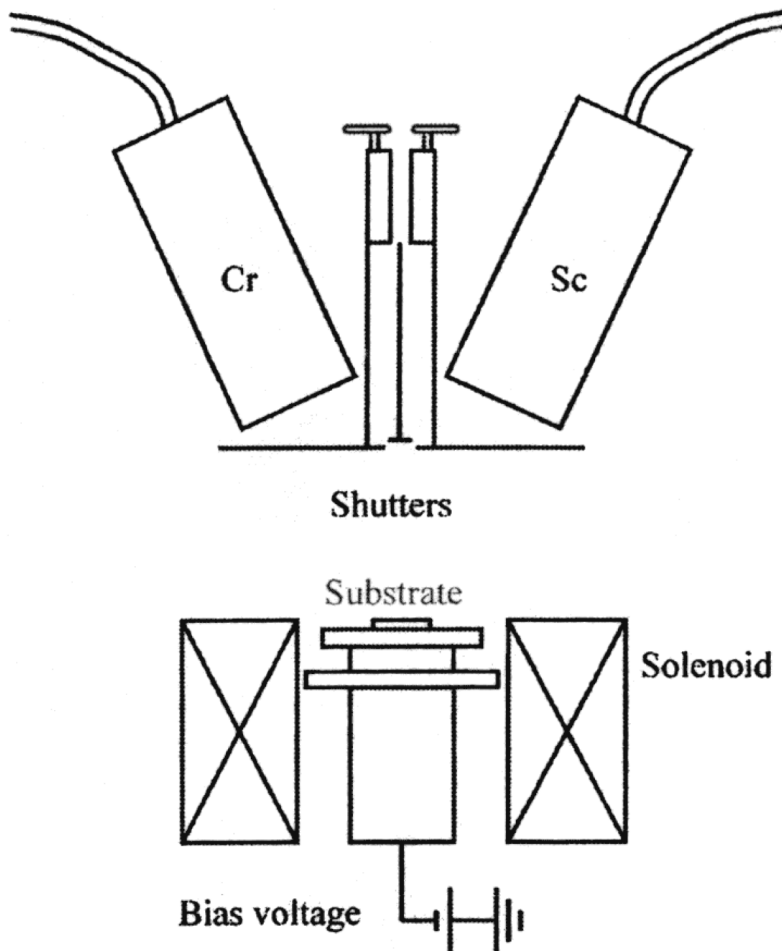
Figure 7 A dual magnetron sputter deposition system, showing magnetrons, shutters, rotating substrate table and surrounding solenoid. A part of the plasma from the magnetrons is extended to the substrate. In combination with the solenoid coil around the substrate and a bias voltage on the substrate ions can be attracted from the plasma, to further assist the deposition process in a more controlled way.
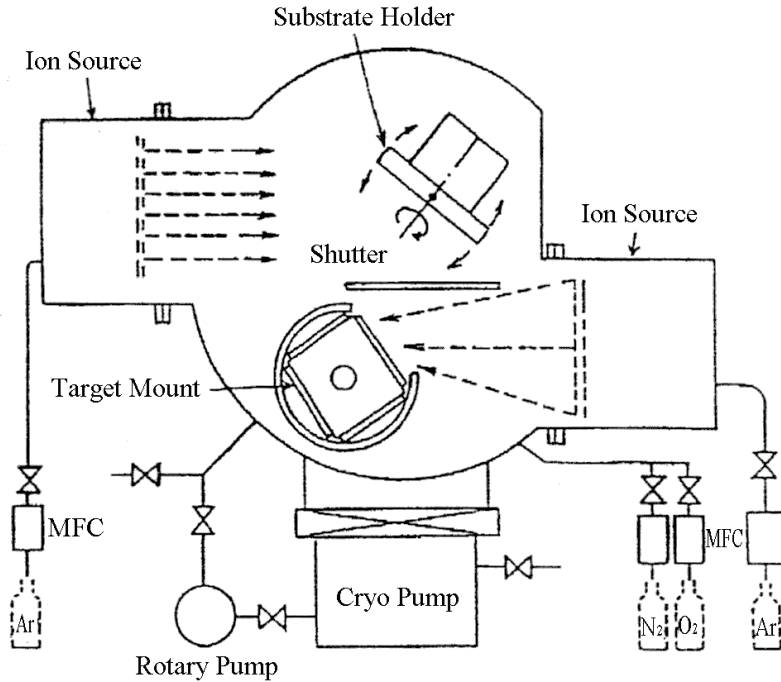
Figure 8 A schematic diagram of an ion beam sputter deposition system. The target mount rotates in order to sputter different materials. A separate ion source is installed for substrate etching or ion assisted deposition.

A smooth layer growth can be achieved by optimising the process by the right choice of the deposition parameters: discharge power and gas pressure. Nevertheless, due to energetic particle impact intermixing at the interface cannot always be avoided. A problem is the conversion of these general deposition parameters into quantified parameters with a physical meaning, like the amount of energy that accompanies each arriving atom. Eriksson et al [7] used magnetron sputter sources of which they configured the magnets in such a way that the plasma of the discharge was extended to the substrate. In combination with a solenoid

coil around the substrate and a bias voltage ions could be attracted from the plasma to the substrate, to further assist the deposition process in a more controlled way (Figure 7). They were able to vary the ion energy from 9 eV up to ~100 eV and could at the same time vary the ion density related to the arrival rate of the sputtered atoms. Basically for a sputter deposition process the layer thickness can accurately be achieved from the deposition time. However, the impact of energetic particles at the substrate will inevitably result in sputtering freshly deposited material from the substrate. And worse, the presence of high mass material underneath will boost the sputter yield of a low mass over layer [8, 9]. As a result, for the first 2 nm the thickness of the growing layer may be no linear function of the deposition time [10].

An alternative sputter deposition system as described by Soyama et al [11] is based on an ion source combined with a rotating target holder (Figure 8). In this system the substrate is not the anode that takes part in the discharge. The advantage is that the substrate is not subject to an uncontrolled impact of electrons and negative ions. As the discharge takes place within a relatively enclosed environment of the source, the working pressure is $< 10^{-3}$ mbar. Therefore, the sputtered particles generally arrive with their full initial energy at the substrate. A second ion source can be mounted to bombard the substrate during or after deposition. Also x-ray reflectometry to monitor the deposition process is possible.

3.4 Pulsed laser deposition

Pulsed laser deposition, as first used by Gapanov [12] to produce multilayers, can be considered as a special case of evaporation. A laser pulse is used for ablation of target material producing a local plasma. This results in a plasma, containing energetic clusters and macro particles. The emission of these macro particles from the laser irradiated surface form a serious drawback. A solution is to use crossed laser-induced ablation plumes to discriminate macro particles ejected from the target [13]. Such a cross beam PLD system dedicated to the deposition of multilayer systems was developed by Gurbunov et al [14].
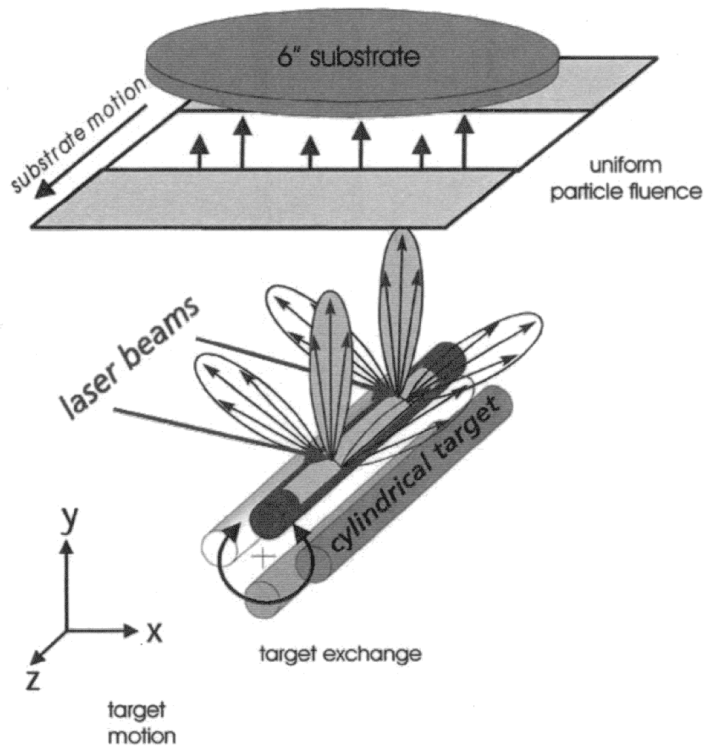
Figure 9 Principle of a dual beam Pulsed Laser Deposition source, designed for large area PLD of nanometre multilayers.

Their system consists of two targets and two lasers (as shown in Figure 9). Each of the laser beams strikes one of the two targets located close to each other. The substrate is positioned in front of the targets on the symmetry axis. A diaphragm that is designed and positioned in such a way that the laser focal points can not be seen from the substrate position forms the essential part of the system. Particle collisions in the intersection region cause a new direction of plasma propagation in vacuum towards the substrate.

The energy of the evaporated material depends on the laser pulse energy. The energy spectrum of the plasma particles consists of a major low-energy part (1-100 eV) and a minor high-energy part (up to a few keV) [15]. As this energetic impact of the evaporated material is kept responsible for a layer growth with smooth surfaces, a choice of the proper laser pulse energy is required. Dietch et al [16] deposited Ni/C multilayers by pulsed laser deposition (PLD) for different pulse energies in the range between 230mJ to 876 mJ. They demonstrated, using High Resolution Transmission Electron Microscopy (HRTEM) and x-ray reflectometry, that the best results were achieved when the PLD process was carried out at moderate pulse energies in the range of 230 mJ.

Each laser pulse is responsible for a well-defined amount of evaporated material. The thickness of each of the multilayer components very accurately depends on the number of laser pulses. Therefore stable ablation conditions are required.

For the deposition of multilayer coatings on larger surfaces special provisions are required. Dietsch et al designed a system based on a dual beam source combined with substrate motion as shown in Figure 9[17]. They have been able to deposit multilayer systems with more than 150 layers from 1 – 10 nm, on substrates of 30 cm diameter with a thickness homogeneity better than 1%

References

1) E. Spiller, A. Segmüller, J. Rife and R.-P. Haelbich, Appl. Phys. Lett.,37,1048 (1980)

2) A.N. Broers and E. Spiller, Scanning Electron `Microscopy 201 (1980)

3) M.P. Bruijn, W.J. Bartels, P. Chakraborty, H.W. van Essen, J. Verhoeven and M.J. van der Wiel, Applications of Thin Film Multilayered Structures to Figured X-Ray Optics, G.F. Marshall editor, SPIE Proc. 563,182 San Diego (1985)

4) J. Verhoeven, H. Zeijlemaker, E.J. Puik and M.J. van der Wiel, Vacuum 41, 1327 – 1329 (1990)

5) T.W. Barbee, Opt. Eng., 25, 893 (1987)

6) E. Kay, F. Parmigiani and W. Parrish, J. Vac. Sci. Technol. A5, 44 (1987)

7) F. Eriksson, G.A. Johanson, H.M. Herz and J. Birch, Opt. Eng., 41, 2903 (2002)

8) J.M.E. Harper, S. Berg, C. Nender, I.V. Katardjiev and S. Motakef, J. Vac. Sci. Technol., 10, 1765 (1992)

9) S. Berg, A.M. Barklund, C. Nender, I.V. Katerdjiev and H. Barankova, Surface and Coating technology 54-55, 131 (1992)

10) A.E. Yakshin, Thesis, Marseille 1996

11) K. Soyama, W. Ishiyama and k. Murakami, J. Phys. Chem. Solids, 60, 1587 (1999)

12) S.V. Gapanov, F.V. Garin, S.A. Gusev, A.V. Kochemasov, Y.Y. Platonov, N.N. Salashenko and E.S. Gluskin, Nucl. Instrum. And Meth., 208, 227 (1983)

13) S.V. Gaponov, A.A. Gudkov and A.A. Frearman, Sov. Phys. Tech. Phys.,27, 1130 (1982)

14) A.A.Gorbunov, W. Pompe, A. Sewing, S.V. Gaponov, A.D. Akhsakhalyan, I.G. Zabrodin, I.A. Kas'kov, E.B. Klyenkov, A.P. Morozov, N.N. Salaschenko, R. Dietch, H. Mai and S. Völlmar, Appl. Surf. Sci., 96-98, 649 (1996)

15) A.D. Akhsakhalyan, Yu.A. Bityurin, S.V. Gaponov, A.A. Gudkov, and V.I. Luchin, Sov. Phys. Tech. Phys.,27, 696 (1982)

16) R. Dietsch, Th. Holz, H. Mai, C.-F. Meyer, R. Scholz and B. Werner, Appl. Surf. Sci., 127 – 129, 451 (1998)

17) R. Dietsch, Th. Holz, D. Weissbach and R. Scholz, Appl. Surf. Sci. 197, 169-174 (2002)

4   Smoothing surfaces

Abstract

The development of surface roughness during deposition of the multilayer components forms one of the causes of interface roughness. The use of energetic ions during or after deposition of the multilayer components to reduce the surface roughness is reviewed. For the metal-carbon systems the best results have been achieved by a post-deposition ion etch of the metal component. This process is based on the removal of an excess layer by ion etching after deposition. The required thickness of this excess layer depends on the growth mode of the layer. For nickel the first 4 nm appeared to grow on carbon as separated islands. In contrast, the first 2 nm of tungsten on carbon formed a closed layer. Intermixing of the interface underneath by residual energy from the ion impact limits the application of ion beam smoothing. The metal on carbon interfaces appeared to have a high stability. The metal on silicon interfaces were easily intermixed in contrast with the silicon on metal interface. For the molybdenum-silicon combination the best results were achieved after a post deposition etch procedure of silicon. For the tungsten silicon combination Ion Assisted Deposition of tungsten additional to post deposition etched silicon gave the best results. Ion beam assisted deposition using a magnetron has successfully been applied for the deposition of Cr-Sc.

4.1 Introduction

As mentioned in chapter 1 interface roughness forms the main reason for the reflectivity to deviate from theory. Interface roughness can be introduced by the development of surface roughness during deposition of the components. It is even possible that due to the formation of islands the first nanometres do not form a closed layer. Basically the chemical interaction between the multilayer components is responsible

for the growth mode of the film. By a proper choice of deposition parameters like working pressure, residual gas composition, deposition rate and substrate temperature the growth process can be influenced. The influence of the working pressure and the residual gas composition was demonstrated by Bruijn et al [1]. They investigated the deposition by e-beam evaporation of W on C in a hydrogen as well as in an oxygen environment of 10^{-6} mbar. Growth of W on C resulted in a layer with a higher surface roughness for the oxygen environment than for the hydrogen environment. Experiments on the deposition of Cr on Si revealed that a deposition rate lower than 0.5 nm/s did not result in a closed layer for thicknesses < 2nm [2].

However, depending on the deposition technique, in spite of the proper choice of deposition parameters, the development of surface roughness often can not be avoided. A possible solution is formed by additional energetic input during or after the deposition process. As mentioned before this can be done by heating of the substrate and by the impact of energetic particles.

The first experiments that revealed the effect of reduction of the surface roughness of a film using energetic ions were done by Verhoeven [3]. The investigation concerned the deposition by e-beam evaporation of nickel on a carbon surface. The deposition process and the etch process were monitored by interference of in situ reflectometry [4,5]. It was shown that hydrogen ions with an energy of 2 keV not only caused etching, but that during the etch process the roughness of the nickel surface decreased.

In this chapter an overview is given of experiments on the application of energetic ions to reduce the surface roughness of metal deposited on carbon and metals on silicon as well as silicon on metals.

4.2 Metal-carbon multilayers

4.2.1 Treatment by low energy ions after deposition.

Spiller [6] had observed that Mo/Si multilayers deposited by sputter deposition always showed a better reflectivity than multilayers deposited by evaporation. He ascribed the difference by the higher

energy of the vapour achieved by sputtering, resulting in less interface roughness. Also bombardment of the substrate by energetic particles cannot be avoided during a sputter deposition process. Spiller [6] was therefore the first to publish an investigation on the use of low energy ions to reduce the interface roughness of a RhRu/C multilayer. For these experiments an ion gun was installed at an angle of 10^0 from grazing with the substrate. Deposition was done by e-beam evaporation and he used in-situ x-ray reflectometry to monitor the whole process. A RhRu/C multilayer with a periodicity of 6 nm was grown without any treatment. This was followed by a similar deposition of a multilayer of which a small selection of the layers was treated after deposition for 5 minutes by 300 eV argon ions. From the increase of the interference amplitude of the in-situ reflected signal, smoothing of the treated surface could be observed. (Figure 10) The reflectivity as a function of angle of both mirrors was measured afterwards for a wavelength of 0.154 nm (CuKα) and 4.8 nm (Synchrotron Brookhaven). The increase of the reflectivity of 0.154 radiation for the first order maximum from 40% to 69% clearly indicated the effect of interface roughness reduction. Detailed analysis of the reflectivity spectra revealed r.m.s values (σ) of 0.95nm for the non-treated multilayer and 0.63 nm for the ion treated multilayer, an improvement of 0.32 nm. The test with synchrotron radiation in the $\lambda = 4.4 - 5.8$ nm region showed an increase of the reflectivity by more than a factor of 2. Reduction of the layer thickness by ion etching could not be observed from the in-situ reflection signal. The small angle of incidence of the ions may have been responsible for a low sputter yield. However, the number of layer thickness errors was larger for the ion beam treated multilayer system. This might have been caused by small thickness changes due to sputtering. As an example, a layer thickness error was reported to occur during the deposition of layer 16. From the reflectometry data it is shown that the carbon layer (13) as well as the following RhRu layer (14) are treated by ions (Figure 10). Especially a small error of the layer thickness of RhRu caused by etching results in an error in the thickness of a whole period. Additional deposition of a carbon layer until the next interference minimum is reached will not compensate for the error in the period underneath. Moreover the in situ resonant reflection of the whole stack underneath is still disturbed by that one deviated period.
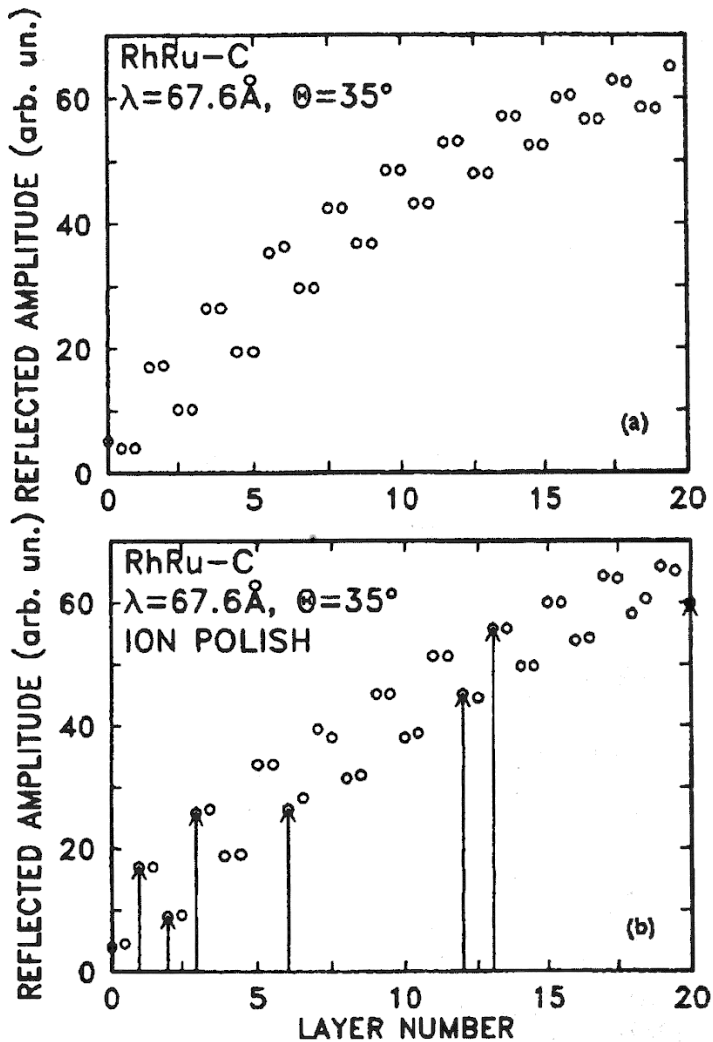
Figure 10 (a) Reflected amplitude at the start and end of each layer measured during deposition of the first 20 layers with $\lambda = 6.76$ nm at a grazing angle of 35^0. (b) Measurements for a similar deposition run, where the surfaces indicated by a vertical arrow were treated with 5 min of bombardment with Ar ions of 300 eV at a grazing angle of 10^0.

This will still affect the layer thickness of periods grown on top using interference from reflected radiation.

Spiller [7] also used e-beam evaporation and x-ray reflectometry to monitor the layer thickness for the production of Co/C multilayers. The multilayer was to be applied for normal incidence reflection in a wavelength region between 4.4 and 7.5 nm. In order to avoid ion beam induced crystallization of Co, only carbon was treated by energetic ions. Spiller explored grazing angles of incidence for the ion beam between 4 and 10 degrees and energies between 30 and 500 eV. The best results were obtained with an ion energy of 500 eV, a grazing angle of 4^0, a current of 15 mA and a polishing time of 5 minutes. The deposition of a stack of 60 Co/C layers was monitored by in situ real time reflectometry of 3.16 nm radiation at a grazing angle of 30^0. The ion polishing process was applied at 8 positions in the stacks. While an r.m.s roughness (σ) of 0.45 nm was achieved throughout the entire stack, the thickness errors were again slightly larger than for a non-polished multilayer. They ascribed this to a slight removal of material during the polishing process. Nevertheless the reflectivity in the wavelength region around 5 nm increased by a factor of 2.

Sequel to earlier experiments on etching of Ni by 2 keV protons [3], Verhoeven et al [8] investigated the application of 750 eV protons and argon ions for high spatial resolution depth profiling. X-ray reflectometry based on the reflection of N Kα radiation (λ = 3.16 nm) under a grazing angle of 35^0 was used to in situ monitor the growth and the etch process of single layers and multilayers. A combination of nickel and carbon was chosen to be investigated. Silicon (111) wafers with $\approx$ 2nm natural oxide were used as a substrate, with an initial r.m.s. roughness σ = 0.4 nm. The layers were deposited by e-beam evaporation. A 3 cm diameter Kaufman ion source was installed at an angle of 45^0, providing energetic ions with energies > 100 eV. They started their experiments with the growth of a single 12.5 nm thick nickel layer on the silicon substrate, followed by the ion etch process (Figure 11a). The fact that the first interference maximum during deposition is lower than the second interference maximum indicates that the first 1.4 nm of the nickel layer is not closed. Apparently nickel initially grows on natural silicon oxide as islands for at least the first 1.4 nm. Most surprising were the results of sputtering with argon ions.
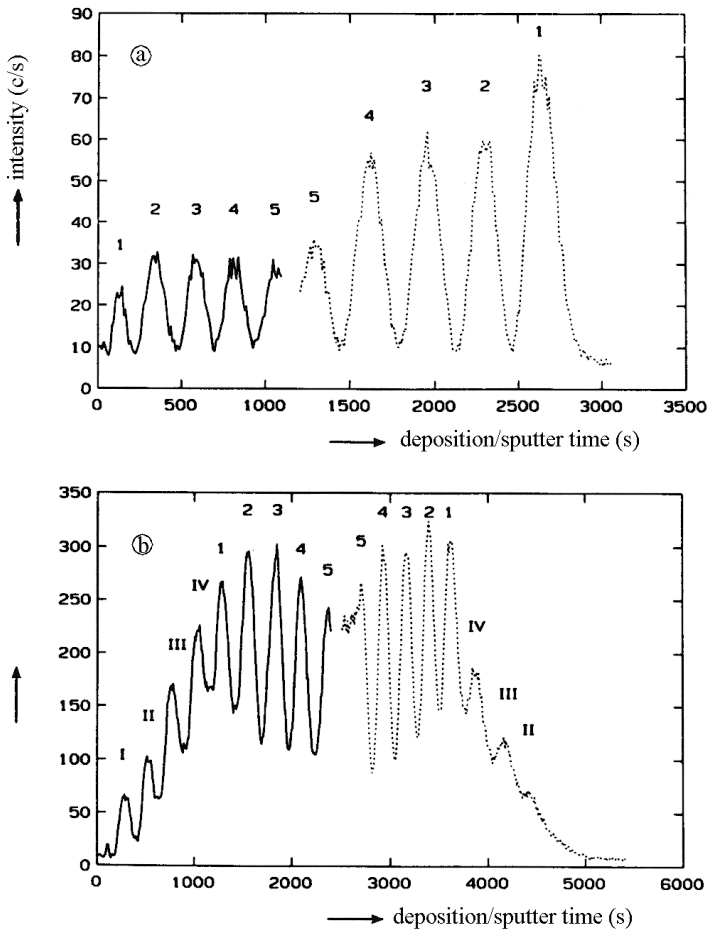
Figure 11 (a). The reflectivity of N-Ka radiation (λ = 3.16 nm) at a grazing angle of 35^{0} as a function of the Ni layer thickness during growth on the surface of a silicon wafer (solid line), followed by an etch procedure by 750 eV Ar ions (dotted line). The maximum Ni thickness was 12.5 nm. (b) The reflectivity of N-Ka radiation (λ = 3.16 nm) at a grazing angle of 35^{0} during deposition of a four period (2.7 nm) Ni-C multilayer with a 12.5 Ni over layer (solid line) Followed by etching of the complete stack by 750 eV Ar ions (dotted line).

42

While an increasing surface roughness due to etching was expected, the increase of the interference amplitude of the reflected x-rays (Figure 11a) during etching with 750 eV argon ions indicated an initial decrease of the surface roughness. The experiments were repeated with a 12.5 nm thick nickel layer on top of a nickel carbon multilayer consisting of a small number of periods of 2.7 nm (Figure 11b). The first as well as the second interference maximum of the nickel over layer growing on the Ni/C multilayer underneath turned out to be smaller than the third interference maximum. This indicates a non-closed layer consisting of islands for the first 4 nm for deposition on carbon. From a further decrease of the interference amplitude of the reflected radiation during deposition an r.m.s. roughness of 0.8 nm could be deduced for the final surface of a 12.5 nm thick nickel layer. Etching by 750 eV argon ions again demonstrated a decrease of the surface roughness of the thick nickel over layer. However, the reflection amplitudes representing the multilayer underneath partly disappeared (Figure 11b). This was explained by ion induced intermixing of the interfaces of the multilayer. This effect was very clear for etching with protons, where during the etching process no interference effects could be observed at all. Due to a high penetration depth interfaces appear to have intermixed right from the beginning of the etching process. Later experiments [9] on deliberate ion beam mixing of tungsten and nickel into carbon only revealed the formation of crystallites at the interfaces. As no intermixing could be observed, the before mentioned disappearance of the interference pattern may have been caused by crystallization at the interface resulting in an increased interface roughness.

Puik at al [10,11,12,13] continued to investigate the possibility to use energetic ions for improving the reflectivity of multilayers. The investigation concerned Ni/C and W/C multilayers with a periodicity of 2.7 nm. It was observed before that when carbon grows on top of a rough subsurface the surface roughness of carbon itself decreases during deposition. This effect was even used to compensate for the surface roughness of a material underneath [14]. Therefore the experiments only concerned smoothing of the metal components by energetic ions.

For deposition e-beam evaporation was used, combined with x-ray reflectometry of N Kα radiation at a grazing angle of 35^0 to monitor the growth and etch process. The ion source was mounted at an angle of 45^0. From TRIM [15] calculations it became clear that for argon ions
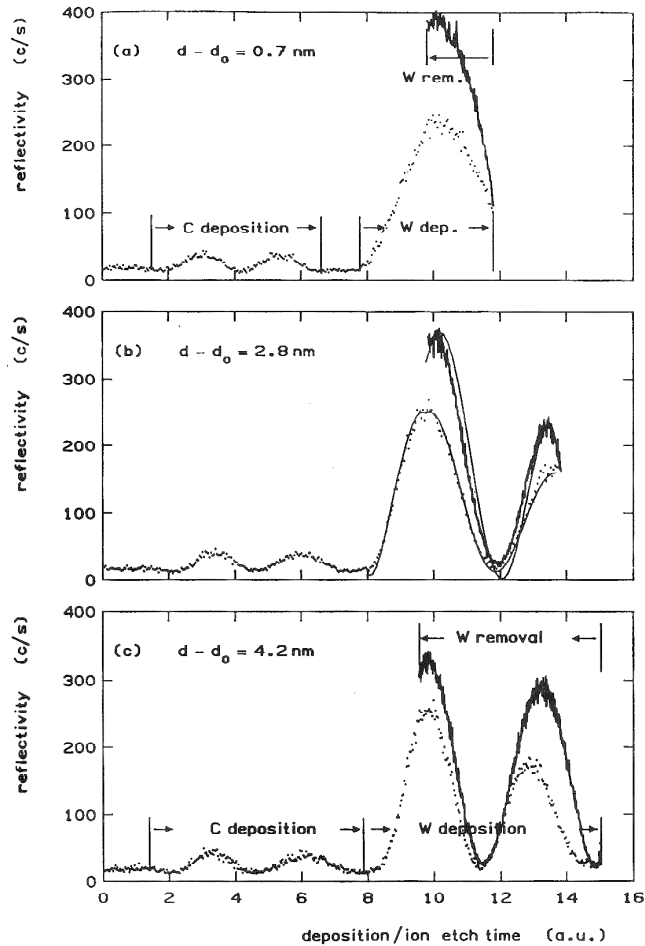
Figure 12. The measured reflectivity behaviour during deposition (dotted line) of two C periods (5.6 nm) followed by subsequently .75, 1.5 and 2 periods of W ((a), (b) and (c) respectively). The solid line corresponds to the measured reflectivity during removal of the W over layer by 200 eV Ar ions. The reflection measurements obtained during etching have been time reversed and scaled with the deposition. The smooth solid line in (b) is a simulation. Note that in all cases the reflectivity at the first maximum, representing a W layer with a thickness of 1.4 nm, is higher for ion etched layers as compared to as deposited.
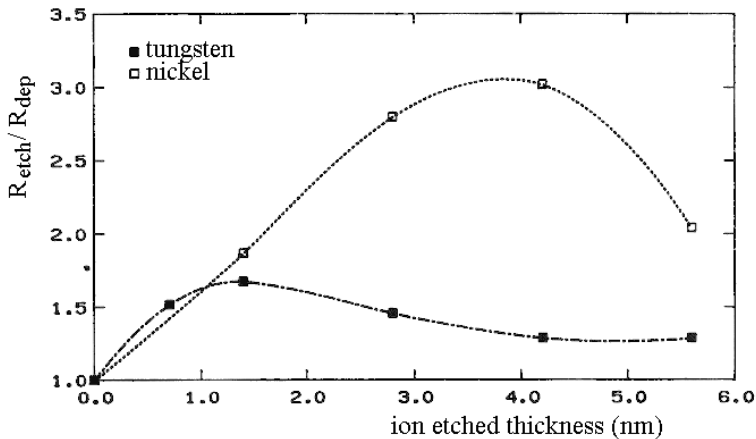
Figure 13. Ratio of reflected intensities at $\lambda = 3.16$ nm at a grazing angle of 35^0 after ion etch and as deposited for a (remaining) layer thickness of 1.4 nm Ni and W as a function of the ion etched over layer thickness. The lines are guides to the eye.

the energy should not exceed 200 eV, in order to prevent damage at the next interface.

Firstly they performed some basics experiments concerning how much extra nickel or tungsten had to be grown on carbon and removed afterwards by ion etching for a maximum reflection. Carbon was deposited on a silicon wafer to a reflection minimum ($\approx$ 6 nm). On top of that carbon layer tungsten or nickel were grown to a maximum interference (1.4 nm layer thickness) with a subsequently extra thickness of 0.7, 1.4, 2.8, 4.2 and 5.6 nm. That extra amount of tungsten or nickel was removed by 200 eV argon ions until the first interference maximum representing a thickness of 1.4 nm. The reflection at that first maximum is a measure for the improvement. Figure 12 shows three of those experiments for tungsten. It is obvious that in all cases the reflectivity at this first maximum is always higher after ion etching as compared to as deposited. The ratio of the reflected intensities for a remaining nickel and tungsten thickness of 1.4 nm after etching and as deposited as a function of the over layer thickness that was removed by etching is shown in Figure 13. The best result for tungsten was achieved

for an etch thickness of ≈ 1.4 nm while for nickel an etch thickness of ≈ 4 nm was required for the best reflectivity.

The effect of smoothing was explained by preferential sputtering of the most loosely bound surface atoms responsible for surface roughness, like having less neighbouring atoms. Examples are atoms or very small islands on atomically flat surfaces or atoms forming the top of islands. Also an enhanced surface migration is expected to be responsible. The initial growth of three-dimensional islands, of which the first 4 nm do not form a closed layer, can be held responsible for the requirement to remove an excess of 4 nm nickel. A high Schwoebel barrier, preventing nickel atoms to leave the island and contribute to a lateral growth, can explain the preferential three-dimensional island growth.
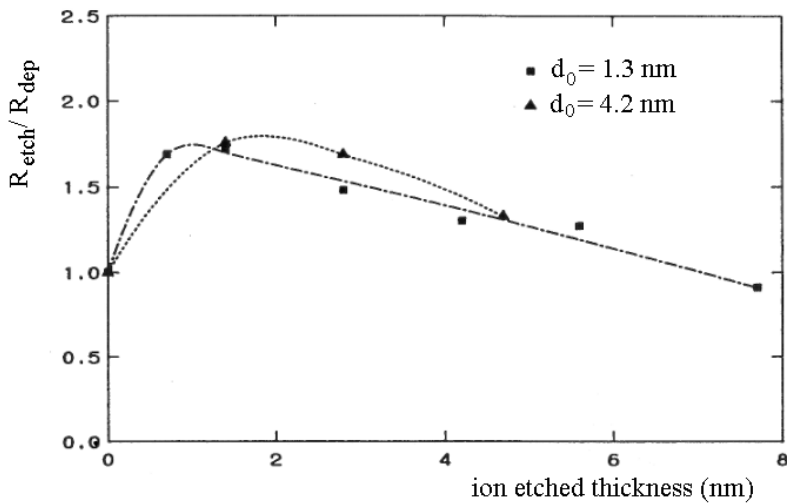
Figure 14 Ratio between the measured reflected intensity for a W layer of thickness d_0 = 1.4 nm (squares) and d_0 = 4.2 nm (triangles) after ion etching and as deposited, as a function of ion etched over layer thickness. The lines are guides to the eye.
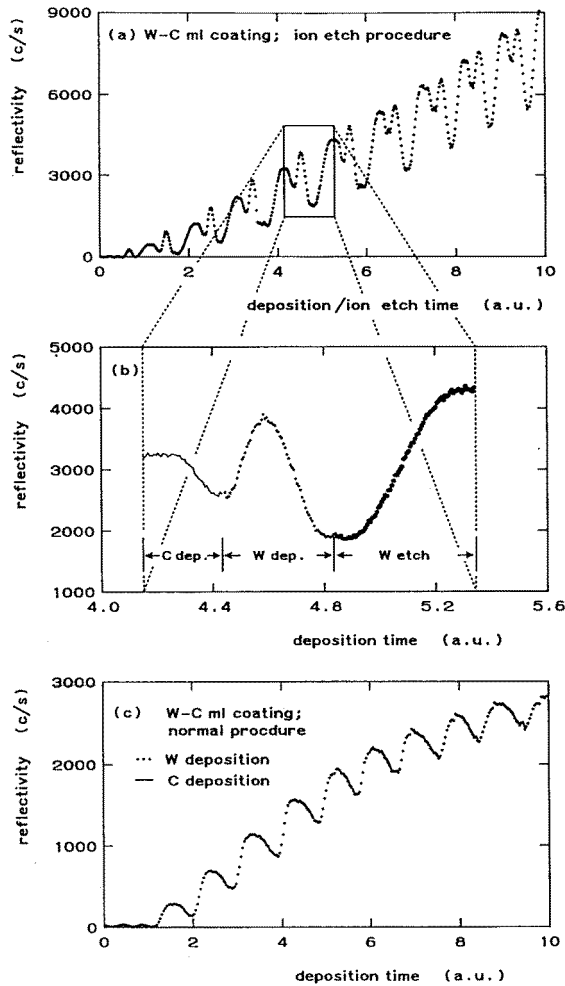
Figure 15 The reflectivity behaviour during deposition of a W/C multilayer coating after etching of each W layer by 200 eV Ar ions to a residual thickness of 1.4 nm (a). As can be seen from this figure after removal the reflectivity of the remaining W layer is considerable higher than for the as deposited layer with the same thickness of 1.4 nm. For clarity the deposition process for one period is enlarged in figure 6 b. Figure 6 c shows the growth of a reference multilayer, without any treatment by ions.

In order to obtain an impression of possible intermixing at the interface of the W-C system the before described experiments were repeated for a residual tungsten layer of 4.2 nm instead of 1.4 nm. Note that 4.2 nm corresponds to the second interference maximum in the reflectivity during growth of the tungsten layer. Since the mean penetration depth of 200 eV argon ions into W is about a factor of 10 smaller than 4.2 nm and a factor of 3 smaller than for 1.4 nm, the fluence of argon ions reaching the interface was expected to be negligible for 4.2 nm compared to a 1.4 nm over layer thickness. The same gain in reflectivity has been measured for the same ion etched thickness of approximately 1.4 nm (this situation is shown in Figure 14). Therefore it was concluded that either the fluence of argon ions reaching the interface through a 1.4 nm thick tungsten layer could be neglected or that the no additional intermixing took place. The latter can be explained by a low residual ion energy after passing 1.4 nm tungsten or a high chemical stability of the interface.

In order to optimise the reflectivity Puik et al [11,12] combined e-beam deposition and an ion etch procedure of all W layers to grow a W/C multilayer with a 2.7 nm periodicity. Contrary to the normal procedure tungsten was not deposited until the first maximum of reflectivity, but until the subsequent minimum was reached. Then from each tungsten layer ≈ 1.4 nm was removed by sputtering with 200 eV argon ions until a maximum reflectivity was obtained. Next carbon was deposited until a minimum reflectivity was reached and the whole procedure on tungsten deposition and etching was repeated. Figure 15 shows the reflected N Kα radiation intensity (3.16 nm) during a regular deposition process, resulting in a reference coating of 10 periods and the ion etch included process also resulting in a coating with 10 periods. It is clear that the etch procedure results in a coating with 3 times higher in situ reflectivity of 3.16 nm radiation than for the reference coating.

As a consequence of a long process time they did not apply the optimised process that requires the removal of an excess of 4 nm nickel. After the basic layer of carbon they deposited 4.2 nm nickel subsequently removed 2.8 nm to a residual thickness of 1.4 nm. Nevertheless a gain by a factor of 3 was achieved after deposition of 10 periods.

Characterisation of the multilayers by CuKα diffraction revealed a gain in the reflectivity at the first Bragg order due to the ion etch process of a factor 4 and 2 for Ni/C and W/C respectively. The interface roughness was obtained from a computational scheme in which thickness errors could be incorporated, solving the Fresnel equations. This scheme was used to simulate the reflection curve as function of the angle around and at the second Bragg order with the Debye-Waller roughness as a parameter. This resulted in an interface roughness σ = 0.45 nm for an untreated W/C multilayer and σ= 0.3 nm for an ion treated system. For the Ni/C combination the ion treatment resulted in an decrease of the interface roughness from σ = 0.44 nm to σ = 0.28 nm.

A striking difference with the polishing experiments done by Spiller [7] is that the etch procedure was completely controlled by reflectometry. A by reflectometry visible amount of material was removed for each period. Therefore unintentional thickness errors could be avoided. Also the improvement of the reflection after the etch procedure of each period could be observed. Louis et al [16] optimised Co/C and Ni/C multilayers with a periodicity of 3.95 nm by etching the metal component with low energy ions. The multilayers were to be applied as dispersive elements for space research in the wavelength region from 4.4 to 8 nm. Evaporation was used as deposition technique and with reflectometry by N Kα radiation the deposition as well as the etch process were monitored. For optimisation they varied the energy of Kr as well as Ar ions from 300 to 1000 eV. The best results were obtained for a Co-C combination of which an excess layer of 1.3 nm was removed by sputter etching at an angle of 20^0 with 500 eV krypton ions. The reflectivity of a 158-layer system improved at least 10% in the wavelength region from 4.4 to 8 nm.

4.2.2. Ion Assisted Deposition

Puik et al [11] also investigated the effect of Ion Assisted Deposition in combination with e-beam evaporation on the reflectivity of a Ni/C multilayer system. The Ni/C system was chosen since the influence of ion etching had shown to be most dramatic for this combination of materials. In-situ reflectometry of N Kα radiation during deposition was
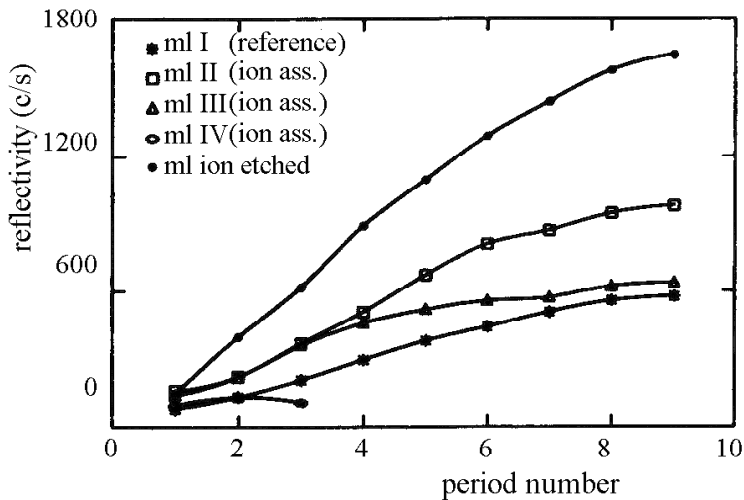
Figure 16. Maximum reflected intensities at $\lambda = 3.16$ nm and a grazing angle of 35^0 after deposition of each of the 1.4 nm Ni layers in various Ni-C multilayer coatings. Multilayer I is the as-deposited reference mirror. Multilayer II consisted of Ni layers up to .9 nm deposited without any ion treatment, followed by ion assisted deposition (200 eV Ar^+) for the next .5 nm. For multilayer III only the first 0.6 nm Ni was deposited without ion treatment, while the residual 0.8 nm was deposited by ion assistance. For multilayer IV the whole Ni layer was deposited by ion assistance. The highest reflection is obtained for the multilayer for which an etch procedure was applied after deposition.

used as a diagnostic tool. This resulted in periods of 2.7 nm for a grazing reflection angle of 35^0. They started to grow a reference system in the classical way. Carbon was deposited until, due to destructive interference a reflection minimum was obtained. Nickel was subsequently grown to a reflection maximum. The next two coatings consisted of nickel layers, which were partly as deposited and partly deposited with ion assistance. Bombardment with 200 eV argon ions at an angle of 45^0 was started after deposition of 0.9 and 0.5 nm respectively. For the last coating ion bombardment was applied during the deposition of the whole nickel layer. For all coatings Figure 16

50

shows the reflectivity at their maximum after deposition of the nickel layer, as a function of the layer number. disappearance of any reflectivity during total ion assisted deposition of nickel can be ascribed by intermixing, taking into consideration that at an angle of 45^0 the mean penetration depth of 200 eV argon ions is .4 nm.

The same curve is added for the etch procedure after deposition. From Figure 16 it is clear that low energy ion treatment after deposition of the nickel layer gives the highest reflectivity. Nevertheless also ion assisted deposition after an initial deposition without ion bombardment results in a higher reflectivity than for an as-deposited multilayer. Only ion assistance right from the beginning of Ni deposition appears to destroy the reflectivity completely. These results can be understood when we that realize that several mechanisms explain the influence of energetic ions on the growth of the nickel layer. The improvement of the reflection for partially ion assisted deposited nickel related to an as-deposited system can be explained by a smoother surface as well as by laterally larger islands and hence a more closed nickel layer. A completely closed layer would have resulted in a similar reflectivity as for an after deposition etch procedure. Extension of the islands can be explained by a reduction of the residence time of nickel atoms on top of a nickel island. That means that nickel atoms receive enough energy from the bombarding ions to cross the Schwoebel barrier and to find a position at the island edge. The disappearance of any reflectivity during total ion assisted deposition of nickel can be ascribed by intermixing, taking into consideration that at an angle of 45^0 the mean penetration depth of 200 eV argon ions is .4 nm.

51

4.3 Metal-silicon multilayers

4.3.1 Molybdenum Silicon

The reduction of the size of structures of electronic components has required the development of lithographic processes based on short wavelengths. For wavelengths longer than 100 nm transmission optics can still be applied. For shorter wavelengths reflection optics based on multilayers were to be designed. In the beginning of the nineties a choice was made for a radiation source of 13.5 nm. Especially Mo and Si form a suitable combination for a multilayer with a theoretical perpendicular reflectivity of more than 70% for this wavelength. It should be emphasized that the whole optical system required for the lithographic process consists of more than 10 optical elements. Therefore any loss of reflectivity per element should be avoided. Moreover these systems should be stable under radiation impact. Also high accuracy of the shape (< 1 nm) of the optical elements is required. Stress in the coatings can be a cause for deformation of the optical elements. All these problems have been a reason for an extended investigation of the Mo/Si the last decennium by many groups.

The first experiments on modification of the Mo/Si system by low energy ions was done by Verhoeven et al [17]. They investigated the influence of the impact of 300 and 800 eV argon ions on the surface roughness of Mo on Si and intermixing at the interface. Both materials were deposited by e-beam evaporation. Reflectometry of N Kα radiation (3.16 nm) under a grazing angle of 35^0 with the surface in combination with Auger Electron Spectroscopy were used for monitoring the growth and etch processes. The experiments took place in an UHV system with an ultimate vacuum of 10^{-8} Pa. During evaporation the pressure increased to 10^{-6} Pa, while argon ion etching even caused a pressure rise to 10^{-3} Pa. On a silicon (111) substrate with a natural oxide thickness of $\approx$ 2nm, 2.7 nm silicon was grown, corresponding to the first interference period in contrast with the oxide layer underneath (Figure 17). This was followed by the deposition of 10.8 nm Mo, corresponding to 4 more interference periods. All layers were subsequently removed by 300 eV argon ions. The decrease of the

interference peaks during deposition suggests an increase of the surface roughness. From the fact that peak 5' is higher than peak 5 it can be concluded that the ion etch procedure initially reduces the surface roughness of the Mo layer. The decrease of peaks 4' and 3'cannot be explained by ion beam mixing at the interface of Mo with Si underneath. The maximum penetration depth of 300 eV argon ions bombarding the substrate for an angle incidence of 45^{0} is according to TRIM [15] calculations < 2.5 nm. Peak 3' represents a layer thickness of 5.4 nm for Mo on Si. Only an increase in the roughness can be responsible for this decrease in reflectivity. This contradicts Molecular Dynamics (MD) calculations from Klaver et al [18], who predict surface roughening right from the beginning of the etch process. They used a single crystalline layer in their model, while the real layers are polycrystalline on top of an amorphous layer of 1 or more nm. On the contrary, the disappearance of peak 2' can only be explained by the disappearance of the interface of Mo with Si underneath due to intermixing. In contrast with TRIM, according to MD simulations [18] this effect can be expected for Mo layer thicknesses < 1 nm. The reappearance of peak 1' corresponding with the basic Si layer suggests that eventual reflection loss due to intermixing with the oxide layer underneath is compensated by an increase in density due to intermixing with Mo. Auger spectra of the Mo MNN peak and the Si LMM peak were recorded for a Mo layer thickness corresponding with an interference maximum or minimum of the reflectometry spectrum (Figure 17). It is clear that after deposition of 1.4 nm Mo still 20% of the Si LMM peak is present. Taking into consideration the escape depth of 90 eV electrons (Si LMM) it could be concluded that the Mo did not form a homogeneously closed over layer. The presence of the Mo MNN peak at the very end of the etch process in the region where only silicon is expected, confirms intermixing. Mo can even be observed after removing all Si from its oxide substrate. Apparently in the residual mixture of Mo and Si, the latter is preferentially sputtered in competition with recoil implantation of Mo. Similar deposition and etch experiments were repeated for 800 eV argon ions. Figure 18 shows that
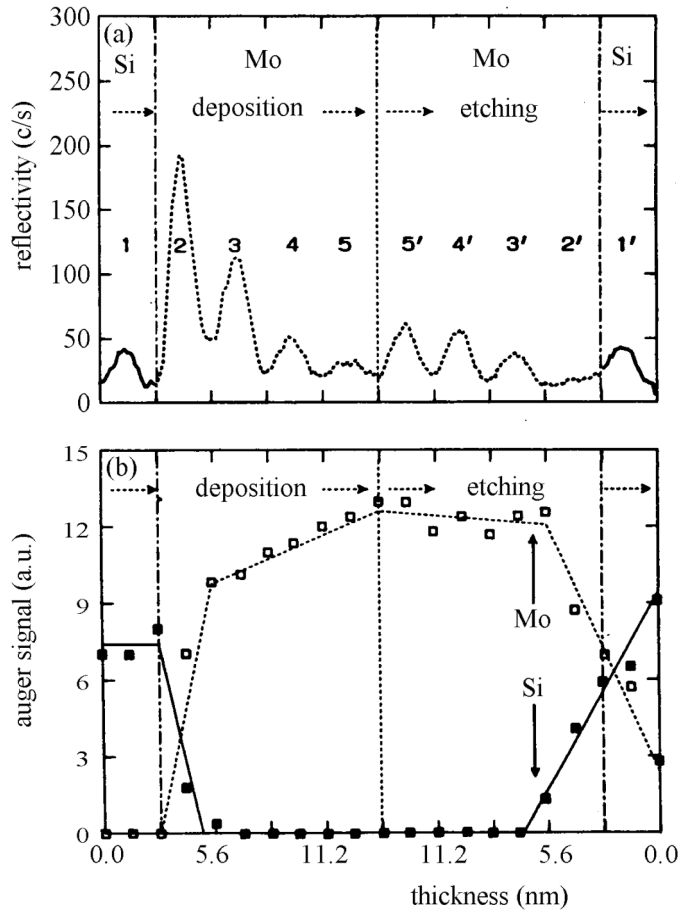
Figure 17 (a) Reflectivity of N-Kα radiation under grazing incidence of 35^0 as a function of layer thickness during deposition of 2.7 nm Si and 10.5 nm Mo on top, followed by etching with 300 eV Ar$^+$ ions. (b) The Auger MNN peak of Mo and the LMM peak of Si as a function of layer thickness during deposition of 2.7 nm Si and 10.5 nm Mo on top, followed by etching with 300 eV Ar$^+$ ions.
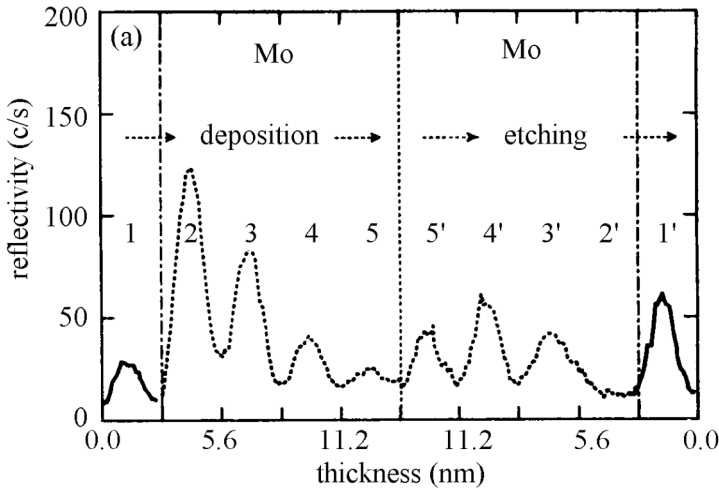
Figure 18 Reflectivity of N-Kα radiation under grazing incidence of 35^0 as a function of layer thickness during deposition of 2.7 nm Si and 10.5 nm Mo on top, followed by etching with 800 eV Ar^+ ions.

etching by higher energy ions results in more reduction of the surface roughness of Mo. Smoothing even continues after removing another interference maximum (4'). Again the roughness of the Mo surface increases after continuing of the etch procedure. Moreover the behaviour of the reflected intensity just after interference peak 3' suggests that intermixing occurs at a larger depth than for 300 eV ions. According to TRIM [15] calculations the maximum penetration depth for 800 eV argon ions into Mo should be 4.5 nm. The growth of the interference peak 1' related to the Si layer on top of the oxide surface confirms density enhancement by intermixing of Mo into Si. The only problem to be solved was why roughening of the Mo surface occurs after an initial smoothing. By comparing the etch rates for 300 eV and 800 eV argon ions it became clear that in all cases roughening occurs after the same ion fluence, being $\approx 6 \times 10^{19}$ ions/cm^2. In order to understand this phenomenon planar TEM was applied on substrates of at a different stage of growth and back etch. These substrates were prepared on a rock salt crystal at the edge of a regular silicon substrate.

The deposition and the etch processes were again monitored by reflectometry. A 5.4 nm thick Si layer was used as the basic layer onto which Mo was deposited and etched. These substrates were covered with 15 nm carbon as an over layer to prevent atmospheric influence during transport. TEM revealed that the first 2.7 nm Mo grows three dimensionally (Stranski-Krastanov) on top of Si. Deposition of a layer of 5.4 nm followed by a 300 eV argon ion etch to a residual thickness of 2.7 nm showed a smooth closed layer. Ongoing deposition beyond 5.4 nm revealed a growth of the crystallites in the Mo layer. From a subsequent back etch to a residual thickness of 5.4 nm it became clear that ion bombardment induced growth of the crystallites. Subsequent etching to 2.7 nm resulted in a moon landscape like surface. From these experiments it was concluded that a sputter etch procedure induces smoothing of a Mo surface. However the effect appeared to be limited by the formation of larger crystallites, after which roughness increases due to preferential sputtering of certain orientations. The formation of larger crystallites in the Mo film was observed for a fluence of $\approx$ 6 x 10^{19} ions/cm^2 for both ion energies. Related to the residual Mo layer thickness, interface mixing could the limiting factor for the choice of the ion etch energy. Schlatmann et al [19] investigated in more detail the growth and ion etch processes of the Mo/Si system, using reflectometry and Auger Electron Spectroscopy (AES). More specifically they investigated the effect of argon and krypton ion bombardment on the surface roughness of Mo on Si as well as Si on Mo. Energies were varied from 200 – 1500 eV and the angle of incidence was 45^0. Krypton has a smaller penetration depth than argon (to study the intermix effect) and a higher sputter rate (to study the fluence effect). X-ray reflectometry and AES on single layer growth followed by ion etching revealed that the surface roughness of a Mo layer increases during growth on Si. As a surprise, during deposition of Si on Mo the reflection amplitude does not change considerably as can be seen in Figure 19. From simulations (Figure 19) it could be concluded that during growth of 5.6 nm Mo the surface roughness had increased to a value of $\approx$ 0.8 nm. An additional deposition of 10.8 nm Si did appear to result in a final roughness < 0.9 nm. As such, the roughness of Si surface could be considered to be a copy of the surface roughness of the Mo surface underneath and slightly dependent of the

layer thickness. For all ion energies etching of Mo as well as Si resulted in smoothing of the surface. Smoothing of Mo appeared to be limited by intermixing and roughening. Figure 19 also revealed that removal of the Si over layer by 800 eV krypton ions did not result in the disappearance of any of interference amplitudes, suggesting that the interface formed by Si on Mo was much less sensitive to intermixing than the interface of Mo on Si. Intermixing only limited the smoothing effect of Si for an over layer thinner than 1.5 nm. Also a thermal treatment results in a much thicker interlayer for Mo on Si than for Si on Mo. Altogether it was concluded that it is more effective to ion etch the Si layer than the Mo layer. Furthermore, it appeared slightly more advantageous to use Kr ions instead of Ar, because of its higher sputter rate and smaller penetration depth.

The above single layer experiments were followed by the deposition of four different Mo/Si multilayers with 10 periods of 6 nm. For one of the multilayers acting as a reference, no ion etch at all was applied. For one multilayer only all Mo layers were ion etched with 300 eV krypton ions. For a third multilayer only all Si layers were etched and of the last multilayer all Mo as well as Si layers were etched. As expected from the single layer experiments the best results were obtained by etching an excess of $\approx$ 1.5 nm from each Si layer only. Related to the reference multilayer a gain of the in-situ reflectivity at the end of the deposition process by a factor of 5 was achieved. Simulations from Cu Kα reflectivity scans after deposition revealed a σ ranging from 0.3 to 1.4 nm for the reference stack. While for the ion etched multilayer a σ of 0.5 nm was found for the Si on Mo interface and 0.3 nm for the Mo on Si interface. The smoothing effect can clearly be observed in the cross section TEM photograph of Figure 20.
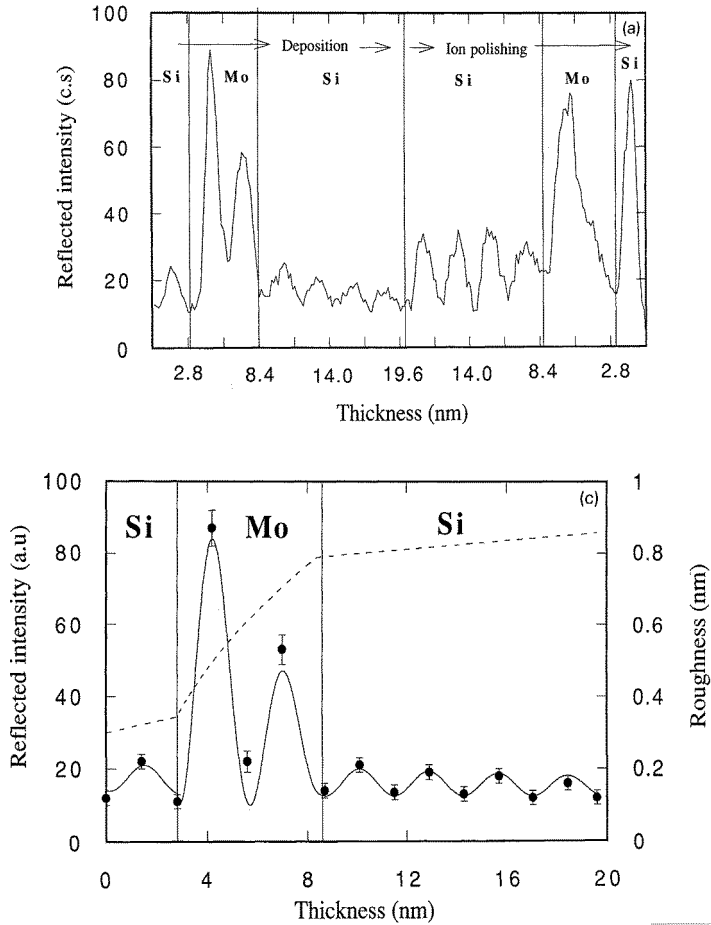
Figure 19 (a) Reflectivity of N-Kα radiation under grazing incidence of 35^0 as a function of layer thickness during deposition of 2.7 nm Si followed by 5.4 nm Mo and another 10.5 nm Si on top, followed by etching with 300 eV Ar⁺ ions. (b) Simulation of the reflectivity of N-Kα radiation as a function of layer thickness during the deposition process, including the roughness development during deposition in order to fit the measured data (represented by the measured values for the interference extremes)
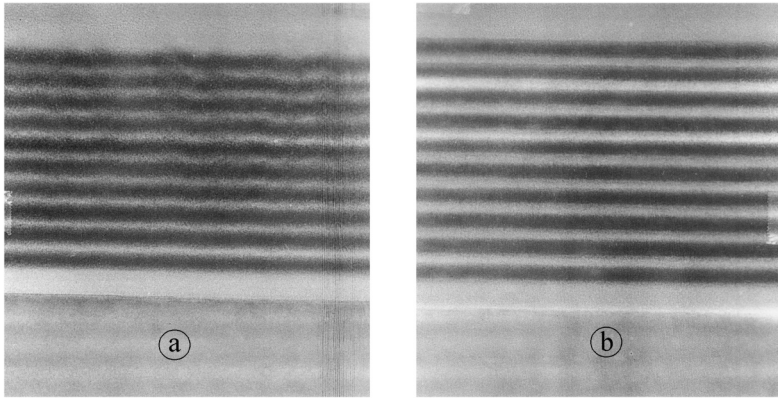
Figure 20 A cross section TEM photograph for a 10 period (d≈ 6nm) Mo-Si multilayer (a) as deposited, (b) after removing an excess of ≈ 1.5 nm from each Si layer by etching with300 eV Kr^+ ions.

From reflectivity scans with Cu Kα radiation it was observed that the period of an ion etched multilayer system was slightly larger than for an as deposited multilayer (6.1 versus 5.9 nm). This effect was ascribed to a densification of the Si layers as a result of the Kr etching process. An increase of 4% of the Si atomic density (also adversely affecting the optical contrast of the multilayer) must be assumed to explain the effect. This densification is not totally unexpected since the density of the as-deposited Si layers is some 90% of the bulk crystalline Si [20]. From extended x-ray (Cu Kα) scattering experiments, Schlatmann et all [21, 22] learned that the laterally shorter-length-scale roughness is removed more strongly by the ion etch procedure than the long-length-scale roughness. Off-specular scans even revealed for all ion eroded multilayers a clear reproduction of the interference peaks that were visible in the specular scan. This suggested a large degree of co formality of the roughness between all interfaces, down to in-plane length scales of less than 20 nm [23, 24]. From the exponential decay

with q_r of the intensity for all transverse scans it could be concluded that viscous flow was the dominant mechanism during ion bombardment [25,26]. At that time the available deposition system did not permit the deposition of a 6.7 nm period multilayer. Therefore no multilayer was available to be tested for perpendicular reflection of 13.5 nm radiation. However, calculations revealed that the roughness results as achieved with an ion etch process would result in a 69 % normal reflectivity for a 6.7 nm multilayer system. Stuik et al [27] investigated the role of the component ratio of the multilayer and finally Louis et al [28] were able to produce the proper multilayers with a 6.7 nm periodicity. Combining evaporation and a krypton ion back etch of Si they achieved a reflectivity of 69.5% for 13.5 nm radiation at an angle 1.5^0 off normal for a Mo-Si multilayer system. Moreover they closed the gap between fundamental research and the development of an optical element and demonstrated the control of a laterally uniformity of the d spacing within +/-0.05% over an area of 6 inch diameter.

4.3.2 Tungsten Silicon

The W/Si combination has widely been applied for the spectroscopic analysis of the composition of materials using fluorescence techniques. The main requirement for application is a proper wavelength resolution in order to distinguish different components. Nevertheless a high reflectivity permits a shorter time for the analysis procedure. When this analysis procedure is part of an energy consuming process like a melting furnace, a decrease with seconds of the total process will reduce the costs considerably. In order to come up with these requirements a proper ratio of the components within the periods have to be chosen and interfaces smoothness is to be optimized [29]. Therefore, Kessels et all [30] recently conducted experiments to study the possibility to improve the smoothness of the interfaces of the W/Si system. E-beam evaporation was used as a deposition source. In situ reflectometry of C Kα radiation (4.4 nm) under a grazing angle of 35^0 was applied to monitor both the processes of growth and etching. A 3 cm Kaufman source under a grazing angle of 45^0 provided energetic ions with energies > 50 eV.

In a similar way like for the Mo/Si combination a considerable improvement could be achieved by treatment of the surface of freshly

grown Si by 300 eV Kr^+ ions. They continued to investigate the improvement of the W surface as a result of Ion Assisted Deposition (IBAD) and a post deposition etch procedure. All experiments on the deposition of W were conducted on Si of which the surface was smoothed. IBAD experiments were carried out using Kr^+ ions with energies from 65 to 200 eV. In combination with the ion current this was transformed into 1 – 65 eV per arriving W atom. For one experiment a post deposition etch of an excess of 0.5 nm W by 300 eV Kr^+ ions was applied. They started to prepare planar TEM substrates by deposition of a Si-W-Si sandwiches of rock salt substrates. This deposition process was controlled by reflectometry on an adjacent silicon substrate. All planar TEM micrographs showed that 2 nm thick W layers deposited by IBAD as well as a post deposition etch procedure were closed. However in-situ reflectometry revealed a highest reflection for an IBAD procedure using $\approx$ 100 eV Kr^+ ions. This was verified after deposition using this IBAD procedure of W/Si multilayers with 10 periods of 4 nm.

For thin films in the order of several nm one needs to discriminate between surface effects and intermixing of the interface underneath. Therefore the investigation of IBAD effects on the surface smoothness as a function of energy added by ions for each arriving atom, a constant ion energy is required. Preferably this ion energy should be low enough to restrict the penetration depth. As that turned out not to be possible they had to discriminate between IBAD enhanced surface smoothing and intermixing of the W-Si interface underneath due to an enhanced ion energy. Therefore a newly developed technique was used [31]. In this method the intensity distribution in a cross sectional TEM micrograph is transformed into a preliminary density distribution. This density distribution is used as an onset for a fitting procedure with reflectometry measurements, which enables a quantitative in depth profile of the structures. This method revealed that even without IBAD intermixing at the W on Si interface could not be prevented. An interlayer of 0.4 nm with graded density was formed. IBAD caused the formation of a more complex structure consisting of two interfaces, one between W and a compound of W and Si forming an interlayer and another between this interlayer and Si underneath. These experiments confirmed competition between smoothing of the W surface during

IBAD and ion induced intermixing at the W-Si interface underneath. energies exceeding. New experiments to further optimise the process is required.

As a second part of the project the formation of WRe/Si multilayers was investigated. The WRe alloy was observed to grow as an amorphous layer [32], with a smoother surface as compared to the surface of a W layer [33]. All experiments on the deposition of WRe were conducted on Si of which the surface was smoothed. In contrast with pure W, planar TEM revealed that WRe did not grow on Si as a closed layer. Application of IBAD was required to obtain closed layers. However, the final peak reflectivity as measured from in situ reflectometry turned out to be lower for WRe/Si multilayers produced by IBAD than for the multilayer deposited without ion treatment. Also a post deposition etch of WRe did not perform better than a regular system for which no ion treatment at all was applied on the WRe layer. Apparently ion induced intermixing with the Si interface underneath is a dominant process that causes a decrease of the reflection. Nevertheless the WRe/Si multilayer without ionic impact during the deposition of WRe still performed better than the best W/Si multilayer.

4.4. Metal-metal Systems

4.4.1 Chromium - Scandium

Multilayers in the so-called "water window" region (2.2 – 4.4 nm) have an important application as optical elements in microscopy of biological specimens. When one of the multilayer components has an absorption edge within this "water window", an enhanced reflection can be achieved slightly beyond this absorption edge due to a negative δ. This can result in a normal incidence reflection as high as 55% [34]. Combined with a broad spectrum from a synchrotron radiation source, the proper wavelength can automatically be selected. The availability of new small scale bright x-ray sources with a wavelength within the "water window" enables the availability of x-ray microscopy at laboratory scale. A good example is the laser plasma based source as described by Johansson et al [39, 35]. A new promising source is based

on Cherenkov radiation [36]. Narrowband, radiation at energies of 453 eV and 512 eV has been generated by 10-MeV electrons in respectively titanium and vanadium foils.

Therefore quite some effort has been put into materials combinations of which one has an absorption edge within the "water window", like the L edges of Sc, Ti and V. A theoretically promising materials combination is Cr-Sc. Sc has an L absorption edge at a wavelength of ≈ 3.12 nm. Schäfers et al [34] used sputter deposition to produce a Cr-Sc multilayer for normal-incidence reflection of Sc L edge radiation. A value of 7% reflectance for this wavelength was achieved for a multilayer with a period thickness of 1.57 nm. By improvement of the stabilisation of the sputter deposition sources, reducing layer thickness errors, they were able to achieve a reflectance of 11% [37]. As discussed in paragraph 3.3, during a classical sputter deposition process the substrate is subject to all kinds of energetic particles and is as such an energetic particle assisted deposition technique. This process is controlled in an indirect way by choice of dc or rf systems, discharge power and working pressure.

Eriksson et al [38] used ion beam assisted sputter deposition to grow Cr-Sc multilayers to operate in the "water window" as condenser mirrors in a soft x-ray microscope. They designed the multilayer for a high-brightness line-emitting laser plasma source utilizing an ethanol liquid jet target, emitting mainly 3.374 radiation. As discussed in the end of 2.1, the absolute value of the interface roughness becomes more important for small multilayer periods. Similarly it can be calculated that a decrease in interface roughness from 0.5 nm to 0.3 nm results in an increase of the perpendicular reflectivity of a 1.692 nm period Cr-Sc multilayer from 3.2% to 28.9% for a wavelength of 3.374 nm.

Their experimental set-up was previously discussed in chapter 3.2. These multilayer systems were designed for near normal reflection of the first and the second order with 400 bilayers and periods of 1.692 and 3.381 nm. During deposition the multilayers were irradiated with argon ions with an energy varying from $9 - 113$ eV. Also the arriving ion-to-metal atom ratio could be varied by a factor of 10, from 0.76 to 7.1 for Cr and 2.5 to 23.1 for Sc. They used reflectometry with Cu-Kα radiation to obtain the nanostructural properties. The near-normal at-wavelength reflectivity of the multilayers was investigated using a soft

x-ray reflectometer with the laser plasma source generating the 3.374 radiation for which the microscope was designed [39]. Eriksson et al [38] observed a competition between the reduction of the surface roughness of the deposited layer and intermixing of the interface underneath. For a high ion-to-metal flux ratio a maximum value for the first order reflection of Cu-Kα radiation was achieved for an ion energy of 24 eV. However for radiation with a wavelength of 3.374 nm a maximum reflection of 5.47% was achieved at a reflection angle of 76^0 with the surface, after a high ion-to- metal flux ratio with an ion energy of only 9 eV. The difference was explained by the fact that hard x-rays are sensitive to atomic scale roughness while soft x-rays are more sensitive to lower spatial frequencies. Thus, it was concluded that for increasing ion energy initially the lower spatial frequency roughness is reduced. Increasing the ion energy results in a decrease of the atomic scale roughness, but at the same time causes intermixing of the interface underneath.

More recently Eriksson et al [40] prepared a 600 bilayer Cr-Sc system designed for near normal incidence for radiation of 3.11 nm (Sc L edge). A peak reflectivity of 14.5% was measured for a reflection angle of 87.5^0. However, according to a simulation, including an interface roughness of 0.34 nm, a value of 25.6% for the peak reflectivity was expected. This deviation could not be ascribed to interface roughness but a constant drift in the material fluxes during deposition as well as impurities of N (15 at.%), O (3 at.%) and C (0.5 at.%) turned out to be responsible.

4.4.2 Nickel - Titanium

Multilayer systems are also widely used as neutron monochromators. Also for this application a low interface roughness related to the d-spacing is required. Soyama et al [41] used a combination of ion beam sputtering and ion beam polishing for the deposition of Ni-Ti multilayers with a period thickness of 12 nm. Their deposition system consisted as a Kaufman ion source for target sputtering and a Kaufman ion source for ion polishing. This system is described in paragraph 3.2 figure 7. They investigated the influence of the time of argon ion

bombardment on the surface roughness of both multilayer components. The argon ion energy was 100 eV and the angle of incidence was 10^0 with the surface. For Ti as well as Ni a reduction from 0.7 to $\approx$ 0.35 nm of the surface roughness was observed. Etching resulting in a decrease of the layer thickness was not observed. On the contrary, bombardment of Ti even appeared to result of an increase of the layer thickness, while the layer thickness of Ni did not change at all. For ion energies of 300 eV and higher similar surface roughness reduction and etching as well were observed.

4.5. Conclusions

Energetic ions to reduce the roughness of a surface of freshly deposited thin films have successfully been applied for different material combinations for multilayer systems. For the metal carbon systems an improvement of the reflectivity of a factor of 3 after application of a post deposition etch procedure has been achieved. The performance of metal carbon systems deposited by Ion Beam Assisted Deposition (IBAD) has turned out to be lower than for the post deposition etch procedure. Limitations are formed by interface mixing and crystallization of the layer. Intermixing of two multilayer components not only depends on the chemical reactivity but also on the interface sequence. Metal-carbon systems appeared to be insensitive for intermixing. Only crystallization of the metal component at the interface has been observed. However, for metal-silicon systems mixing at the interface underneath a deposited layer can, even without ion impact, can not always be prevented. Most intermixing occurs at the metal on silicon interface. For the Mo-Si system a gain in reflectivity of a factor of 3 has been achieved after a post deposition ion etch process of the Si component. For the W-Si combination Ion Beam Assisted Deposition (IBAD) results in an improvement for a properly chosen ion energy.

WRe grows in flat islands on Si, even up to a layer thickness of 6 nm. Ion treatments using energies of 60 eV and higher result in closed layers. However application of ions with energies in the range as used in the experiments to grow a multilayer has resulted in a lower in-situ

measure reflectivity than obtained from a multilayer grown without any energetic ion treatment.

Ion Beam Assisted Deposition using an unbalanced magnetron has successfully been applied to grow Cr-Sc multilayers. Impurities and a drift of the deposition rate appear to form a major limitation for a maximum peak reflectivity.

References

1) M.P. Bruijn and J. Verhoeven, unpublished results (1985).

2) J. Verhoeven, unpublished results (1998)

3) J. Verhoeven, unpublished results (1986)

4) E. Spiller, A. Segmüller, J. Rife and R.-P. Haelbich, Appl. Phys. Lett.,37,1048 (1980)

5) A.N. Broers and E. Spiller, Scanning Electron `Microscopy 201 (1980)

6) E. Spiller, Appl. Phys. Lett., 54, 2293 – 2298 ((1989)

7) E. Spiller, Opt. Eng., 29, 609-613 (1990)

8) J. Verhoeven, H. Zeijlemaker, E.J. Puik and M.J. van der Wiel, Vacuum 41, 1327 – 1329 (1990)

9) Verhoeven, unpublished results (1994)

10) E.J. Puik, M.J. van der Wiel, J. Verhoeven and H. Zeijlemaker, Thin Solid Films, 193/194, 782-787 (1990)

11) E.J. Puik, M.J. van der Wiel, H. Zeijlemaker and J. Verhoeven, Appl. Surf. Sci., 47, 251-260 (1991),

12) E.J. Puik, M.J. van der Wiel, H. Zeijlemaker and J. Verhoeven, Appl. Surf. Sci., 47, 63 (1991),

13) E..J. Puik, M.J. van der Wiel, H. Zeijlemaker and J. Verhoeven, Rev. Sci. Instr. 63, 1415 (1992

14) M.P. Bruijn, P. Chakraborty, H. van Essen, J. Verhoeven, M.J. van der Wiel and W.J. Bartels, Proc. SPIE, 563, 183 (1985)

15) J.F. Ziegler, J.P. Biersack and U. Littmark, The Stopping and Range of Ions in Solids (Pergamon, New York 1985)

16) E. Louis, E. Spiller, S. Abdali, F.E. Christensen, H.-J. Voorma, N.B. Koster, P.K. Frederiksen, C. Tarrio, E.M. Gullikson and F. Bijkerk, SPIE proc. 2515, 194 (1995)

17) J. Verhoeven, Lu Chunguang, E.J. Puik, M.J. van der Wiel and T.P. Huijgen, Appl. Surf. Sci., 55, 97 (1992)

18) P. Klaver, W. Goedheer, F. Bijkerk and B.J. Thijsse, Mat. Res. Soc. Ptoc., 585, 305 (2000)R.

19) Schlatmann, C. Lu, J. Verhoeven, E.J. Puik and M.J. van der Wiel, Appl. Surf. Sci., 78, 147 (1994)

20) R. Schlatmann, A. Keppel, Y. Xue ad J. Verhoeven, Appl. Phys. Lett., 63, 3297 (1993)

21) R. Schlatmann, J.D. Schindler and J. Verhoeven, Phys. Rev. B, 51, 5345 (1995)

22) R. Schlatmann, J.D. Schindler and J. Verhoeven, Phys. Rev. B, 54, 10880 (1996)

23) D.E. Savage, J. Kleiner, N. Schimke, Y.H. Phang, T. Janowski, J. Jacobs, R. Kariotis and M.G. Lagally, J. Appl. Phys., 69, 1 (1991),

24) Y.H. Phang, D.E. Savage, R. Kariotis and M.G. Lagally, J. Appl. Phys., 74, 3181 (1993)

25) W.W. Mullins, J. Appl. Phys., 30, 77 (1959)

26) C. Volkert and A. Polman, in "Phase Formation and Modification by Beam-Solid Interactions", Edited by G.S. Was, L.E. Rehn and D. Follstaedt, Symposia Proceedings

27) R. Stuik, E. Louis, A.E. Yakshin, P.C. Görts, E.L.G. Maas, F. Bijkerk, D. Schmitz, F. Scholze, G. Ulm and H. Haidl, J. Vac. Technol. B17, 2998 (1999)

28) E. Louis, A.E. Yakshin, P.C. Görts, S. Oestreich, R. Stuik, E.L.G. Maas, M.J.H. Kessels, F. Bijkerk, M. Haidl, S. Müllender, M. Mertin, D. Schmitz, F. Scholze and G. Ulm, SPIE 3997-44, Microlithography, Santa Clara (2000)

29) M.J. H. Kessels, J. Verhoeven and F. Bijkerk, to be published

30) M.J.H. Kessels, J. Verhoeven, F.D. Tichelaar and F. Bijkerk to be publishede

31) M.H.J. Kessels, F.D. Tichelaar, J. Verhoeven and F. Bijkerk, J. to be published

32) A.W.D. van der Gon, J.C. Barbour, R. de Reus and F.W. Saris, J. Appl. Phys., 61, 1212-1215 (1987)

33) R.-P. Healbich, A. Segmuller and E. Spiller, Appl. Phys. Lett., 34, 184-186 (1979)

34) F. Schäfers, H-C. Mertins, F. Schmolla, I. Packe, N.N. Salashchenko and E.A. Shamov, Appl. Opt., 37, 719 (1998)

35) H.M. Hertz, G.A. Johansson, H. Stollenberg, J. de Groot, O. Hemberg, A. Holmberg, S. Rehbein, P. Jansson, F. Eriksson and J. Birch, J. Physique IV, 104, 115 (2003)

36) W. Knulst, M.J. van der Wiel, O.J. Luiten and J. Verhoeven, Appl. Phys. Lett. 83, (2003) 4050 - 4052

37) F. Schäfers, M. Mertins, D. Abrahamson, A. Gaupp, H-C. Mertins and N.N. Salashchenko, Nucl. Instr. Meth. Phys. Res., A 467 – 468, 349 (2002)

38) F. Eriksson, G.A. Johansson, H.M. Herz and J. Birch, Opt Eng., 41, 2903 (2002)

39) G.A. Johansson, M. Berglund, F. Eriksson, J. Birch and H.M. Hertz, Rev. Sci. Instr., 72, 58 (2001)

40) F. Eriksson, G.A. Johansson, H.M. Hertz, E.M. Gullikson, U. Kreissig and J. Birch, Opt. Lett., 28, 2494 (2003)

41) K. Soyama, W. Ishiyama and K. Murakami, J. Phys. Chem. Solids, 60, 1587 (1999)

5   Modifying layers

Abstract

The impact of energetic ions on thin films will result in implantation, cause densification and intermixing at interfaces. All these effects can be applied to modify the mechanical, chemical and optical properties of multilayer systems. In this chapter examples are given about ion-induced reduction of stress, ion induced intermixing to form special interlayers and implantation to improve the optical contrast as well as the thermal stability. Intermixing and implantation of hydrogen has been applied to both the Mo-Si and W-Si systems. Different results for intermixing and implantation for these systems are discussed. CH_x^+ ion implantation into Si has demonstrated to improve the thermal stability of the Mo-Si system. The combination of intermixing and implantation was applied for the formation of a NiSi/SiN multilayer system.

5.1. Introduction

As discussed previously in chapter 2, energetic ions can cause densification and intermixing to a certain thickness of a thin film and ions can be implanted to an energy dependent depth. As a result of densification, mechanical stress in a thin film can decrease as well as increase. Intermixing at interfaces underneath a top layer can often not be avoided due to a preferential compound formation of the components. Even systems that are stable at room temperature may be subject to intermixing at elevated temperatures. This thermal instability forms a limitation for the application of certain component combinations for multilayer systems. Ion beam controlled intermixing can be applied to form a thermally more stable compound. As a result a special density distribution within the multilayer periods may be produced. An alternative to thermally stabilize a multilayer system is to

change the chemical composition of one of the multilayer components by implantation. As a result also the optical contrast with the other component may change. In this chapter the application of energetic ions to modify stress in the Mo-Si system will be discussed. This is followed by ion induced intermixing of the Mo-Si as well as the W-Si system. The next paragraphs will deal with implantation of hydrogen into Si in order to improve the contrast and implantation of CH_x^+ ions to improve the thermal stability of Mo-Si multilayers. This chapter will be concluded with a paragraph about the formation of a $NiSi/SiN_x$ multilayer system by a combination of intermixing and implantation of nitrogen.

5.2. Stress reduction

An important problem in Mo-Si multilayers for UEV lithography is stress. Windt et al [1] investigated stress evolution in Mo-Si multilayers produced by magnetron (diode system) sputter deposition as a function of background pressure. For multilayers containing 40 bilayers of ≈ 4.3 nm Si and ≈ 2.6 nm Mo they found an increase in the stress from approximately -280 MPa (compressive) to -450 MPa for a decrease in the residual background pressure from 10^{-5} to 6.0×10^{-8} mbar. For multilayers of the same period but with thicker Mo layers, the dependence on background pressure turned out to be stronger. X-ray (λ = 0.154 nm) reflectometry measurements revealed only a slight increase in interfacial roughness for films deposited at high background pressure, but no evidence was found for any differences in the microstructure of the polycrystalline Mo layers that comprise these structures. They ascribed this phenomenon to the incorporation of hydrogen in the layers and to a decrease in the surface mobility of the ad atoms during deposition due to adsorbed residual gas atoms. Nevertheless, the peak soft x-ray (λ =13,6 nm) reflectance, which is sensitive to interfacial roughness at longer spatial wavelengths, showed no correlation with background pressure or stress. However, internal stress in these multilayers may result in a non-negligible deformation of the accurately fabricated mirror substrates, to the extend that optical properties are affected [2]. Shiraishi et al [3] investigated the possibility to reduce stress by incorporating an extra layer of Ru and by ion beam polishing.

They used a Kaufman source and a rotating target for sputter deposition, combined with a separate Kaufman source for polishing. Their conventional multilayer of 50 layer pairs and a fractional thickness ratio Mo:Si of 0.35 showed also a compressive stress of –450 MPa. By bombarding each Mo layer during 6 seconds with 30 mA 600 eV Ar^+ ions at an angle of 20^0 with the surface, they managed to reduce the stress to –140MPa. Ion polishing of the Si layer did not appear to result in a stress reduction. A residual stress of $\approx$ 14 MPa was achieved from a combination ion beam polishing of Mo and the incorporation of Ru. Shiraishi et al [3] ascribed stress to the formation of an interlayer. Their low stress multilayers had much thinner interdiffusion layers and more abrupt interfaces.

5.3. Intermixing

5.3.1 Mo-Si

As mentioned before, ion bombardment of a Mo over layer with a Si layer underneath easily causes intermixing at the interface. Verhoeven et al [4] used x-ray reflectometry to measure sputtering yields of thin films. It was observed that after removal of a complete over layer of Mo from Si, the sputter yield for Si remained 31% higher than measured for a Si layer that never contained an over layer of another element. This result was ascribed to an increased stopping power due to the presence of intermixed molybdenum resulting in an increased preferential sputtering of Si. An increased sputter yield could even be observed after further removal of 10 nm extra Si, suggesting a continuous ion enhanced diffusion of Mo into Si in competition with preferential sputtering of Si. Harper et al [5] as well as Berg et al [6] reported similar phenomena that they were able to simulate by application of T-DYN. From these results a novel method to fabricate layers with mixed composition was developed by Schlatmann et al [7]. In this process each multilayer period, consisting of one spacer layer and one mixed layer, was formed in three steps. The whole process was monitored by reflectometry. Firstly a full period of Si was deposited, followed by a 3 nm thick over layer of Mo. Finally that whole over layer of Mo was removed by 300 eV krypton ions, ending up at the residual Si thickness

(Figure 21). Repeatedly following this procedure, a stack was grown of which an increase of the amplitude of the in situ x-ray reflectivity signal could be observed. This was a qualitative indication that the formation of an intermixed layer took place and that the interface roughness did not increase throughout the stack. From a cross-section transmission electron microscope picture (Figure 22) it became clear that a layered structure was formed with sharp interfaces. Rutherford backscattering spectroscopy (RBS) and ex situ reflectometry using Cu Ka radiation showed that the multilayer consisted of a 2 nm mixed layer and a 4 nm pure Si layer. The mixed layer had an average atomic ratio of Mo:Si of 1.7±0.3. This is close to the ratio 1.67 of Mo_5Si_3, which is the most stable compound in a Mo rich environment, according to the equilibrium phase diagram and annealed Mo/Si multilayers [8].

To investigate the mixing process in more detail, Schlatmann et al [7] prepared single periods of Mo and Si. A bilayer of 8 nm Mo on top of 8 nm Si was bombarded with Ar and Xe ions of different energies (ranging from 200 to 1500 eV, at a constant current of 20 $\mu A/cm^2$).
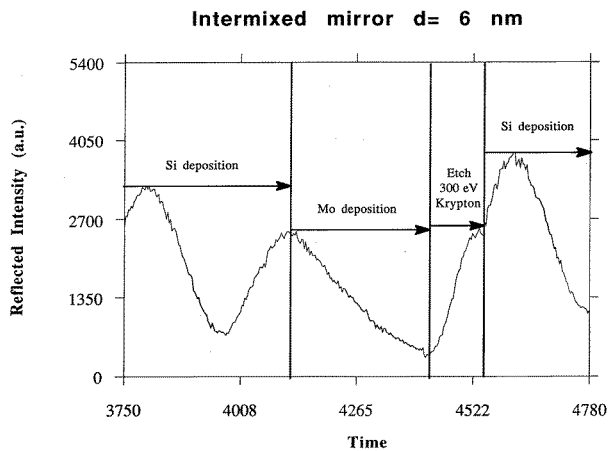

Figure 21. A detail of the deposition as observed by the intensity of C-Kα (4.47 nm) radiation reflected under grazing incidence of 35^0 of a Mo-Si multilayer system where Mo is intermixed into Si. A whole period of Si is deposited until an interference maximum is reached. This is followed by the deposition of half a period Mo. Subsequently all Mo is removed by 300 eV Kr^+ ions.
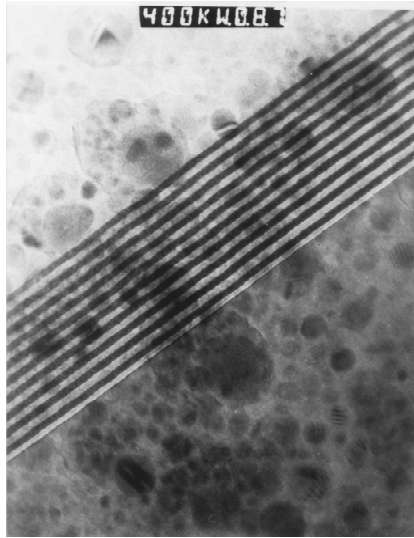
Figure 22. A cross sectional TEM photograph of an intermixed Mo-Si multilayer structure.

Controlled by x-ray reflectometry the etch procedure was continued until a residual layer thickness of 8 nm was reached. The Mo spatial density N_{Mo} was measured using RBS. A plot of N_{Mo} as a function of ion range as calculated by TRIM 89 [9] revealed a linear relationship (Figure 23) Based on the consistency of the calculated concentrations with RBS and reflectivity data for the multilayer sample, the mixed layer was assumed to have an approximately uniform distribution of Mo and Si. Then N_{Mo} is proportional to the layer thickness of the intermixed layer for all samples, assuming a similar composition of all layers. The diffusion of Mo atoms through the mixed layer is ion enhanced and is only significant in the region reached by the ions. So, if the compound formation rate is higher than the sputter rate, the thickness of the mixed layer is simply equal to the ion range in that layer. Consequently, the
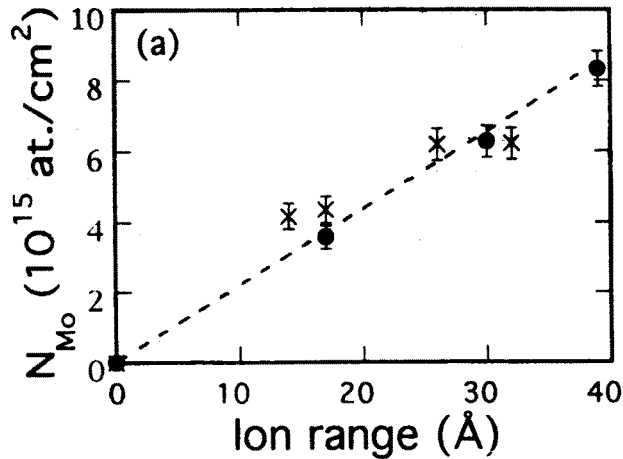
Figure 23. Measured Mo content (N_{Mo}) in the ion beam mixed Mo-Si multilayer as a function of ion range in the solid. The different symbols represent measurements using Ar (dots) and Xe (crosses).

interface between the mixed Mo_xSi_y and the pure Si layer shifts (into the Si layer) as a result of erosion of the top surface. By intermixing the contrast between the layers as well as the absorption in the stack will be reduced. As a consequence more interfaces will contribute to the reflection process resulting in a better wavelength selectivity. Moreover, multilayers consisting of a combination of a metal silicide and silicon have the advantage of an increased thermal stability compared to a stack of layers consisting of the separate elements. E.g. multilayers consisting of alternating $MoSi_2$ and Si layers were shown to be stable in peak reflectivity and multilayer period up to temperatures between 700^0 [10] and 850^0 [11].

5.3.2 W-Si

More recently experiments by Kessels et al [12] were conducted on ion induced intermixing of the W-Si system. E-beam evaporation was used to deposit the multilayer. A 3 cm Kaufman source under a grazing angle
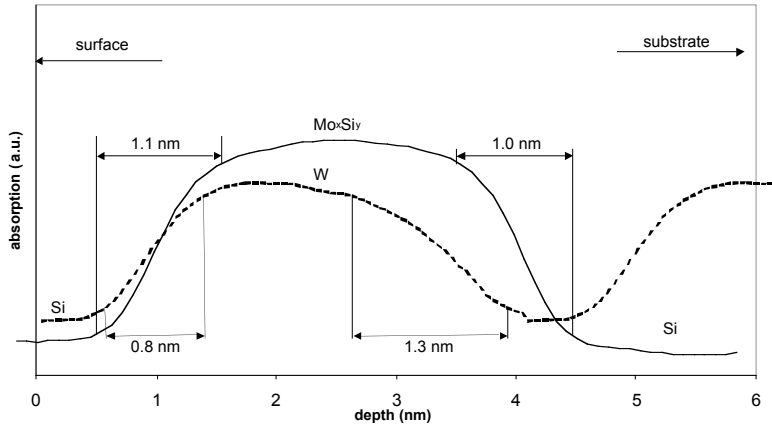
Figure 24 Measured absorption profiles of cross section TEM images of W/Si (dashed line) and Mo/Si (solid line) multilayers. The scales are identical. Note the asymmetric profile of W/Si vs the symmetric profile of Mo/Si, the W-on-Si interface showing the graded profile. The indicated interface widths are determined using absorption levels of 10 % above the minimal value and 10% below the maximum value.

of 45^0 provided energetic ions with energies > 50 eV. In situ reflectometry of C K radiation (4.4 nm) under a grazing angle of 35^0 was applied to monitor both the processes of growth and etching. The multilayers were characterized by θ-2θ reflectometry using an x-ray reflectometer at Cu-Kα wavelength. Cross sectional TEM was used to further investigate the multilayer structure. In order to be able to compare with the intermixing experiments of the Mo-Si combination as discussed in the chapter before, Kr[+] ions with a higher energy were used for the intermixing process. TRIM simulations [37] revealed that to maintain a constant ion energy – mass ratio an energy of 1000 eV was required for the W-Si system as opposed to 300 eV for the Mo-Si system. Experiments including monitoring of the process were conducted in the same way as for the Mo-Si system (Figure 21). For each period 5 nm Si was deposited, of which 1 nm was removed by 300 eV Kr[+] ions. An improvement of the surface smoothness was observed.

This was followed by the deposition of 1 nm W, which was subsequently removed by 1000 eV Kr^+ ions. In Figure 24 the cross section TEM intensity profiles of the intermixed Mo-Si system as obtained from Figure 22 is compared with the same profile for intermixed W-Si. The Mo-Si profile is clearly symmetric, while in contrast the profile for the W-Si system is asymmetric. So it can be concluded that while Mo tends to form a compound with Si, W forms a depth dependant mixture with Si. In order to explain this discrepancy the thermodynamic process depending on the Gibbs free energy ($\Delta G= \Delta H-T\Delta S$) was considered. When the enthalpy of alloy formation (ΔH), the temperature T and the entropy of alloy formation (ΔS) are known, the Gibbs free energy can be calculated. When comparing the W rich compound W_5Si_3 and $MoSi_2$, ΔS is respectively 0.0013 and –0.0015. However, ΔH for W_5Si_3 is −17 and for $MoSi_2$ –44. The resulting lower ΔG for W_5Si_3 can be held responsible for a less likely alloy formation and a more easily dissociation as compared to $MoSi_2$.

5.4. Implantation of hydrogen to improve the contrast

5.4.1 Mo-Si

As already discussed, the reflectivity of a multilayer is determined by the optical contrast and interfacial roughness. The optical contrast is determined by the difference in the optical constant $n = 1 - \delta + i\beta$. δ as well as β are directly proportional to the atomic density of the material. So by reducing the atomic density of the spacer material (e.g. Si), the optical contrast will be enhanced.

For electronic devices, the ability of hydrogen to passivate impurity related states and to eliminate gap states, has rendered doping of amorphous Si feasible. Therefore, the electrical, optical and structural effects of hydrogen in a-Si have been studied extensively. It has been known that the incorporation of H in Si can affect the relative Si atomic density [13,14,15]. For Si layers, deposited by means of a glow discharge in a SiH_4 atmosphere, it was found that when an increasing
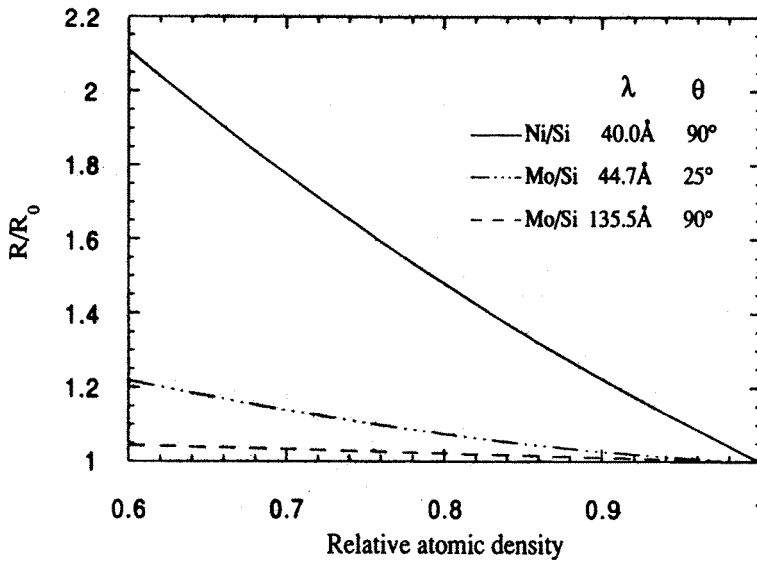
Figure 25. Calculated Bragg reflectivity for multilayers of 100 periods, as a function of the relative atomic density of the spacer, Si. The multilayers are optimised for the wavelength λ and grazing angle θ indicated in the figure, with a constant rms roughness $\sigma=.3$ nm for all interfaces.

amount of H is incorporated in the layer, the Si atomic density is gradually reduced. Reductions as high as 40% have been measured. In low density Si, H is bonded at vacancy or defect positions in the a-Si structure. Layers deposited on low temperature substrates by evaporation already possess a relatively high defect density [16]. By H^+ ion bombardment further structural damage will be caused in the Si layer, to which the hydrogen may be bonded. Schlatmann et all [17,18] investigated the effect of low energy H^+ ion implantation of Si on the improvement of the contrast for a Mo-Si multilayer system. From calculations (Figure 25) of the Bragg reflectivity for multilayers of 100 periods as a function of the relative atomic density of Si shows that for 13.5 nm radiation only a gain of 4.5% can be achieved at normal reflectivity. The effect is particularly strong for the combination of Ni and Si at a wavelength of 4 nm at normal incidence. The relatively low

gain for 13.5 nm is due to the anomalous behaviour of the refractive index of Si around its L absorption edge (12.44 nm).

E-beam evaporation was used for deposition and a Kaufman broad beam ion source provided energetic H^+ ions. In situ x-ray reflectometry (C Kα 4.47 nm) was used to control deposition as well as the implantation process. With Elastic Recoil Detection (ERD) the spatial
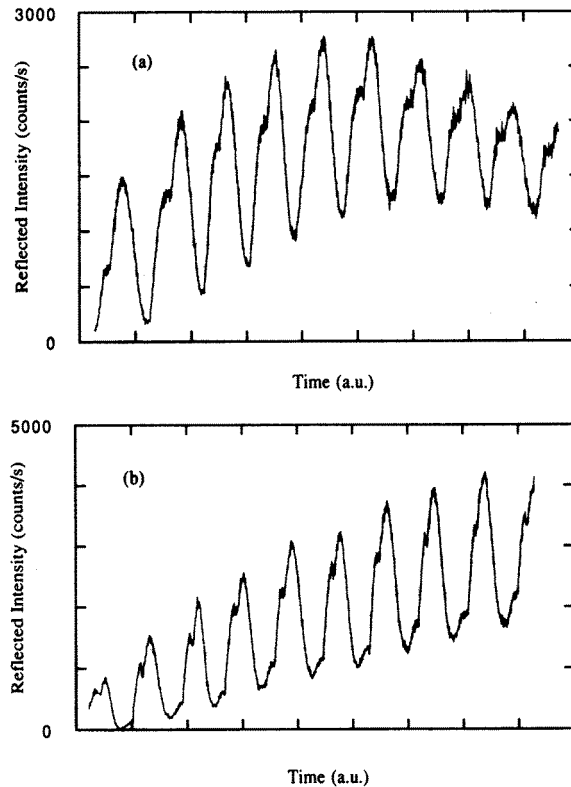
Figure 26. Measured reflection of C-Kα radiation during deposition of a Mo-Si multilayer system as a function of time. (a) As deposited; (b) after implantation of each Si layer by 150 eV H^+ ions.
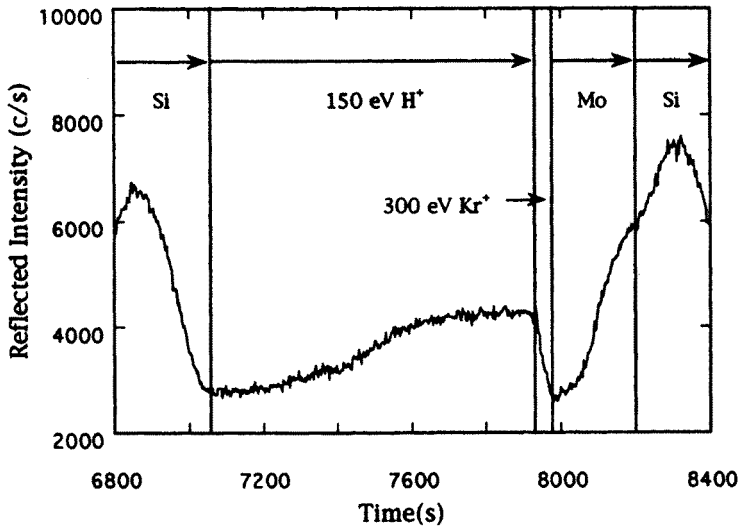
Figure 27. Detail of measured reflection of C-Kα radiation during deposition of a Mo-Si multilayer where implantation of Si by150 eV H$^+$ ions was combined with smoothing by 300 eV Kr$^+$ ions.

density of implanted hydrogen of the multilayer components was measured. From Rutherford Backscattering Spectroscopy (RBS) the spatial densities of Mo and Si could be retrieved. The Si-H vibrational stretching mode region was examined using Fourier transform infrared absorption spectroscopy (FTIRAS). Varying the fluence of 150 eV H$^+$ ions on each of the Si layers, a number of Mo-Si multilayers was deposited. Each consisted of 10 periods of 6 nm, with a cap layer of 6 nm Si to prevent oxidation of Mo after deposition. From the in situ x-ray reflection during the whole production process it became clear that for the implantation of 10^{16} H$^+$ ions/cm^2 a much higher reflectivity was achieved than for an as deposited-system (Figure 26). A qualitative check on the interface roughness by comparison of cross section TEM pictures from both samples did not indicate a large smoothing effect as a result of the H$^+$ implantation. The atomic Si density was found to

saturate at a minimum of 64±5% of the crystalline value. Additionally three multilayers were grown where implantation with a large fluence of H^+ was combined with a back etch with 300 eV Kr^+ ions to reduce the surface roughness [18]. A detail of this deposition process is shown in Figure 27. In this figure Si is deposited until a minimum in the reflected intensity is reached. Then the Si layer is bombarded with a
saturation H^+ fluence of 1.5 x 10^{16} ions/cm^2. The reflectivity signal can be seen to rise and then saturate during the implantation process. This reflectivity signal rise is attributed to swelling of the Si layer. During a much shorter time the layer was etched by 300 eV Kr^+ ions, again down to a minimum in the reflected intensity. Finally Mo is deposited until the next reflectivity maximum was reached. This combination of implantation followed by etching resulted in a Si atomic density saturating at a minimum of 77±5% of the crystalline value. An improvement of 6% was observed for the in situ reflected intensity of 4.4 nm radiation with respect to a non-hydrogenated Mo-Si multilayer. The maximum absorption in the FTIRAS spectrum suggested isolated SiH_2 bonds, $(SiH_2)_n$ polymers [19] and/or Si-H bonds on the internal surfaces of voids [20].

5.4.2. W-Si

Kessels et al [21] applied implantation of hydrogen into the W-Si system, not only to improve the contrast, but also to passivate silicon in order to prevent interdiffusion at the interfaces. A disadvantage of a surface with a low chemical reactivity is the high mobility of the atoms arriving. As a result those atoms tend to form clusters. For the combination of Mo on Si passivated by hydrogen, Lohman et al [22] observed the formation of islands until after a critical layer thickness of 1 nm a closed layer was formed. Therefore Kessels et al [21] studied 3 systems; a regular W-Si system as a reference, a "W-H implanted Si" system and a "W- H implanted Si" system with an extra 0.3 nm thick Si interlayer after implantation. An energy of 500 eV was used for implantation of H^+ ions. All deposition processes involved smoothing of the Si surface by 300 eV Kr^+ ions. For the implanted systems smoothing was done before implantation.
The same procedure and experimental setup for deposition as described in paragraph 5.4.1 was used. Planar TEM substrates were prepared by

deposition of Si-W-Si, Si:H-W-Si and Si:H:Si-W-Si sandwiches onto rock salt substrates. This deposition process was controlled by reflectometry on an adjacent silicon substrate. For each combination full 10 period stacks were deposited, controlled by in situ reflectometry. The total hydrogen content in these full stacks were determined by elastic recoil detection (ERD). From planar TEM it became clear that W on Si formed a closed layer. W on H implanted Si and on H implanted Si with an extra 0.3 nm Si over layer revealed the formation of islands. The average lateral dimensions of these islands were ≈ 2.95 nm for the Si:H-W-Si system and ≈ 3.62 nm for the Si:H:Si-W-Si system. ERD revealed a H content of 34% for the Si:H:Si-W-Si structure and 26% for the Si:H-W-Si structure. The highest maximum reflectivity as measured from in situ reflectivity was achieved by the W-Si:H:Si 10 period multilayer. The reflectivity of the W-Si:H multilayer turned out to be lower than for the W-Si multilayer. That was not expected considering the higher contrast for the W-Si:H system and the absence of intermixing at the interface compared to the W-Si system. This was ascribed to a high roughness at a small lateral scale caused by the growth of small W islands as observed by TEM. For the W-Si:H:Si system at least intermixing for the 0.3 nm Si interlayer could be expected. Nevertheless this increased intermixing appeared to be compensated by a lower roughness at a lateral large scale.

5.5. Implantation of carbon to improve the thermal stability of the Mo-Si system

The reflective coatings of EUV lithography optics must be demonstrated to simultaneously show constant and high reflectivity, appropriate layer thickness profiles of the multilayer period, and extreme stability. The dependency of these properties on time, temperature and exposure to EUV radiation must remain within very tight specifications (typically within 0.05%). High reflectance of the multilayer, comprising more than 60 layer pairs, is crucial because of the strong dependence of the throughput of the optical system on the number of multilayer-coated surfaces [23,24]. For the past fifteen years the reflectance of Mo/Si multilayers has therefore been optimised via

extensive studies of their structural dependence on the deposition conditions and post-deposition treatments. At specialised facilities, near-normal incidence reflectivity values above 69% are nowadays routinely achieved at wavelengths around 13.5 nm [25,26].

A well-known problem of Mo/Si multilayers is that characteristics like reflectivity and multilayer period deteriorate under high loads of photons or particles or when the mirror is exposed to elevated temperatures [27,28]. The mechanisms behind these changes are diverse, but the most prominent are compound formation, compaction of the silicon layers and intermixing of the two materials at the interfaces between Mo and Si. Since a high reflectivity of the multilayer is so critical, a fundamental approach of mitigation of these effects needs to be found. The aim is to find a material combination of Mo, Si and additional elements that show an increased thermal stability of the multilayer reflectivity and period up to 430K where the deterioration effects are known to start. Future investigation has to show if this method provides enough thermal stability for practical applications.

Alink et al [29] investigated the possibility to stabilize the Mo/Si system by post deposition implanting of the Si layer by CH_x^+ ions. The motivation for using carbon is based on its optical properties at a wavelength of 13.5 nm, which are close to those of silicon so that its use should not reduce the reflectivity too much. The feasibility of stabilizing Mo/Si multilayers by regular deposition of thin carbon layers between Mo and Si has been shown previously [25,30]. The thickness of such carbon layers must be large enough to act as a diffusion barrier, but still remain as small as possible to prevent a significant reduction of the multilayer reflectivity.

The experiments started with the study of the growth behaviour of single Si layers and the results of implantation. The base pressure of the vacuum system used for these experiments was below 10^{-9} mbar and approximately 2×10^{-9} mbar during deposition. A Kaufman broad beam ion source mounted under an incident angle of 45° with the substrate surface was available. Methane was used as a source for CH_x^+ ions. To obtain a stable ion beam discharge, neon was added and the gas mixture, consisting of 50% methane/50% neon, was fed to the Kaufman source. To prevent charging of the substrates, the ion beam was neutralised by intermixing with electrons emitted from a separate

filament. In-situ soft x-ray reflectometry with C-K radiation (λ = 4.47 nm) was used to monitor the layer thickness during deposition as well as during treatment with ions. A description of the monitoring process is given in ref. [31]. In-situ Auger Electron Spectroscopy (AES) was used to determine the surface composition of the deposited layers. AES was especially useful as from the position of the C KLL peak the formation of silicon carbide can unambiguously be distinguished from pure silicon [32].

Another deposition chamber, with a base pressure of 10^{-8} mbar and a working pressure of 10^{-7} mbar, was used for the deposition of full stack multilayers. The in-situ reflectometer was set at an incident angle of 23.5^{o} to obtain a multilayer periodicity of 6.3 nm. A quartz crystal was used to monitor the deposition rate. The deposition rates of Mo and Si were respectively 0.06 nm/s and 0.03 nm/s. During deposition, the substrate temperature was approximately T = 300 K.
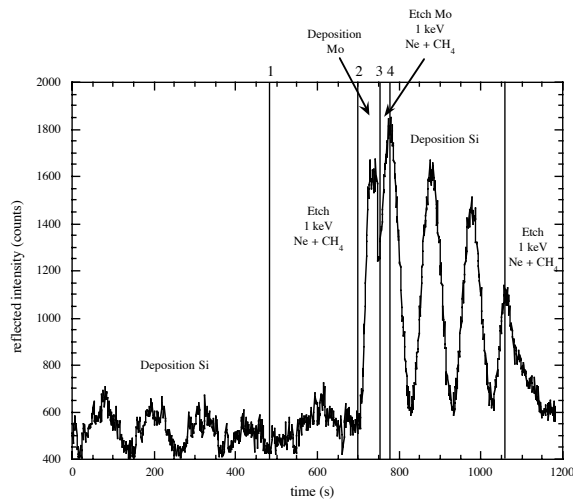

Figure 28. Reflected intensity of C-K radiation during Si and Mo deposition, and during ion treatment of Mo and Si surfaces. The numbers 1 to 4 indicate the moments Auger spectra were recorded. The reflectivity is highest at position 4, indicating a smoothing of the multilayer by the etching of the methane/neon mixture.
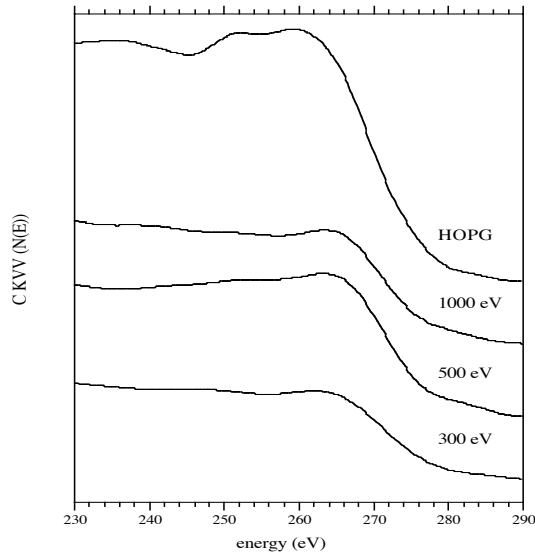
Figure 29. Comparison of the C *KLL* Auger spectra (N(E)) for Highly Oriented Pyrolitic Graphite (HOPG) and for Si implanted with CH_x^+ ions of 300, 500 and 1000 eV. The matching of the Auger peak position indicates the presence of carbon after methane etching.

The temperature stability was tested by annealing of the multilayers in a vacuum furnace at 2×10^{-8} mbar. Grazing incidence x-ray reflectometry with Cu-Kα radiation ($\lambda = 0.154$ nm) was applied to determine the multilayer period before and after annealing.

First, the effect of CH_x^+ / Ne^+ bombardment of single Si and Mo layers was investigated. Ion energies have been varied up to 1500 eV during bombardment. As an example Figure 28 shows the reflected intensity during deposition and subsequent etching. The experiment started with the deposition of ≈ 12 nm Si, represented by 4 interference periods in Figure 28. In this case the Si layer was implanted by 1 keV CH_x^+ / Ne^+
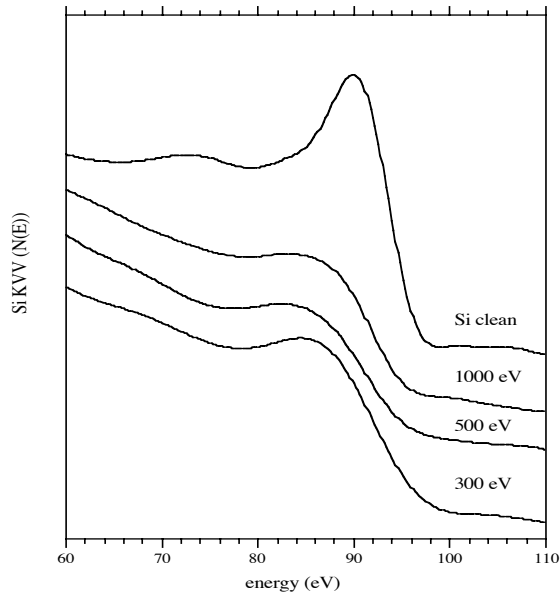
Figure 30. Comparison of the Si *KVV* Auger spectra (N(E)) for pure Si and for Si implanted with CH_x^+ ions of 300, 500 and 1000 eV. The change of the Auger peak recorded on the silicon sample after methane etching indicates the presence of carbon.

ions from the Kaufman source. The reappearance of a reflection peak during the implantation process (600 s) shows that Si is being removed. Moreover, the increased height of the interference maximum during etching (compare peaks before and after etching, i.e. at 425 and 600 s) is a sign of a decrease of the roughness of the top surface. Subsequently, 2.9 nm of Mo was deposited. The Mo layer was then bombarded with 1 keV CH_x^+/Ne^+ ions (between position 3 and 4 in Figure 28). The increase in peak reflectivity after etching of Mo again indicates smoothing of the top surface. This process was followed by the deposition of 12 nm of Si. The large decrease of the peak intensities during the Si deposition suggests that Si roughens significantly when grown on top of the treated Mo layer. The procedure of etching and

simultaneous implantation of CH_x^+ ions was also studied for higher and lower ion energies. Implantation at all energies showed a significant increase of the Si roughness when grown on top of a treated Mo layer. To investigate the results of the CH_x^+ ion implantation, the Auger spectra taken at positions 1, 2, 3 and 4 of Figure 28 have been systematically analysed. Figure 29 shows the Auger C *KLL* spectrum after CH_x^+ ion implantation of Si (position 2 in Figure 28), and a reference Auger C KLL spectrum taken on Highly Oriented Pyrolitic Graphite (HOPG). This confirms the presence of carbon at the silicon surface after ion treatment. From a comparison of the positions of these C *KLL* spectra and the reference spectrum we conclude that there is no indication of the formation of pure graphite. The Si *LVV* spectra recorded for pure Si (position 1 in Figure 28) and those after treatment with Ne^+ / CH_x^+ ions (position 2 in Figure 28) are shown in Figure 30. A comparison of the peak positions reveals that bombardment with 500 eV ions results in a shift of the Si *LVV* peak position from 90 eV to about 84.5 eV, while a shift down to about 83 eV can be observed for bombardment using higher ion energies. We ascribe this shift to the formation of silicon carbide at the silicon surface [33]. The cause of such a shift is the difference in the valance band density of states with regard to p-states near the valance band edge in carbon [34]. Figure 31 compares the extended Auger spectrum including the Mo *LMM* peaks before and after bombardment with 1 keV ions. The appearance of a C *KLL* spectrum with a characteristic peak at 268 eV (position 4 in Figure 28) demonstrates the presence of carbon after etching Mo with the ion mixture. No shifts of he Mo *LMM* peaks could be observed. Also from the C *KLL* part of the spectrum the formation of carbide is not evident. Although successful deposition of carbon on both Mo and Si was demonstrated, the increased surface roughness of Si grown on top of an ion treated Mo surface is considered unacceptable for full stack multilayer depositions. As a result, for the multilayers that were prepared for the thermal stability studies, only the Si surface was treated with CH_x^+ ions. To investigate the multilayer stability after CH_x^+ ion implantation in more realistic Mo/Si multilayer systems, several multilayers were prepared, using the second deposition chamber. All multilayers consist of a 20 period Mo/Si stack with 6.3 nm d spacing. Two multilayers, to be used as references, were deposited without CH_x^+

ion implantation. To smoothen the interfaces for one of these multilayers Si was etched with Kr^+ ions [35], while for the other sample Ne^+ ions were used. All other multilayers were prepared using the Ne^+/CH_x^+ etching procedure for Si, with ion energies up to 1.5 keV. Figure 32 shows a detail of the in-situ
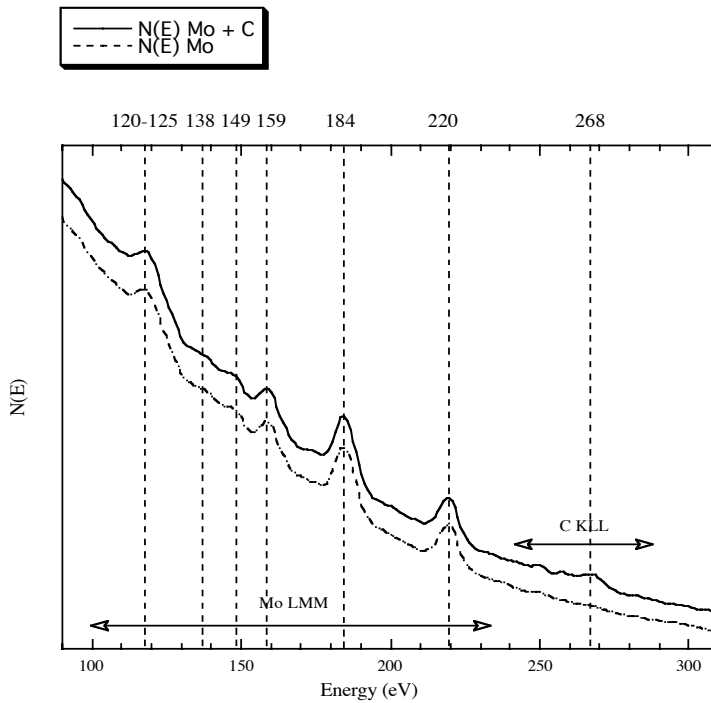

Figure 31. Comparison of the Mo *LMM* Auger spectra (N(E)) before (a.) and after (b.) implantation with 1 keV CH_x^+ ions. Note the appearance of the C *KLL* peak at 268 eV after implantation, showing the presence of carbon after methane etching. The dashed lines indicate the energies of the peaks of both spectra.
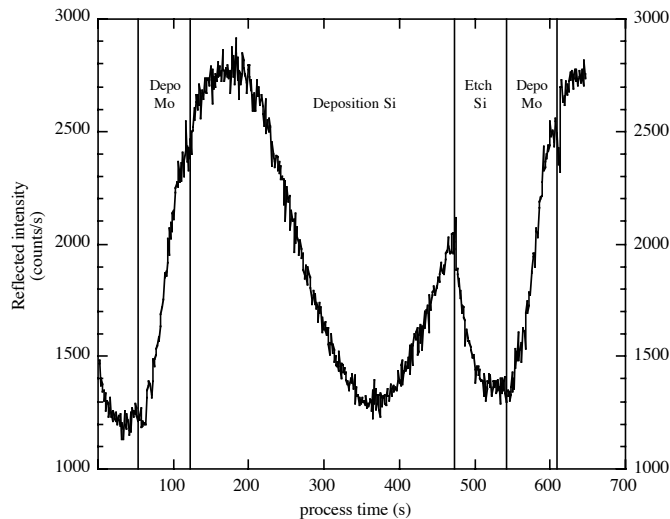
Figure 32. Detail of the intensity of the reflected C-K radiation during deposition of one period of a 20 period Mo/Si multilayer. An excess of a quarter of a period of Si was removed using 500 eV Ne^+ and CH_x^+ ions.

reflectometry signal during the multilayer deposition. For each Si layer, an excess of a quarter period is removed by bombardment with energetic Ne^+/CH_x^+ ions to an interference minimum. This is followed by the deposition of Mo until the interference maximum is reached. The total reflectivity of the multilayer that was treated by the 500 eV Ne^+/CH_x^+ ions was comparable with the reflectivity of the two reference multilayers. Higher Ne^+/CH_x^+ ion energies resulted in lower reflectivity. This is ascribed to ion induced intermixing at the Si-on-Mo interfaces. Both the reference multilayer etched with 500 eV Ne^+ ions and the multilayer which was prepared using 500 eV Ne^+/CH_x^+ ions have been annealed up to temperatures of 430 K to study the thermal stability. The annealing was done for 8 hours in an ultra high vacuum furnace.

Figure 33 and Figure 34 show Cu-Kα grazing incidence x-ray reflectivity scans for both multilayer systems, before and after annealing. After annealing the reference multilayer, a shift of the Bragg peaks is clearly observed (Figure 34). This shift corresponds to a change

Figure 33. Grazing incidence x-ray reflections from a Mo/Si multilayer before and after annealing at 430 K for 8 hours. The surfaces of all Si layers were treated with 300 eV Kr^+ ions for smoothening. The shift of the Bragg peaks are caused by a contraction of the multilayer period on annealing.

of the multilayer period from 6.59 nm before annealing to 6.55 nm after annealing, corresponding to 0.6 ±0.15%. This reduction of the multilayer period is a phenomenon that has been described in literature [3, 4] and is commonly perceived to be caused by both the formation of enlarged silicide interlayers and the contraction of the silicon layer due to annihilation of voids. In the case of the CH_x^+ implanted multilayer, annealing does not result in a change of the position of the Bragg peaks in the reflection spectrum within the measurement accuracy, as shown in Figure 34. A detailed analysis of the relative height of the Bragg peaks in the reflection curves does show a small difference before and

after annealing. Such a redistribution of peak heights is expected to be caused by the change in the composition of the periods following annealing [36].

Moreover, these results also suggest that treatment of the silicon layer with a mixture of 500 eV Ne^+ / CH_x^+ ions stabilizes both interfaces of Si with Mo by CH_x^+ implantation. This can be explained by a conversion of most of the Si layer into carbide. without causing damage to the Si on Mo interface. It cannot be excluded that no carbide is formed at the Si
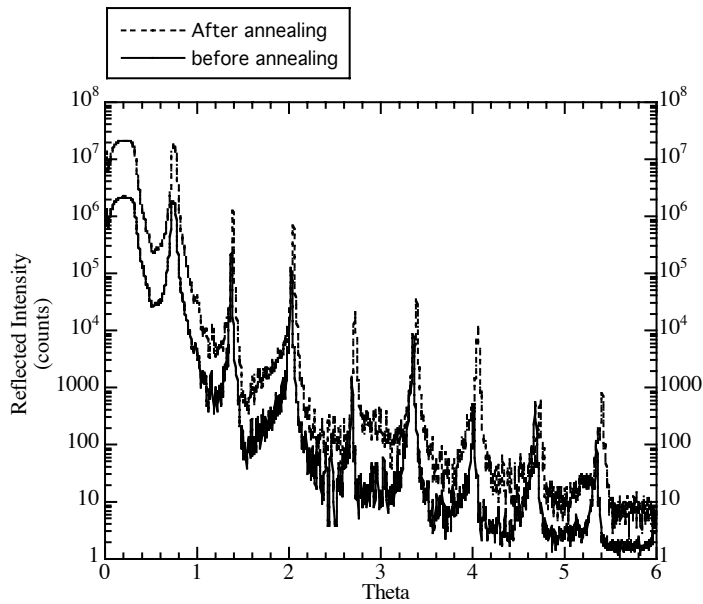

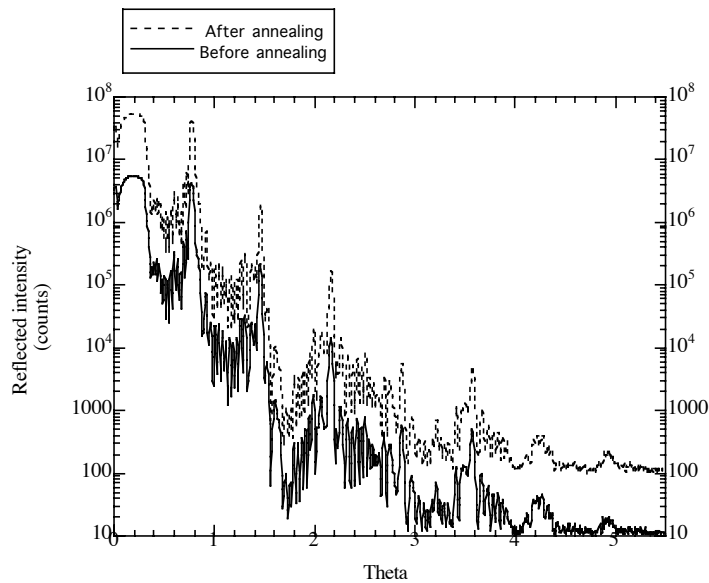Figure 34. Grazing incidence x-ray reflections from a Mo/Si multilayer before and after annealing at 430 K for 8 hours. The surfaces of all Si layers were treated with a mixture of Ne^+ and CH_x^+ ions for smoothening and implanting carbon.

on Mo interface, but the intrinsic temperature stability for this interface should then be significantly higher than that for Mo on Si to explain a thermally stable multilayer.

TRIM [37] calculations were conducted for 500 eV and for 1000 eV C^+ ions impinging (incident angle 45°) on a double layer consisting of 3 nm Si on top of 3 nm Mo. Although, according to these calculations, 500 eV C^+ ions penetrate deep into the Mo layer, these ions have already lost most of their energy before reaching the Si/Mo interface. For 1000 eV C^+ ions however, the simulations do show a considerable energy transfer at the interface. This suggests ion induced intermixing of Mo and Si may play an important role at high ion energies.

The presence of loosely bound hydrogen after implanting Si with CH_x^+ ions is not very probable, because annealing would have driven out the hydrogen. This would also result in a contraction of the Si layers [18], an effect that is not observed. The presence of carbon in some other phase cannot be excluded. It should be mentioned that for a wavelength of 13.5 nm the real part n of the complex refractive index of silicon carbide matches that of silicon, so that the use of silicon carbide does not compromise the optical contrast with molybdenum. However, the conversion of the full silicon layer into silicon carbide would result in a threefold increase of the absorption component k of this layer and therefore compromise the reflectivity.

5.6. Intermixing and implantation

Water is highly transparent for radiation in the wavelength region from 2.4 – 4.4 nm. However, absorption by carbon with its K edge at 4.4 nm is high. Below 2.4 nm the K absorption edge of oxygen causes considerable absorption. Microscopy using radiation in this so-called "water window" has the advantage of a high contrast for carbon and is as such applicable in biological research. As Ni and Si have no absorption edges in the water window, these materials form suitable components for multilayers to be applied as optical elements in this wavelength region. However this material combination is highly chemically active and thick intermixed layers (amorphous nickel silicide) at each interface have been observed by Wang et al [38].
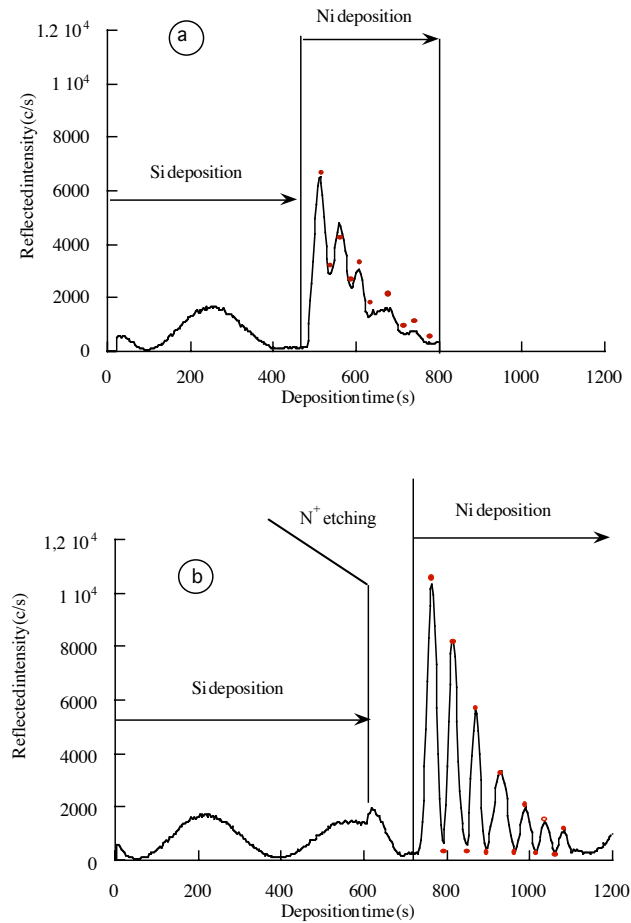
Figure 35. (a) The reflected intensity of C-Kα radiation (35^0 grazing incidence) measured during the growth of 20 nm Ni onto a 4 nm thick silicon layer. The dots represent the extremes of a simulation of the reflected intensity during Ni deposition. According to this simulation a $\approx$ 2-nm-thick silicide layer was formed. (b) The reflected intensity of C-Kα radiation measured during the growth of 28 nm Ni onto a silicon layer previously implanted by 300 eV N$^+$ ions. According to simulations (dots representing the interference extremes) only an intermixed layer of < 0.3 nm was formed.

Cilia et al [39] reduced the chemical reactivity by combining silicon nitride and nickel silicide as multilayer components. Therefore they investigated the formation of silicon nitride by implantation of low energy N[+] ions into Si. This procedure is known to lead to the formation of a stoichiometric silicon nitride (Si_3N_4) film, shown to be a good barrier against silicide formation [40,41]. Ion beam mixing was applied to produce a controlled nickel silicide layer [42,43]. E-beam evaporation was used as deposition technique. The deposition, implantation and intermixing processes were controlled by in situ x-ray reflectometry. In the deposition system Auger Electron Spectroscopy (AES) was available for determination of the surface composition. AES was especially useful as from the position of the Si LVV peak silicon nitride can unambiguously be distinguished from nickel silicide or pure silicon. Pure Si as well as nickel silicide display an Auger LVV peak in the differentiated spectrum at 91 eV [44], while the peak shifts to 84 eV for stoichiometric silicon nitride (Si_3N_4) [45,46].
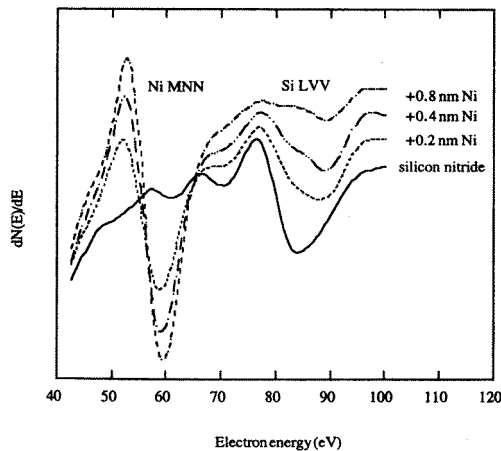

Figure 36. Evolution of the Auger electron spectrum including the Ni (NMM) and Si (LVV) peaks during sequential deposition of 0.2 nm nickel; to a total thickness of 0.8 nm, onto a Si layer implanted by 300 eV N[+] ions.

The experiments started with the growth of single layers Ni on Si, Ni on Si implanted by N^+ ions and Si on Ni. Figure 35a shows the reflected intensity of C $K\alpha$ radiation during deposition of 4 nm Si, followed by 20 nm Ni. A simulation of the evolution of this reflected signal (dots in Figure 35a) could be fitted with the formation of a homogeneous amorphous nickel silicide layer $\approx$ 2nm thick, with a density of 8.2 g/cm^3 and a composition close to Ni_2Si. This value is in relatively good agreement with those reported by Holloway et al [47]. An increasing surface roughness from 0.3 to 0.7 nm for the full thickness also had to be included in the simulation. Figure 35b represents the growth of 6 nm Si followed by bombardment with 300 eV N^+ ions/cm^2. During this process 2 nm of the Si layer was removed. From the initial increase of the reflected intensity after starting the N^+ etch procedure, a reduction of the surface roughness can be observed as an additional effect. A layer of 28 nm Ni was subsequently deposited on this by nitrogen treated Si. The evolution of the reflected signal fits with an intermixed layer of < 0.3 nm. However, this simulation indicated a similar surface roughness evolution like that for Ni deposition on pure Si, resulting in a final roughness (σ) of 1.2 nm for the full layer thickness. Figure 36 shows the evolution of the differentiated Auger spectra measured during sequential deposition of Ni on top of Si treated by N^+ ions. The initial surface shows clearly a single peak at 84 eV, confirming the formation of nitride. After deposition of 0.2 and 0.4 nm Ni, the appearance of a 91 eV peak can be observed. This confirmed the formation of a thin silicide interlayer after deposition of Ni on the nitrided Si layer. However, the interface between stoichiometric Si_3N_4 and Ni has been demonstrated to be stable up to 1370 K [48,40]. From this it could be concluded that the process of N^+ implantation had not resulted in a stoichiometric nitride. Similar experiments on the growth of Si on Ni revealed the formation of a silicide interlayer not thicker than 0.5 nm. This contradicts the observation of a symmetric silicide formation at the Ni-Si interface from Holloway et al [47]. Similarly as observed for the growth of Si on Mo [31] the surface roughness only increased to $\sigma = 0.3$ nm for 160 nm layer thickness.

The next problem to be solved was the interaction of N^+ ions with the interface of Si and Ni underneath. To that purpose an AES depth profile was made using N^+ as well as Ne^+ ions, having roughly the same
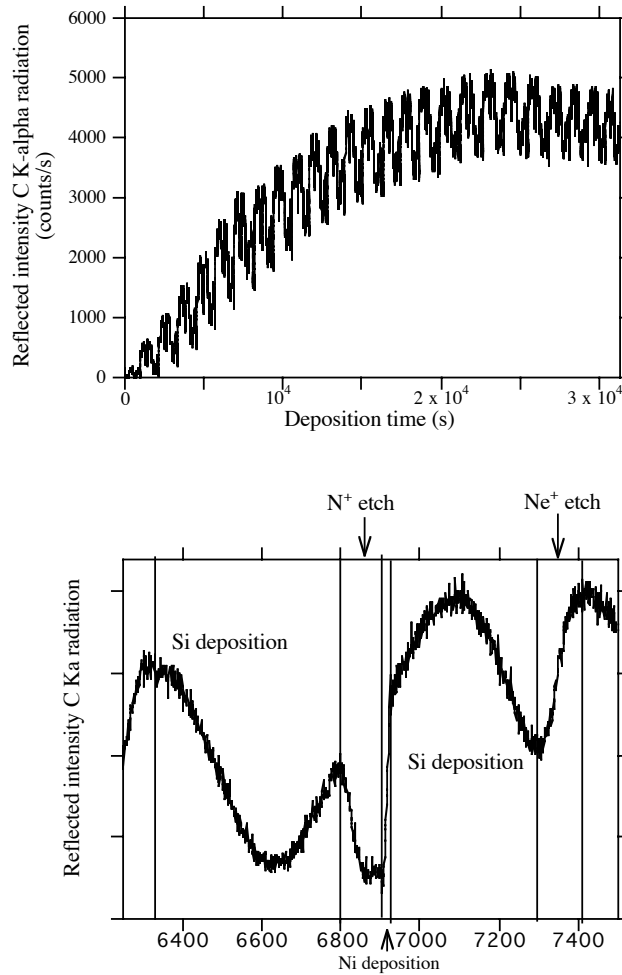
Figure 37. (a) The reflected intensity of C-Kα radiation measured during deposition of a Ni-Si based multilayer (periodicity 4 nm, 25 periods). (b) Detail of the deposition process. A period is started by the deposition of 3 nm Si, followed by removing 1 nm by 300 eV N+ ions. The process was continued by the deposition of 1 nm Ni, followed by ≈ 2nm Si. At the end of the period 1 nm of Si was removed by 300 eV Ne ions.

95
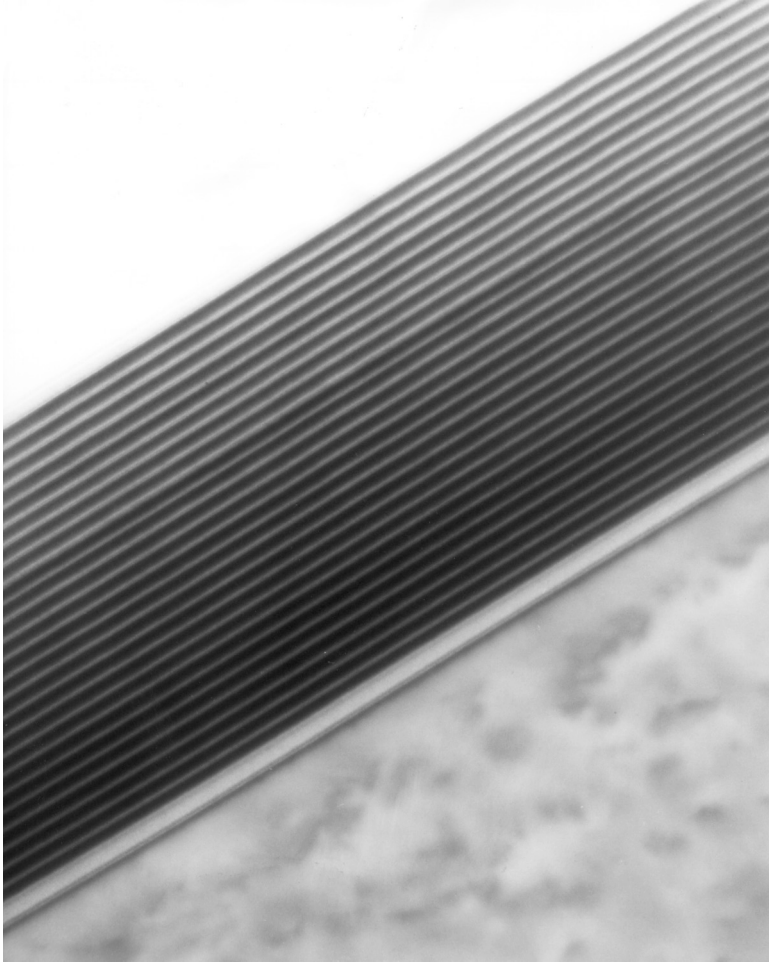
Figure 38. Cross-section TEM photograph of the nickel silicide – nitrided silicon multilayer structure (25 periods of 4 nm).

penetration depth. From these experiments it was learned that while N^+ bombardment did not cause an increase of the thickness of the previously formed silicide interlayer, considerable intermixing was induced by Ne^+ bombardment, as demonstrated previously by others [42]. These observations gave rise to a novel design based on ion implantation and ion beam mixing to form a multilayer system composed of nitride as a spacer and silicide as the scattering component.

The deposition process was monitored by x-ray reflection and is shown in Figure 37 (a total deposition process and b one period in detail). Silicon nitride was formed by growing 3 nm Si, followed by a removal of 1 nm by 300 eV N^+ ions ending up in a reflection minimum related to destructive interference. The next step was the deposition of a layer pair of 1 nm Ni and 2 nm Si on top. From the Si over layer 1 nm was removed by 300 eV Ne^+ ions ending up in a reflection maximum related to constructive interference, to produce a silicide layer. A cross section TEM image (Figure 38) revealed smooth interlayers between the components. Electron diffraction showed an amorphous structure for all multilayer components. Elastic Recoil Detection (ERD) revealed a composition of Si_2N for the spacer instead of Si_3N_4. However, application of Si_2N in combination with Ni_2Si to simulate the evaluation of the reflected signal during the deposition process still was not satisfactory. It became clear that a better fit could be achieved from NiSi than the stoichiometric Ni_2Si composition.

The main disadvantage of using nitrogen in a multilayer to be applied in the "water window" is the introduction of an absorption edge at 3.16 nm. Depending on the nitrogen content, absorption limits the application of such a multilayer system to a wavelength region > 3.16 nm.

5.7. Conclusions

In this chapter it is demonstrated that energetic ions can be used to modify mechanical and optical properties and to improve the thermal stability of multilayer systems. Energetic ion bombardment of Mo results in a release of stress in a Mo-Si multilayer system. Energetic

ions can be applied to form mixed layers of which the thickness is determined by the penetration depth of the ions, which is controlled by the choice of ion mass and energy. For the Mo-Si system the application of this technique results in a stack of Si and homogeneously mixed Mo_xSi_y layers ($x/y \approx 5/3$) with smooth interfaces ($\sigma \approx 0.4$ nm). Application of the same process to the W-Si system resulted in a graded density profile on the W-on-Si interface. The difference can be explained by the heat of compound formation.

Implantation of H into Si of a Mo-Si system has successfully been applied to decrease the atomic density and hence to improve the optical contrast. Saturation to a minimum atomic density of $\approx 64\%$ of the crystalline value was found. W was observed to grow as islands on H implanted Si. As a result, in spite of an improved contrast the optical performance of the W-SiH system turned out to be lower than for the W-Si system. An improvement was achieved by including an interlayer of ≈ 0.3 nm Si in between SiH and W.

Implantation of CH_x^+ ions was applied to improve the thermal stability of e-beam deposited Mo-Si multilayers. While the d-spacing of standard Mo-Si multilayers change by more than 1% upon annealing at 430^0C during 8 hours, no change could be observed for a system of which Si was implanted by CH_x^+ ions.

It was demonstrated that a combination of low energy nitrogen ion implantation and neon ion beam mixing is a promising technique to be applied in the production of a nickel-silicon based multilayer system with a periodicity of 4 nm. Additional interface roughness reduction due to sputtering during these processes has been observed. The composition of the components deviate from the expected stoichiometry.

References

1) D.L. Windt, W.L.Brown, C.A. Volkert and W.K. Waskiewicz, J. Appl. Physics, 78, 2423 (1995)
2) K. Murakami, T. Oshino, H. Kinoshita, T. Watanabe, M. Niibe, M. Ito, H. Oizumi and H. Yamanashi, Jpn. J. Appl. Phys., 37, 6750 (1998)

3) Masayuki Shiraishi, Wakana Ishiyama, Tetsuya Soshino and Katsuhiko Murakami, Proceedings SPIE, 3997, 620 (2000)

4) J. Verhoeven, A. Keppel, R. Schlatmann, Y. Xue and I.V. Katerdjiev, Nucl. Instr. Methods, B94, 395 (1994)

5] J.M.E. Harper, S. Berg, C. Nender, I.V. Katardjiev and S. Motakef, J. Vac. Sci. Technol., 10, 1765 (1992)

6) S. Berg, A.M. Barklund, C. Nender, I.V. Katerdjiev and H. Barankova, Surface and Coating technology 54-55, 131 (1992)

7) R. Schlatmann, A. Keppel, S. Bultman, T. Weber and J. Verhoeven, Appl. Phys. Lett., 68, 2948 (1996)

8) O.B. Loopstra, W.G. Sloof, Th.H. de Keijser, E. Mittemeijer, S. Radelaar, A.E.T. Kuiper and R.A.M. Wolters, J. Appl. Phys., 63, 4960 (1988)

9) J.F. Ziegler, J.P. Biersack and U. Littmark, The Stopping and Range of Ions in Solids (Pergamon, New York 1985)

10) V.V. Kondratenko, Yu.P. Pershin, I.V. Kozhevnikov, S.I. Sagitov, V.A. Chirkov, V.E. Levashov and A.V. Vinogradov, Appl. Opt., 32, 1811 (1993)

11) U. Kleineberg, H.-J. Stock, A. Kloidt, B. Schmiedeskamp, U. Heinzmann, S. Hopfe and R. Scholz, Phy. Status Solidi, A145, 539 (1994)

12) M.J.H. Kessels, J. Verhoeven, A. Yakshin, F.D. Tichelaar, F. Bijkerk NIM B Vol 222/3-4 484-490 (2004)

13) M.J.M. Pruppers, (PhD Thesis, University of Utrecht, 1988), chap.4,

14) P. John, I.M. Odeh, M.J.K. Thomas, M.J. Tricker, J.I.B. Wilson, J.B.A. England and D. Newton, J. Phys. C14, 309 (1981),

15) J.F. Sadoc and R. Mosseri, J. Phys., C14I, 189 (1981)

16) J.C. Bean, Appl. Phys. Lett., 36, 59 (1980)

17) R. Schlatman, A. Keppel, Y. Xue, J. Verhoeven and M.J. van der Wiel, Appl. Phys. Lett., 63, 3297 (1993),

18) R. Schlatmann, A. Keppel, J. Verhoeven, C.H.M. Marée and F.H.P.M. Habraken, J. Appl. Phys., 80, 2121 (1996)

19) G. Lucowsky, J. Non-Cryst. Solids, 76, 173 (1985)

20) H. Wagner and W. Beyer, Solid state Commun.,48, 585 (1983)

21) M.J.H. Kessels, J. Verhoeven, F.D. Tichelaar and F. Bijkerk, to be published

22) M. Lohman, F. Klablunde, J. Blasing, P. Veit and T. Drusedau, Thin Solid Films, 342, 127-135 (1999)

23) E. Spiller, "Soft X-ray optics", SPIE, Bellingham (1994) ISBN:0-8194-1655-X

24) D.G. Stearns, R.S. Rosen and S.P. Vernon, Appl. Opt. 32 (1993) 6952-6960.

25) E. Louis, A.E. Yakshin, P.C. Gorts, S. Oestreich, R. Stuik, E.L. Maas, M.J. Kessels, F. Bijkerk, M. Haidl, S. Mullender, M. Mertin, D. Schmitz, F. Scholze, G. Ulm, Proc. SPIE, vol.3997, (2000), p.406-11

26) S. Braun, H.Mai, M. Moss, R. Scholz and A. Leson, Jpn. J. Appl. Phys. Vol. 41 (2002) pp. 4074–4081

27) Z. Jiang, X. Jiang, W. Liu and Z. Wu, J. Appl. Phys. 65 (1989) 196-200.

28) H. Nakajima, H. Fujimori and M. Koiwa, J. Appl. Phys. 63 (1988) 1046-1051.

29) L.G.A.M. Alink, R.W.E. van de Kruijs, E. Louis, F. Bijkerk and J. Verhoeven, to be published

30) H. Takenaka and T. Kawamura, Jounal of Electron Spectroscopy and Related Phenomena 80 (1996) 381.

31) R. Schlatmann, C. Lu, J. Verhoeven, E.J. Puik and M.J. van der Wiel, Appl. Surf. Sci., 78, 147 (1994)

32] V. van Elsbergen, T.U. van Kampen and W. Mönch, Surface Science 365 (1996) 443-452.

33) V. van Elsbergen, T.U. van Kampen and W. Mönch, Surface Science 365 (1996) 443-452.

34) R. Weissmann, W. Schnellhammer, R. Koschatzky and K. Muller, Appl. Phys. 14 (1977) 283-287.

35) E. Louis, H.-J Voorma, N.B. Koster, L. Shmaenok, F. Bijkerk, R. Schlatmann, J. Verhoeven, Yu. Ya. Platonov, G.E. van Dorssen en H.A. Padmore, Microelectronic Engineering 23 (1994) 215-221.

36) E. Spiller, Review Phys. App. 23 (1988) 1687-1700.

37) J.F. Ziegler, J.P. Biersack, http://www.srim.org, 1984-2003, Annapolis, MD.

38) W.H. Wang, H.Y. Bai and W.K. Wang, Mater. Sci. Eng., A179/180, 229 (1994)

39) M. Cilia and J. Verhoeven, J. Appl. Phys., 82, 4137 (1997)

40) F. Weitzer and J.C. Schuster, J. Solid State Chem., 70, 178 (1987),

41) E.H. Andrews, W. Bonfield, C.K.L. Davies and A.J. Markham, J. Mater. Sci.,7, 1003 (1972)

42) B.Y. Tsaur, Z.L. Liau and J.W. Mayer,. Appl. Phys. Lett., 34, 168 (1979)

43) R.S. Averback, L.J. Thompson, J. Moyle and M. Schalit, J. Appl. Phys., 53, 1342 (1982)

44) J.A. Roth and C.R. Crowel, J. Vac. Sci. Technol.,15, 1317 (1978)

45) Ph. Avouris, F. Boszo and R.J. Hamers, J. Vac. Sci. Technol., B5, 1387 (1987)

46) J.A. Taylor, Appl. Surf. Sci.,7, 168 (1981)

47) K. Holloway, R. Sinclair and M. Nathan, J. Vac. Sci. Technol., A7, 1479 (1989)

48) E. Heikinheimo, A. Kodentsov, J. A. van Beek, J.T. Klomp and F.J.J. van Loo, Acta Metall. Mater., 40, 111 (1992),

6 The application of energetic CH_x^+ ions to form a Si/SiC multilayer systems for reflection of radiation between 20 and 80 nm.

Abstract

Implantation of CH_x^+ ions with an energy of 1 keV into Si as well as deposition of Si assisted by bombardment with 500 eV CH_x^+ ions (Ion Beam Assisted Deposition (IBAD)) were applied to form Si/SiC multilayers. For deposition, e-beam evaporation was used, while a Kaufman broad-beam ion source was available for ion bombardment. After deposition of a Si layer and subsequent ion bombardment, Auger Electron Spectroscopy combined with sputter etching was used to achieve a depth profile of the carbon content. As expected a graded mixture of carbon and silicon was observed to an implantation depth that scaled with the ion energy. However, from the shift of the Si LMM Auger peak it became clear that for 500 eV ions carbide was only formed near the surface, while for 1 keV the maximum carbide concentration appeared at a depth of around 2 nm. In order to demonstrate the feasibility of the implantation as well as the IBAD process, multilayers with a periodicity of 10.8 nm were grown. The structures were characterized by $\theta : 2\theta$ Cu Kα reflectometry. As the optical contrast between Si and C can be neglected compared to the contrast between Si and SiC, this technique revealed for both multilayer production processes the formation of a periodic Si/SiC structure. A preliminary fitting procedure with the measured Cu Kα reflectometry curves confirmed that the system produced by implantation with 1 keV ions contains a carbide layer localized within 0.6 nm. In the IBAD deposited system an amount of 25% carbide is distributed over a layer

thickness of ≈ 5nm as a part of a mixture with C and Si. This results in a lower contrast than for the implanted system.

6.1. Introduction

The development of lasers generating higher order light in the wavelength region < 100 nm requires optical elements that can be applied in this wavelength region. The reflection of radiation by solid surfaces decreases considerably below a wavelength of 100 nm, while the absorption increases. A solution is the application of multilayer systems. Reflection by such systems is based on positive interference of radiation reflected by a sequence of interfaces. In first approximation maximum reflection occurs when the well-known Bragg relation $n\lambda=2d\sin\theta$ is satisfied. The applicability of these systems has been demonstrated for reflection of radiation with a wavelength < 20 nm. In order to optimize the reflectivity a proper choice of the multilayer components is required. Especially in the wavelength region from 20 to 100 nm absorption seriously limits the number of interfaces that contributes to the total reflected intensity. According to calculations by IMD software [1], the combination of SiC/Si turned out to be a good choice for the 20-100 nm wavelength range.

Deposition of multilayer systems by e beam evaporation, controlled by x-ray reflectometry has been applied successfully in the past decades [2]. However this technique cannot be applied for SiC, since this material easily dissociates during evaporation. Therefore we investigated two processes to form SiC: implantation of carbon ions and carbon ion beam assisted deposition (IBAD). Formation of multilayers by implantation was achieved by a sequence of deposition of silicon by evaporation and implantation of carbon containing species. This results in a graded carbon content within each period. The implantation profile depends on the ion energy. For IBAD the carbon ion source was periodically switched on and off during deposition of Si by evaporation. This study concerns the efficiency to form SiC due to implantation by CH_x^+ ions and the depth profile. Finally the whole procedure based on implantation as well as IBAD to grow multilayer systems was investigated.

6.2. Experimental

The experiments to investigate carbon depth profiles in a silicon layer after bombardment with 500 eV and 1 keV CH_x^+ ions were done in a UHV system with a base pressure $< 10^{-9}$ mbar. For Si deposition we used e-beam evaporation. A 3 cm Kaufman ion source, mounted in a differentially pumped chamber under an angle of 45^0 with the substrate, was available for etching as well as implantation of the substrate. The changes of the layer thickness during deposition as well as during energetic ion treatment were monitored in real time by interference of C Kα radiation (4.47 nm) reflected under a grazing angle of 35^0[2, 3]. The measured in-situ signal used to determine the layer thickness depends on the interference of reflected radiation at the top layer with radiation reflected at interfaces underneath. Based on the Bragg equation the thickness deposited between two interference maxima is equal to 3.89 nm. From the behaviour of the amplitude of the reflected intensity as a function of layer thickness we could also obtain an impression of the surface roughness [2] of the layer during deposition as well as energetic ion treatment.

We used in-situ Auger Electron Spectroscopy (AES), based on a retarding field electron analyser, to measure the surface composition. As a consequence of a strong variation of the pressure during deposition and the different ion treatments it was not possible to obtain a stable and reproducible electron emission of the cathode. Therefore the application of AES was not reliable enough to determine the quantitative surface composition. However, from the shift in the Si LVV peak position we were able to retrieve chemical changes. The spectra were not differentiated in order to determine this peak position with an accuracy comparable with the energy resolution of the analyser ($< 0.5\%$). Additional qualitative depth profiling was obtained by combining AES and back etching with 500 eV Kr^+ ions. Besides information on the changes in the chemical composition as a function of depth a rough estimate of the penetration depth of carbon could be obtained. The thickness of the layer removed during depth profiling was monitored by interference of C Kα radiation[2].

For complete multilayer systems with 10 periods a different UHV system with a base pressure $< 10^{-8}$ mbar was available. In this system in-situ reflectometry of C Kα radiation under a grazing angle of 25^0 was applied to control the deposition process. Each interference period represents a layer thickness of 5.4 nm. For implantation by CH_x^+ ions as well as for surface smoothing by Kr^+ ions, a 3 cm Kaufman source mounted under an angle of 45^0 with the substrate was used. It turned out that supplying the ion source with pure CH_4 caused instabilities in the ion yield. This could be ascribed to deposition of a non-conducting diamond like carbon (DLC) layer within the source, resulting in a decrease of the ion yield due to charging. Therefore we back filled the ion source with a mixture of 50% CH_4 and 50% Ne for implantation, where the impact of Ne ions prevented the growth of a DLC layer. An X-ray reflectometry system (Philips X'pert) using Cu Kα radiation was available for further optical characterisation of the multilayer.

The reflectivity of multilayer systems as a function of wavelength and materials combination as well as the deposition process under x-ray reflection could be simulated by IMD and Multimul [1,4]

6.3. Results and discussion.

6.3.1. Interaction of Si with CH_x^+ ions

We started to investigate the interaction of 500 eV and 1 keV CH_x/Ne ions with a freshly evaporated Si layer. For the application of multilayers as radiation mirrors, the thickness accuracy of the components of each period should be better than several tenths of a nanometre. The application of in-situ reflectometry during the deposition process enables this accuracy by using the interference extremes to accurately determine the layer thickness. However, while the CH_x part of the mixture is expected to be implanted as C^+ and CH_x^+ ions, forming carbides, hydrides etc, also sputtering cannot be neglected. Also the Ne component contributes to the sputter process.

Therefore compensation for sputter etching is required. Therefore an excess layer of Si has to be deposited to compensate for this thickness decrease. In order to match the implantation fluence with a required extra Si layer thickness, we needed at least a rough estimate of the etch

rate of Si for the before mentioned ion mixture and energies. Therefore in-situ reflectometry experiments by C Kα radiation were conducted to measure the etch rate for the different ion energies, by measuring the decrease of the layer thickness as a function of time [3]. As a result it was found that implantation of Si by a total fluence of 1.5 x 10^{17} CH_x / Ne ions/cm^2 with an energy of 500 eV caused a decrease of the layer thickness by 2 nm. The same amount of Si was removed during
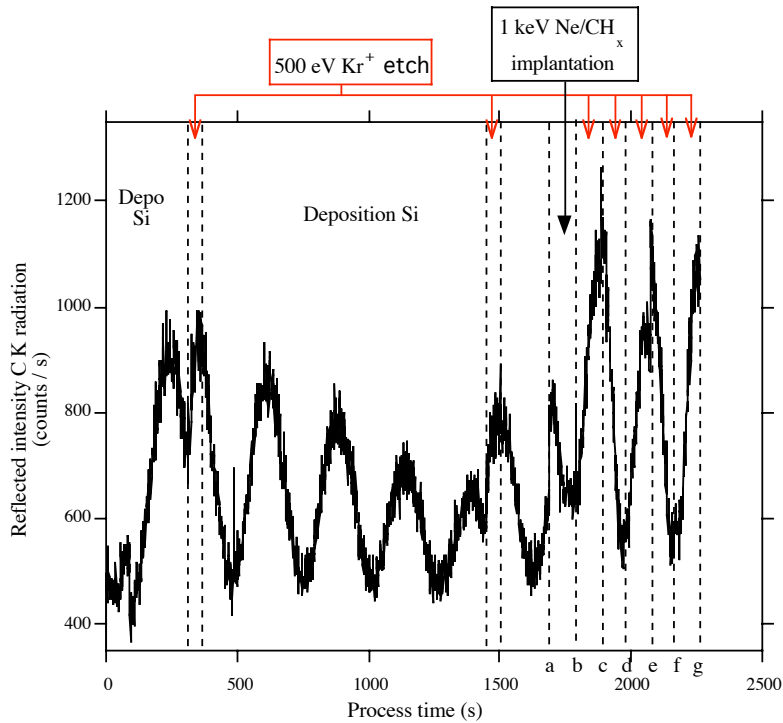
Figure 39 An example of the reflected intensity of C K radiation during a process of Si deposition followed by implantation (1 keV CH$_4$/Ne ions). After implantation a crude depth profile is obtained by combining sputter etching with 500 eV Kr$^+$ ions and Auger Electron Spectroscopy.
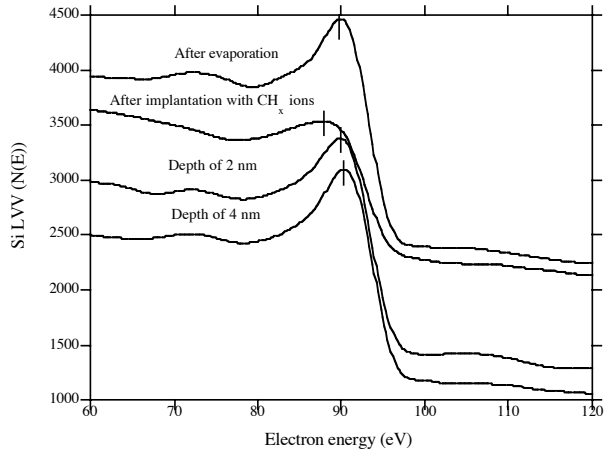
a
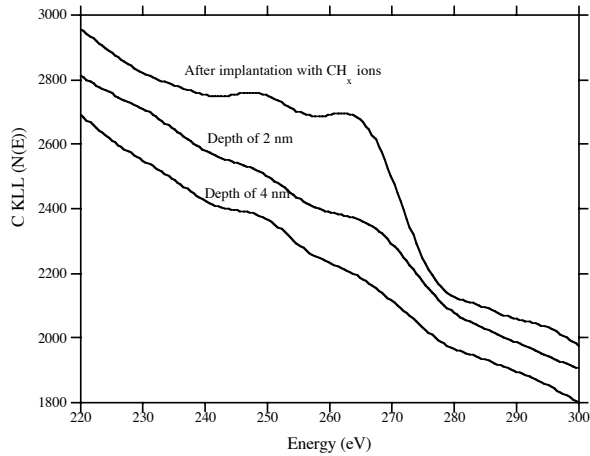
b

Figure 40 a) The Si LVV Auger spectrum for a clean Si layer, after implantation with 500 eV CH_4/Ne ions and after 500 eV Kr^+ etching to a depth of 2 and 4 nm. b) The C KLL Auger spectrum after implantation with 500 eV CH_4/Ne ions and after 500 eV Kr^+ etching to a depth of 2 and 4 nm.

implantation by a fluence of only 1×10^{17} CH$_x$/Ne ions/cm^2 and an energy of 1 keV.

We subsequently investigated the process of the growth of Si layers, ion induced surface smoothing and made depth profiles after bombardment with 1.5×10^{17} CH$_x$/Ne ions. An example of this whole process as monitored by interference of reflected C K radiation is shown in

Figure 39. Five and a quarter interference periods representing a total thickness of 20.4 nm Si was deposited on a silicon wafer having a natural oxide layer on top. The deposition of Si was interrupted twice by a short etch with 500 eV Kr$^+$ ions in order to reduce the surface roughness of the deposited layer. The reduced roughness is clearly demonstrated by an increased reflectivity. At the end of the Si deposition process (position a) the first Si LVV AES spectrum of the clean surface was measured. This was followed by bombardment with 1.5×10^{17} CH$_x$ / Ne ions. Figure 39 represents an example of implantation by1 keV CH$_x$ / Ne ions with a fluence of 5×10^{16}, resulting in a removal of 1/4 period (to an interference minimum = 1 nm, position b). At this position (b) the Si LVV as well as the C KLL Auger spectrum was measured, representing the composition of the top surface after implantation.

A qualitative depth profile was obtained by removing the implanted layer by 500 eV Kr$^+$ ions. After each 2 nm the Auger Si LMM and C KLL peaks were measured (positions c, d, e, f and g). A similar procedure was followed for implantation with 500 eV CH$_x$ / Ne ions and a fluence of 7.5×10^{16}.

6.3.2 Depth profiles after bombardment with 500 eV CH$_x$ / Ne ions

Figure 40 shows these Si LMM and C KLL Auger spectra for different depths after the bombardment with 500 eV CH$_x$ / Ne ions. The highest concentration of carbon can be observed at the surface of the substrate after implantation. We have not been able to deduce from the shape of the C KLL spectrum the chemical phase of carbon. However, a partial transformation into carbide can be held responsible for the shift of the Si LMM peak from 89.9 eV to 87.5 eV when compared with
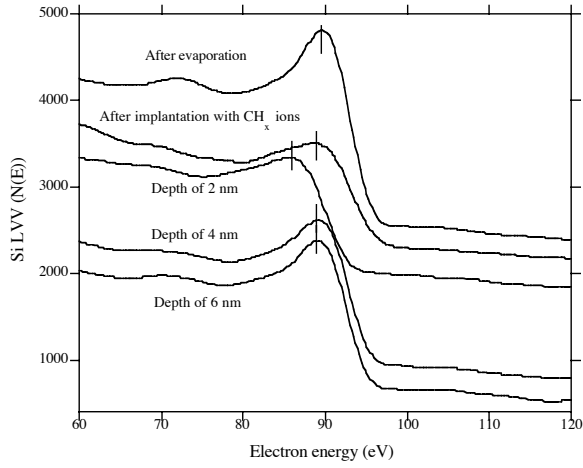
a
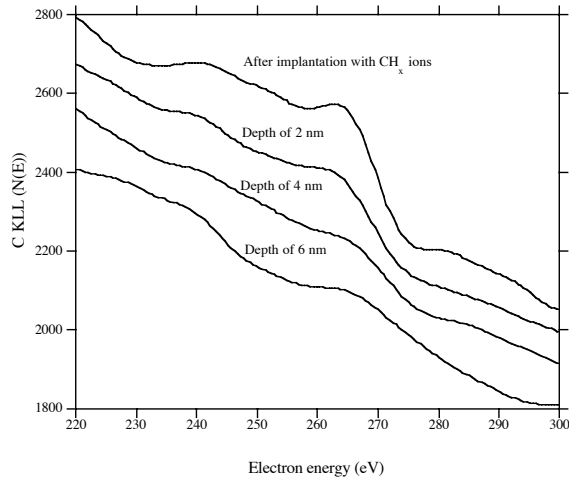
b

Figure 41a) The Si LVV Auger spectrum for a clean Si layer, after implantation with 1 keV CH_4/Ne ions and after 500 eV Kr^+ etching to a depth of 2, 4 and 6 nm. b) The C KLL Auger spectrum after implantation with 1 keV CH_4/Ne ions and after 500 eV Kr^+ etching to a depth of 2, 4 and 6 nm.

freshly evaporated Si. This downward energy shift is a consequence of the difference in the valance band density of states with regard to the p-states near the valance band edge [5]. A shift back of the Si LMM peak to the value of 90.3 eV for crystalline Si can be observed at a penetration depth of 2 nm. The C KLL peak as a function of depth decreases fast and cannot be observed any more at a depth of 6 nm. This leads to the conclusion that, while some carbide formation can be observed at the surface, the residual amount of carbon at larger depth is not present as carbide. According to calculation by SRIM-2003 [6] a 6 nm effective penetration depth can be expected for 500eV C^+ ions into Si. These calculations do not take into account the removal of material by sputtering.

6.3.3 Depth profiles after bombardment with 1 keV CH_x / Ne ions

Figure 41 shows the Si LMM and C KLL Auger spectra as a function of depth after bombardment with 1 keV CH_x/Ne ions. A striking difference with bombardment by 500 eV (Figure 40) is that the position of the Si LMM peak of the substrate surface after bombardment with CH_x/Ne ions has not remarkably shifted to lower energies. A weak shoulder near 85.4 eV might indicate the onset of the formation of carbide. This suggests that only a minor amount of carbon has been transformed into carbide. Most carbon appears to be intermixed into silicon but also the formation of a thin over layer of diamond like carbon cannot be excluded [7,8]. Only at a depth of 2 nm transformation of most silicon into carbide can be deduced from a shift of the whole peak to 85.4 eV. At 4 nm carbon is still present, however the shift of the Si LMM peak to 90.3 eV again suggests that the presence of carbide can be neglected.

In general, the C KLL Auger spectra show that for bombardment with 500 eV as well as 1 keV ions the highest carbon concentration is present at the surface of the Si layer. According to the carbon concentration represented by the C KLL Auger peak in Figure 41b, for 1 keV the penetration depth does not exceed 6 nm. SRIM-2003 [6] confirms an effective penetration depth of 6 nm. However a concentration maximum is expected at a depth of 4 nm. SRIM [6] simulations confirm that an initial C over layer delays implantation into Si underneath due to

capture of C and causes further growth of the over layer. Actually the process is rather complicated as the substrate is bombarded by a mixture of C^+, CH_x^+ and Ne^+ ions at the same time. The C^+, CH_x^+ ions will be implanted and can form silicon carbide as well as a carbon based (graphite, diamond like) over layer [7,8]. The growth rate and the phase of a carbon over layer depend on the energy of the C^+, CH_x^+ ions arriving at the surface[8]. However, a growing carbon over layer is also subject to sputtering during the process. This is mainly caused by Ne^+ ions, having a higher mass than C^+, CH_x^+ ions. Therefore an equilibrium thickness during implantation will depend on the ratio of growth to etch rates of this layer. In which case the etch rates as we measured concern the etch rate of carbon, enhanced by the near vicinity of the interface with the Si containing intermixed layer underneath [9]. When comparing the 500 eV implantation process with the 1 keV process, for increasing ion energy the deposition of the carbon over layer appears to dominate sputter etching. Another process for the formation of carbon within the implanted layer that requires consideration is ion-induced breaking of the SiC bond. Similar effects are not to be neglected for depth profiling where 500 eV Kr^+ ions are used. Bond breaking by energetic ions could be responsible for the disappearance of carbide at a depth of 2 nm after the 500 eV implantation process. However, in that case no carbide should have been observed in the depth profiles for the 1 keV implantation process. Nevertheless, preferential sputtering during depth profiling can be responsible for a decrease in the amount of C as a function of depth.

6.4. Formation of multilayer systems.

The experiments were continued by the deposition of Si/SiC multilayers with 10 periods of 10.8 nm. Considering the low implantation depth, 500 eV CH_x/Ne^+ ions were only applied for Ion Beam Assisted Deposition (IBAD) of multilayers. Ions of 1 keV ions were used to produce multilayers by implantation. As mentioned before, the surface of a Si layer after a treatment with CH_x/Ne^+ ions may be covered by a thin carbon (or diamond-like carbon) layer. Therefore we compared
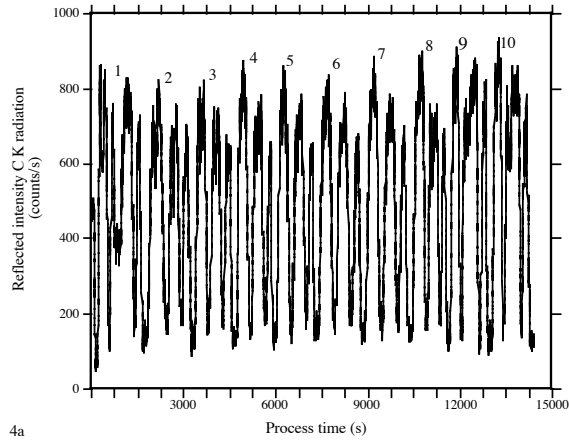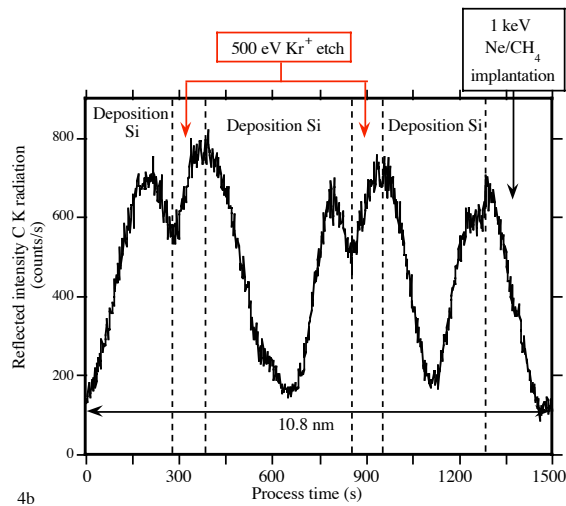
Figure 42 a) The deposition process of a 10.8 nm Si/SiC multilayer produced by implantation with 1keV CH_4/Ne ions, as represented by the reflected intensity of C K radiation. b) A detail of the reflected intensity of C K radiation, representing the deposition of one period. The carbon interlayer formed during implantation was not removed by an etch procedure.

113

Figure 43 a) The deposition process of a 10.8 nm Si/SiC multilayer produced by implantation with 1 keV CH_4/Ne ions, as represented by the reflected intensity of C K radiation. b) A detail of the reflected intensity of C K radiation, representing the deposition of one period. The carbon interlayer formed during implantation was removed by a short etch of 500 eV Kr^+ ions.

depositions where this presumed carbon over layer was removed by a short 500 eV Kr^+ etch with depositions without that extra treatment. Silicon wafers with a natural oxide layer on top were used as substrates.

6.4.1. Multilayers formed by implantation

The deposition process as monitored by in-situ reflectometry by C K radiation of a SiC/Si multilayer of 10,8 nm based on implantation with 1 keV ions is shown in Figure 42a, with the details of the deposition of one period in Figure 42b. Si was deposited with constant rate of $\approx$ 0,04 nm/sec. Within one period the deposition was interrupted twice after each interference maximum in order to smooth the Si surface by an etch procedure with 500eV Kr^+ ions. The smoothing effect can clearly be observed from an increase of the interference maximum. After deposition of 13.5 nm Si (2 interference periods + 2.7 nm) the implantation process with 1 keV CH_x/Ne^+ ions was started. This was accompanied by etching and the implantation process was stopped after removing 2.7 nm, indicated by the foregoing interference minimum. For implantation a total fluence of 1.35 x 10^{17} ions/cm^2 was used.

A simulation of the reflectometry curves representing the deposition process was made by IMD [1] as well as Multimul [4]. It should be emphasized that both programs cannot accurately simulate a graded density within the periods. The deposition process of a Si/SiC multilayer monitored by reflectometry using C K radiation should be represented by a gradual decrease of the interference period amplitudes. A simulation that corresponds qualitatively the closest to the more or less constant interference periods in real reflectometry curves of Figure 42a suggests a carbon interlayer with a thickness of only $\approx$ 0.2 nm.

Simulations for different layer thicknesses of SiC could not be properly distinguished from each other. It was therefore not possible to obtain any reliable information about the SiC layer thicknesses.

6.4.2 Multilayers formed by implantation and etching of the implanted layers.

The deposition process including the short 500eV Kr^+ etch after each implantation, in order to remove the thin carbon over layer that was formed on the Si surface during implanting is shown in Figure 43.

Figure 44 a) The deposition process of a 10.8 nm Si/SiC multilayer produced by Si deposition assisted by bombardment of 500 eV CH_4/Ne ions, as represented by the reflected intensity of C K radiation. b) A detail of the reflected intensity of C K radiation, representing the deposition of one period. The carbon interlayer formed during implantation was not removed by an etch procedure.
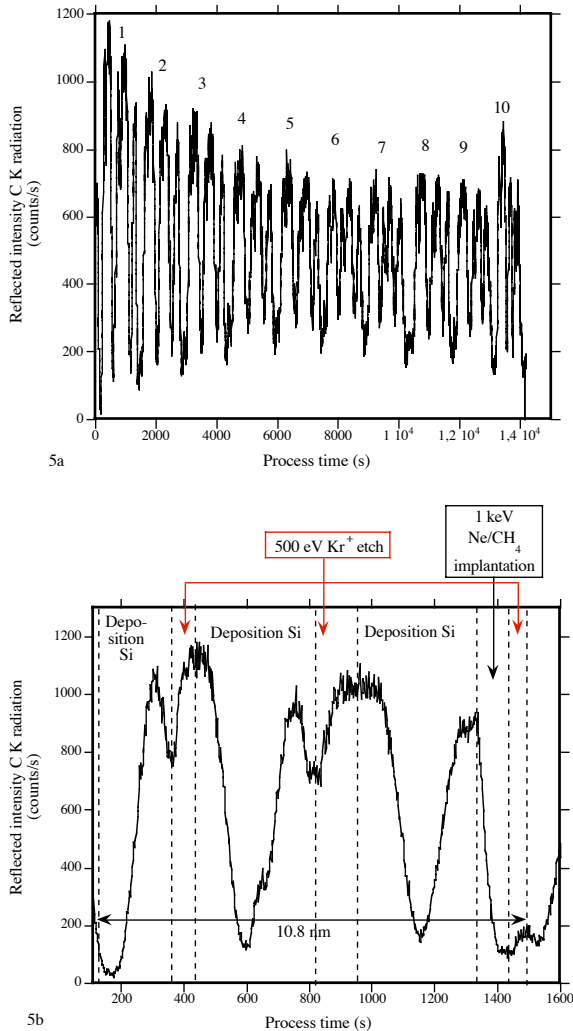
116

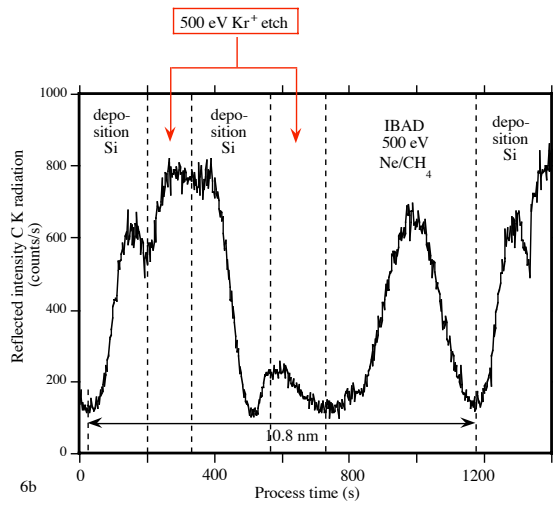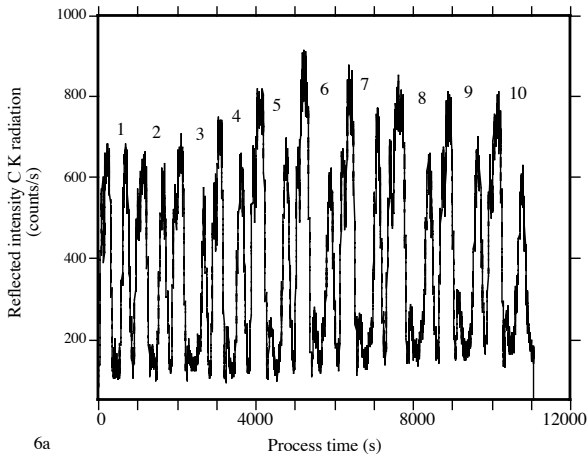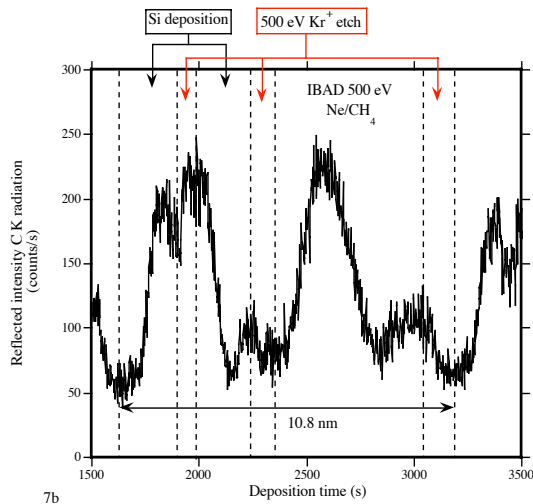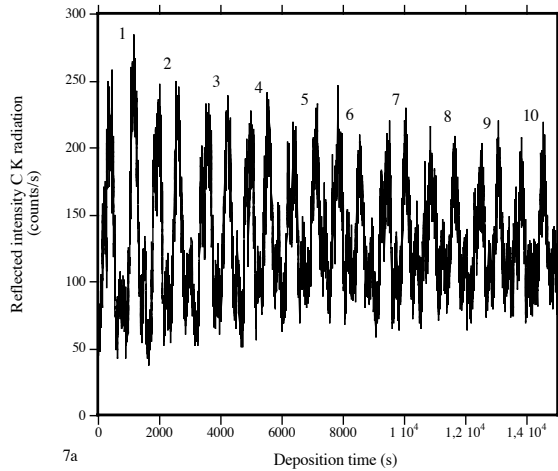Figure 45 a) The deposition process of a 10.8 nm Si/SiC multilayer produced by Si deposition assisted by bombardment of 500 eV CH_4/Ne ions, as represented by the reflected intensity of C K radiation, b) A detail of the reflected intensity of C K radiation, representing the deposition of one period. The carbon interlayer formed during implantation was removed by a short etch of 500 eV Kr^+ ions.

Comparison of the reflectometry curves measured during the deposition process as represented by Figure 42 with the deposition process represented by Figure 43 demonstrates a clear influence of the Kr+ etch procedure. The gradual decrease of the interference period amplitudes during the deposition process as seen in Figure 43a approximates the formation of a SiC/Si multilayer without an extra carbon interlayer. Simulations of these reflectometry curves by IMD [1] as well as Multimul [4] confirmed the absence of the extra carbon interlayer. From these simulations we were not able to information to obtain about the presence of loose carbon as a solution in the layer.

6.4.3 Multilayers formed by IBAD

Figure 44 represents the deposition of a 10.8 nm multilayer using IBAD with 500 eV CH_x/Ne^+ ions. After deposition of $\approx$ 5.4 nm Si, interrupted by a Kr^+ etch procedure at two positions, deposition of the next 5.4 nm Si was continued to a total thickness of 10.8 nm during simultaneous bombardment with CH_x/Ne^+ ions (IBAD). From the reflectometry graph detail (Figure 44b) representing the whole deposition process it can be seen that for IBAD of the subsequent layer of 5.4 nm $\approx$ 400 s is required. During this process a substrate of 4 cm^2 is bombarded by 3.75 x 10^{13} CH_x ions /s cm^2 or a total fluence of 1.5 x 10^{16} CH_x ions /cm^2. The deposition rate of Si as measured by the quartz crystal microbalance was 0.015 nm/s that is an equivalent of 7 x 10^{13} atoms / s cm^2. So the Si atoms and CH_x^+ ions arrive at a ratio of $\approx$ 1.9. The presence of a carbon interlayer can be held responsible for the initial increase of the interference period amplitudes in Figure 44a. A simulation that corresponds qualitatively the closest to the real reflectometry curve of Figure 44 suggests that this interlayer is $\approx$ 0.3 nm thick. Figure 45 represents a similar process where an extra etch procedure with 500 eV Kr^+ ions was applied after IBAD. The decrease of the interference period amplitudes as can be observed in Figure 45 can be explained by the removal of a carbon interlayer.

6.4.4 Characterisation

Finally, we used Cu-Kα reflectometry to further characterise the multilayer systems. As Si and C have a density of respectively 2.3 and 2.2 g / cm^3 and SiC a density of 3.3 g / cm^3, for Cu-Kα radiation the

contrast between a mixture of C and Si with pure Si can be neglected compared to the contrast between SiC and Si. It is therefore not possible to use this technique to distinguish between the processes with and without the Kr^+ post etch to remove a carbon over layer. Figure 46 shows the results for the 1 keV implanted multilayer system (a) and the system prepared by IBAD (b). For both systems an extra Kr^+ ion etch after respectively implantation or IBAD was applied. The appearance of the relatively strong first-order Bragg peaks confirms the formation of a periodic structure containing SiC for both multilayer structures. The appearance of strong higher-order diffraction peaks for the multilayer formed by implantation is an indication of a higher optical contrast compared to the multilayer produced by IBAD. Broadening of the higher order diffraction peaks is an indication of thickness errors. It is therefore not possible to obtain a perfect fit by simulation. However a best fit for the reflectometry curve suggests that each period of the multilayer produced by IBAD contains an about 5 nm thick mixture of SiC, Si and C, with the SiC content in this mixture being about 25%. As the arrival ratio for Si atoms and CH_x^+ ions was $\approx$ 1.9, it can be concluded that half of the arriving CH_x^+ ions was converted into carbide. AES taken at the surface confirms that bombardment of Si with 500 eV CH_x/Ne^+ ions results in a partial carbide formation. According to Figure 44 this intermixed layer extends over a thickness of $\approx$ 5 nm.

A best fit for the reflectometry spectrum of the implanted multilayer suggests that each period contains a pure SiC layer with a thickness of at least 0.6 nm. Depth profiling combined with AES gives additional insight in the structure. As can be seen in Figure 41 implantation by 1 keV CH_x/Ne^+ ions forms a more complete carbide layer at a depth of 2 nm. As at 4 nm no carbide was observed, it could be estimated that the layer that contains carbide is restricted to a total thickness of about 2 nm. Moreover, carbide is not expected to form an interlayer with sharp interfaces and will be present as a graded distribution within $\approx$ 2 nm.
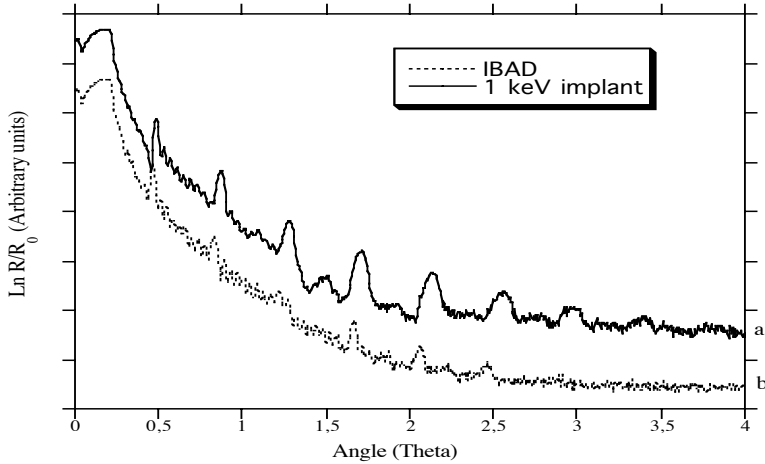
Figure 46 Angular reflectivity scans using Cu-Kα radiation, for a) a 10-period multilayer deposited by implantation with 1keV CH_4/Ne ions; b) a 10-period multilayer deposited by IBAD with 500 eV CH_4/Ne ions

Nevertheless, comparing with the reflectometry results from the by IBAD deposited structure a higher contrast suggests a higher and localised SiC content within a layer thickness of ≈ 2 nm. In order to calculate the efficiency for carbide formation we assume a localised pure carbide layer with an as determined thickness of 0.6 nm. This corresponds to 4.5 x 10^{15} molecules in that 0.6 nm carbide layer. If we neglect sputtering and back scattering and assume that the total fluence of 6.75 x 10^{16} CH_x^+ ions is implanted, the efficiency of transformation of CH_x into SiC is only ≈ 7%. So 93% of carbon is just implanted forming a mixture with Si. The residual 10.2 nm consists of Si mixed to a depth of ≈ 6 nm with C according to a graded concentration profile.

6.5. Conclusions

It has been demonstrated that implantation as well as IBAD using CH_x^+ ions can successfully be applied to produce SiC/Si multilayer systems.

Auger Electron Spectroscopy (AES) combined with depth profiling revealed that implantation of 500 eV CH_x^+ ions into Si results in the formation of a mixture of C, Si and a low concentration of SiC within the first monolayers. At a depth of 2 nm below the surface only a mixture of C and Si is observed. In contrast, for 1 keV implantation the formation of a high concentration SiC layer is observed about 2 nm underneath the surface, while a mixture of Si and C is formed at the surface. Therefore CH_x^+ ions with an energy of 500 eV were used to deposit multilayer systems by IBAD. CH_x^+ ions with an energy of 1 keV were applied to produce multilayer systems by alternate deposition of silicon and implantation. For multilayers deposited by IBAD, Cu-Kα reflectometry revealed the formation of a periodic system of which each period consists of a silicon layer and a mixed layer of SiC, Si and C with a thickness of $\approx$ 5 nm. According to a best fit the SiC content of this layer is $\approx$ 25%. For multilayers produced by implantation with 1 keV CH_x^+ ions, Cu-Kα reflectometry revealed the presence of a layer of $\approx$ 0.6 nm pure SiC. About 7% of the implanted CH_x^+ ions appeared to react with Si to form carbide. While the efficiency for carbide formation is lower for the implantation process than for IBAD, a higher contrast was obtained due to a more localized high concentration of SiC. From the in-situ reflectometry measurements using C K radiation during the deposition process it became clear that after bombardment of Si by CH_x^+ ions, for both energies a carbon interlayer of $\approx$ 0.2 nm was formed. This interlayer could be removed by an extra Kr^+ etch after bombardment with the CH_x^+ ions. The process of the formation of SiC is not well understood and requires further investigation.

References

1) David Windt Computers in Physics 12 (4), 360-370 (1998). (IMD Version 4.1, http://www.bell-labs.com/user/windt/idl)
2) E. Spiller, A. Segmüller, J. Rife and R.-P. Haelbich, Appl. Phys. Lett.,37,1048 (1980)
3) J. Verhoeven, A. Keppel, R. Schlatmann, Y. Xue and I. Katardjiev, Nucl. Instr. Meth. B 94 p. 395 (1994)

4) Written by P. van Loevezijn and R. Schlatmann (AMOLF 1996) based on Fresnel equations for the reflectivity coefficient.

5) R. Weissmann, W. Schnellhammer, R. Koschatzky and K. Muller, Appl. Phys.14, 283 (1977)

6) Ziegler ([SRIM.com]).

7) Yoshikatsu Namba and Toshio Mori, J. Vac. Sci. Technol., A3, 319 (1985)

8) Rajnish Sharma, O.S. Panwar, Sushil Kumar, D. Sarangi, A. Goullet, P.N. Dixit and R. Bhattacharyya, Appl. Surf. Sci., 220, 313-320 (2003)

9) S. Berg, A.M. Barklund, C. Nender, I.V. Katardjiev and H. Barankova, Surface and Coating Technology, 54-55, 131 (1992)

7 Concluding remarks

In the foregoing chapters it has clearly been demonstrated that ions with energies up to 2 keV can successfully be applied to control the roughness of a thin film surface and the formation of an interlayer between components of a multilayer. As discussed in chapter 2, ions striking a material transfer their energy to the near environment of their path, while further penetrating the bulk and end up as implanted. The transferred energy causes displacements, resulting in damage to a crystal structure, destruction of an interface with a material underneath, densification or viscous flow. Viscous flow is an effect that involves a whole layer and is ascribed to stress relaxation [1]. Part of the energy is transferred back to the surface and causes detachment of atoms within a few monolayers from the surface followed by diffusion over the surface or total removal.

For each material one or more of the before mentioned phenomena can be held responsible for ion induced surface smoothing. Smoothing based on detachment of loosely bound adatoms followed by removal combined with diffusion to energetic more stable positions [2, 3] forms a useful model for metal surfaces. However, preferential sputtering of different crystalline orientations will cause an increase of the surface roughness. As metal layers in general start to grow in an amorphous phase and become polycrystalline at a thickness of one or more nanometre, an ion induced smoothing process can only be applied to a limited layer thickness. Furthermore, ion bombardment itself also induces crystallisation, which introduces an extra limitation to the layer thickness for which this process can be applied. It should be emphasised that the minimum roughness that can be achieved after ion-induced smoothing depends strongly on the initial roughness of a layer after deposition and hence the growth mode. It should be noted that the first nanometres do not necessarily grow as a closed layer. Therefore, the development of an ion-induced smoothing process will have to be based

on the growth process for each particular materials combination. The eventual process can be further optimised by deposition and ion induced smoothing at low substrate temperature.

Although ion-induced viscous flow can be held responsible for a decrease of the surface roughness of an amorphous Si layer, also the effects of sputtering and surface diffusion are to be considered. The contribution of these effects can be studied by ion bombardment under a critical grazing angle for which penetration into the bulk can be neglected. As explained in chapter 2, the presence of an interface with a high-mass material underneath will induce an enhanced energy transfer back into the Si layer. Depending on the ion energy, for Si on Mo or W, interface-induced sputtering will be limited to layers with a thickness smaller than $\approx$ 2 nm. However, as viscous flow is a bulk effect, interface-induced effects can be expected to occur for thicker Si layers. It can be concluded that for better understanding of these interface-induced phenomena, more experiments are required.

Interlayers are formed by intermixing, which depends on the chemical reactivity of the layer material with its substrate. Elevated temperatures and impact of energetic radiation will cause an increased intermixing. Therefore the application of any process using energetic ions to reduce the surface roughness is limited by ion-induced intermixing at the interface with the material underneath.

Basically, intermixing can be considered as alloy formation. The well-known Miedema model for alloy formation[4] compares the Gibbs free energy representing the separate components and the alloy. An alloy will be formed if a gain for the total Gibbs free energy can be achieved. However, an initial input of energy to break the chemical bond for each component is required. The stability of e.g. the metal/carbon system can therefore be explained by the high binding energy of carbon. Interlayer formation for the metal/silicon system appears to be too complicated to be described by thermodynamics alone. Even without extra energy input, interlayer formation cannot be prevented. An asymmetry has been observed for interlayer formation for the metal-on-Si interface compared to the Si-on-metal interface. It is also not understood why for the Mo/Si system a homogeneous silicide layer with sharp interfaces was formed by ion beam intermixing, while the same process resulted in an interlayer with a graded metal distribution for the W/Si and Ni/Si

systems. Up to now no model is available that can be used to predict the formation of the interlayers as observed. A model should be considered that is based on thermodynamics in which preferential diffusion is included. Also a Molecular Dynamics approach may in the future provide a deeper understanding. This requires accurate knowledge of interaction potentials.

Although the formation of an interlayer improves the adhesion of a thin film to a substrate, it reduces the reflection of short-wavelength radiation due to diffuse scattering. A solution to achieve a sharp interface is to reduce the chemical reactivity of the components by choosing a more stable alloy for one of the original components. Formation of a stable silicon compound by implantation with H^+, N^+ or CH_x^+ ions has been demonstrated to be a successful technique. A decrease of the chemical interaction between the components will inevitably result in a higher mobility of the first atoms arriving at the surface. This can be the onset for island formation. As a consequence the layer will not be closed initially and will continue to grow with a surface roughness determined by the dimensions of the initial islands. This was clearly observed for W on Si, compared to W on H-implanted Si. Although this was not observed for other metal/Si combinations, it cannot be ruled out that more subtle changes in layer growth occurred which would require a more thorough study.

For a better understanding of the development of surface roughness during deposition and the decrease of the surface roughness due to ion bombardment new techniques are to be applied. Variable temperature scanning probe microscopy has demonstrated to be a powerful technique to investigate layer growth from sub-monolayer level and can be used to monitor the decrease of the surface roughness due to ion bombardment. As the chemical composition of a surface determines the growth of a layer, Photo Electron Spectroscopy can be considered as an additional in situ technique to monitor the surface composition and chemical states. To study intermixing more quantitatively, good results have been achieved by combining cross section TEM and x-ray reflectometry [5].

Finally, on a different note, I would like to mention what I consider a highlight of this thesis, namely the work on the Mo-Si system. This system can be considered as a good example for a

successful spin-off of fundamental materials research to an industrial application. In the beginning of the nineties it became apparent that the new generation of wafer steppers would be based on a radiation source with a wavelength of 13.5 nm. The Mo/Si multilayer system was selected as most appropriate for the required reflection optics. An STW project enabled Schlatmann to spend his time as a PhD student to investigate this system. As mentioned in the forgoing chapters, layer growth, ion beam smoothing, intermixing and implantation were studied. Although Schlatmann was not able to produce a multilayer with the proper periodicity of 6.7 nm, he clearly demonstrated that ion polishing of Si had the potency to optimise the reflectivity. Based on these results it was the group of Bijkerk at the FOM Institute for Plasma Physics which not only produced a multilayer system with the proper periodicity and high reflectivity (Louis et al [6]), but also made - in collaboration with Zeiss - accurate depositions at large curved substrates. This collaboration continued as problems on temperature stability and radiation-induced chemical instability of the top surface had to be solved.

References

1) H. Trinkaus, Nucl. Instr. & Methods B in Phys. Res.,146, 204 (1998)

2) H.-J. Ernst, Surf. Sci.383, L755 (1997)

3) J.B. Hannon, C. Klunker, M. Giesen, H. Ibach, N.C. Bartelt and J.C. Hamilton, Phys. Rev. Lett., 79 2506 (1997)

4) A.R. Miedema, Philips Technisch Tijdschrift, 36, 225 (1976)

5) M.J.H. Kessels, J. Verhoeven, F.D. Tichelaar, F. Bijkerk accepted for publication in: J. Appl. Phys. 2005

6) E. Louis, A.E. Yakshin, P.C. Görts, S. Oestreich, R. Stuik, E.L.G. Maas, M.J.H. Kessels, F. Bijkerk, M. Haidl, S. Müllender, M. Mertin, D. Schmitz, F. Scholze and G. Ulm, SPIE 3997-44, Microlithography, Santa Clara (2000)

8   Summary

Since the second half of the 20th century the number of application of thin films and coatings have increased considerably. This was especially made possible by the development of the required techniques at industrial scale. Well-known applications are anti reflection coatings, hard coatings for cutting tools, decorative coatings and the application in microelectronics. At the end of the seventies multilayer systems for x-ray reflection emerged as a new application. The total reflection of these systems is based on resonant reflection by the interfaces. The intrinsic requirement for resonant reflection of radiation with a specific wavelength λ by a multilayer with period thickness d is given by the Bragg relation $\lambda = 2d \sin\theta$, where θ is the reflection angle with the surface. For the wavelength region as considered, the periodicity (d) of the multilayers will be 1 nm or higher. As a consequence, the reflection of a multilayer system is wavelength selective. A high sharpness of the interfaces between the components forms the main requirement for a high reflectivity. There are two causes for less sharp interfaces: intermixing of the components and surface roughness of the deposited layer.

A widely used technique to grow layers is physical vapour deposition, based on the arrival of atoms or molecules at a substrate surface. The process of layer growth depends on the activation energy of the arriving atoms related to the surface of the substrate as well as the growing layer. Depending on the activation energy and the external input of energy during or after the deposition process a displacement of the atoms is possible. Displacements in the bulk and at the surface of the layer are responsible for the layer density, layer morphology and the roughness of the surface. External energy is provided by the energy of the arriving atoms, heating of the substrate and the impact of energetic particles. Energetic ions also cause sputtering and may be implanted. Three sources for physical vapour deposition are available: evaporation

by heating, sputtering, and pulsed laser ablation. Atoms evaporated by heating arrive at the substrate with thermal energy. Sputtered atoms arrive with energies in the order of tens of eV. Additionally energetic neutrals and ions will provide extra energy to the substrate. Depending on the pulse energy, laser ablation generates energetic atoms and energetic clusters. An important part of the process is control of the layer thickness. When the discharge power is kept constant, for sputter deposition the deposition time can be used to determine the layer thickness. For pulsed laser the number of laser pulses required to grow a layer can accurately determine deposition the layer thickness. A well-established technique to control the layer thickness during deposition by thermal evaporation is based on in situ reflectometry by radiation with a well-known wavelength.

Energetic ions have been applied during or after deposition of the multilayer components to reduce the surface roughness. For the metal-carbon systems the best results have been achieved by a post-deposition ion etch of the metal component. This process is based on the removal of an excess layer by ion etching after deposition. The required thickness of this excess layer depends on the growth mode of the layer. For nickel the first 4 nm appeared to grow on carbon as separated islands. In contrast, the first 2 nm of tungsten on carbon formed a closed layer. Intermixing of the interface underneath by residual energy from the ion impact limits the application of ion beam smoothing. The metal on carbon interfaces appeared to have a high stability. The metal on silicon interfaces were more easily intermixed in contrast with the silicon on metal interface. Additional to smoothing of the surface, densification of the freshly deposited silicon layer has been observed. For the molybdenum-silicon combination the best results were achieved after a post deposition etch procedure of silicon. For the tungsten silicon combination Ion Assisted Deposition of tungsten additional to post deposition etched silicon gave the best results. The improvement can be ascribed to a decrease of the tungsten surface roughness. This process turned out to be in competition with intermixing at the interface with silicon underneath.

It was demonstrated that energetic ions have been applied to reduce stress in Mo-Si systems ion induced intermixing to form special interlayers and implantation to improve the optical contrast as well as

the thermal stability. Intermixing and implantation of hydrogen has been applied to both the Mo-Si and W-Si systems. Different results for intermixing and implantation for these systems are discussed. CH_x^+ ion implantation into Si has demonstrated to improve the thermal stability of the Mo-Si system. The combination of intermixing and implantation was applied for the formation of a NiSi/SiN multilayer system.

Implantation of energetic CH_x^+ ions into Si as well as deposition of Si assisted by energetic CH_x^+ ions (IBAD) was used to form Si/SiC multilayers. For deposition evaporation was used and a Kaufman broad beam ion source was available for implantation. Auger Electron Spectroscopy combined with sputter etch depth profiling revealed the formation of a thin carbon over layer and a graded density carbide layer underneath. As expected the implantation depth scaled with the ion energy. However, for energies higher than 1 keV a decrease of the carbide density, ascribed to sputtering, was observed. In order to demonstrate the feasibility of the process, multilayers with a periodicity of 10.8 nm were grown using implantation with 500 eV and 1 keV ions as well as IBAD with 500 eV. In situ x-ray reflectometry during deposition was used to control the deposition process. This technique revealed that the carbon over layer formed during both processes clearly influences the reflection of the multilayer systems.

9   Samenvatting

Modificatie van oppervlakken en grensvlakken van multilaagsystemen met behulp van energetische ionen

Alvorens in te gaan op het onderwerp dat in dit proefschrift is behandeld volgt hierbij enige achtergrondinformatie, noodzakelijk om de meer geïnteresseerde leek inzicht te verschaffen in het onderwerp.

De toepassing van dunne lagen heeft dankzij de ontwikkelingen van depositie systemen op industriële schaal de tweede helft van de twintigste eeuw een grote vlucht genomen. Er kan daarbij worden verwezen naar de harde coatings op snijgereedschappen, goudkleurige lagen als decoratie, metaallagen op plastic auto-onderdelen, niet te vergeten de toepassing in de micro-elektronica, en optische coatings voor verschillende toepassingen.

De toepassing van multilaagssystemen in optische elementen vormt de basis van dit onderzoek. Optiek speelt in ons dagelijks leven een belangrijke rol. Daar zijn brildragers zich zeker van bewust. Ook fotografie en microscopie zijn bekende optische toepassingen. Het is vaak minder bekend dat zonder optiek de CD speler en de streepjescode scanner niet zouden bestaan. Ook de communicatie in de vorm van lichtgeleiding is een toepassing van de optiek. Velen realiseren zich niet dat de miniaturisering van de elektronica voor een belangrijk deel op een fotografisch proces berust. Alvorens hierop verder in te gaan is enige fundamenteel begrip van optische verschijnselen noodzakelijk. De beschrijving van licht als een golfverschijnsel werd het eerst door Christiaan Huygens geïntroduceerd. De kleur van licht wordt bepaald door de golflengte. Daarbij moet worden gedacht aan enkele tienden van een micrometer (0,000001 m) voor zichtbaar licht. De golflengte vormt dan tevens de beperking voor het kleinst mogelijk waar te nemen object. Dat wil zeggen dat met licht met een golflengte van 0,5 micrometer voorwerpen van minder dan 0,5 micrometer niet meer waarneembaar zijn. Het betekent ook dat een voorwerp niet optisch verkleind kan worden tot een beeldgrootte kleiner dan 0,5 micrometer.

Het streven in de micro-elektronica is de vergroting van het aantal elektronische experimenten per oppervlakte eenheid. Omdat daarvoor de

afmetingen van de elektronische elementen navenant kleiner moeten worden zal het benodigde fotografische proces gebruik moeten maken van licht met steeds kortere golflengte. Optiek met licht van 150 nanometer (1 nm = 0,001 micrometer) vormt heden ten dage de "state-of-the-art". De ontwikkeling van de "memory stick" geheugenkaarten zoals ook in de digitale fotografie toegepast en muziekopslagmedia zoals de iPod zijn hiervan het resultaat.

Voor een verder verkleinen van de dimensies van elektronische elementen zal voor het afbeeldingproces de toepassing van licht met een golflengte < 100 nm (extreem ultraviolet en zachte röntgenstraling) noodzakelijk zijn. Optische afbeelding is gebaseerd op breking van licht aan een grensvlak van een transparant medium zoals glas of reflectie aan een reflecterend medium. Voor afbeelding met zichtbaar licht wordt gewoonlijk gebruik gemaakt van lenzen. Het belangrijkste probleem is dat als gevolg van geringe breking en hoge absorptie voor dit golflengtegebied geen bruikbare materialen bestaan die kunnen worden toegepast in lenzen. Ook een geringe reflectie verhindert het gebruik van simpele reflectie optieken. De enige bruikbare oplossing bestaat uit een combinatie van meervoudige reflectie en interferentie. Interferentie ontstaat als twee lichtgolven met dezelfde golflengte die aan twee evenwijdige vlakken worden gereflecteerd in fase lopen. Dat wil zeggen dat beide golven synchroon moeten lopen, waardoor de intensiteiten bij elkaar worden opgeteld. Daarvoor moet er een bepaalde relatie bestaan tussen de afstand van de reflectievlakken, de reflectiehoek en de golflengte van het licht. De basis voor een bruikbaar reflectieoptiek wordt dan gevormd door een multilaagsysteem bestaande uit verschillende componenten met een zo hoog mogelijk contrast en met afstanden tussen de grensvlakken in de orde van de gereflecteerde golflengte. Dat betekent dus dat het systeem golflengte (kleur) selectief reflecteert. Als gevolg daarvan is het ook mogelijk een multilaagsysteem toe te passen om licht van verschillende golflengte te scheiden (spectroscopie). Spectroscopie wordt toegepast als analysetechniek voor de chemische samenstelling van materialen. Dergelijke toepassingen kunnen bijvoorbeeld worden gevonden in de betonindustrie, de staalindustrie en de halfgeleider industrie.

Ook in de microscopie bepaalt de golflengte van het licht wat de afmetingen zijn van het object dat nog kan worden waargenomen en vergroot. Speciaal voor de biologische microscopie is het golflengtegebied tussen 2 en 4,4 nanometer interessant. Licht in dit golflengtegebied wordt extra geabsorbeerd door koolstof. Aangezien koolstof een belangrijke component

vormt van biologische materialen, levert dit een extra contrast op voor microscopie.

Voor een bruikbare reflectie moeten multilaagsystemen aan de volgende voorwaarden voldoen:

a)   De laagdikte van de multilaag componenten moet binnen 0,1% reproduceerbaar en nauwkeurig zijn. Er moet dan worden gedacht aan waarden van tienden van nanometers.

b)   Voor een optimale reflectie moet de grensvlak ruwheid te verwaarlozen zijn vergeleken met de golflengte van het gereflecteerde licht. De beperkingen hierbij worden gevormd door chemisch intermixen op grensvlakken en de vorming van oppervlakteruwheid tijdens de laag aangroei.

Het navolgende gedeelte van deze samenvatting heeft tot doel geïnteresseerde leken verder inzicht te geven in: waarom dit onderzoek werd gedaan, welke technieken zijn gebruikt, wat de problemen waren en tot welke resultaten dit heeft geleid. Dit deel beperkt zich daarom tot de resultaten die in relatie tot toepassing het meest aanspreken.

In hoofdstuk 2 wordt een kort overzicht gegeven van de aangroei van dunne lagen met behulp van fysische depositie. Bij fysische depositie komt een damp van atomen of moleculen aan op een substraatoppervlak en vormt een laag. De aangroei kan atoomlaag voor atoomlaag plaats vinden, maar er kan ook eilandvorming optreden. In het laatste geval wordt het oppervlak van de laag ruw. Dit alles is een gevolg van de beweeglijkheid van de atomen na aankomst op het substraat en de vorming van barrières die deze beweeglijkheid beperken. In de praktijk wordt het aangroei proces bepaald door: de keuze van het dunne laag materiaal in relatie tot het materiaal van het substraat, de depositiesnelheid en de energie die gedurende het proces in de aangroeiende laag beschikbaar is. De atomen die op het substraat aankomen hebben afhankelijk van het verdampingsproces energie. Extra energie kan worden verkregen door het substraat te verwarmen of te beschieten met energetische deeltjes in de vorm van ionen. Beschieting van een vaste stof met ionen kan aanleiding geven tot implantatie van die ionen, verandering van de dichtheid van de toplaag van het materiaal en verstuiven (sputteren) van atomen op het oppervlak. Afhankelijk van de laagdikte en de ionenenergie kan intermixen optreden aan het grensvlak van een dunne

laag en het substraat. Al deze effecten vormen de basis voor het groeien van multilagen met scherpe grensvlakken.

In hoofdstuk 3 wordt een kort overzicht gegeven van de technieken die worden gebruikt voor de fysische depositie van dunne lagen. De eenvoudigste manier voor het produceren van een damp is thermisch verdampen van een materiaal door middel van weerstandsverhitting of bombardement met hoogenergetische elektronen. De atomen komen dan aan op het substraat met de thermische energie die overeenkomt met de verdampingstemperatuur. Verdampen kan ook gebeuren met behulp van een laser. Daarbij wordt niet alleen damp gevormd, maar ook atoomclusters. Bovendien is de energie waarmee deze atoomclusters aankomen op het substraat veel hoger dan de energie overeenkomend met de verdampingstemperatuur. Een andere veel gebruikte techniek berust op verstuiven met behulp van energetische ionen (sputter depositie). Een basistechniek voor sputter depositie wordt gevormd door een gasontlading tussen een kathode (target) en een anode (substraat). Kathodemateriaal wordt verstoven en groeit aan op de anode als een dunne laag. De versputterde atomen hebben afhankelijk van de ontladingsgasdruk een aanzienlijk hogere energie dan met verdampen mogelijk is. Bij deze techniek is bombardement met andere energetische deeltjes niet te voorkomen.

Hoofdstuk 4 behandelt het gebruik van energetische ionen om de ruwheid van het oppervlak van een aangroeiende laag te verlagen. In dit hoofdstuk wordt onderzoek gepresenteerd aan de combinaties Ni-C, W-C, W-Si, en Mo-Si. Voor al deze systemen is thermische verdamping gebruikt als depositietechniek. Een sprekend voorbeeld van praktische toepassing wordt gevormd door het Mo-Si systeem. Deze combinatie vormt de basis voor toekomstige optische systemen voor de productie van geïntegreerde elektronische componenten met dimensies ver beneden 1 micrometer. Met behulp van een proces waarbij de ruwheid van het oppervlak van de Si laag door middel energetische van krypton ionen wordt verlaagd, is een reflectiviteit van ≈ 70% bereikt. Aangezien het benodigde optische systeem uit 10 of meer spiegel elementen zal bestaan betekent dat een totale transmissie van $0,7^{10} = 2,8\%$. Vandaar dat elke procent winst per spiegel meetelt in de totale transmissie.

Een ander sprekend voorbeeld wordt gevormd door het Cr-Sc systeem, dat speciaal ontwikkeld wordt voor biologische microscopie. In tegenstelling

tot alle vorige paragrafen is hier gebruik gemaakt van sputter depositie. Door een slimme keuze van een combinatie van magnetisch en elektrisch veld is het mogelijk om een deel van de in de ontlading gevormde ionen met gecontroleerde energie naar het substraat te brengen. Op deze manier wordt het substraat op gecontroleerde wijze gebombardeerd met ionen van een bepaalde energie gedurende het depositieproces.

In hoofdstuk 5 wordt aangetoond hoe met behulp van implantatie van energetische ionen de chemische samenstelling van één van de multilaagcomponenten wordt gewijzigd. Daarvan kan op twee manieren gebruik van worden gemaakt. Het optisch contrast kan worden aangepast met als resultaat een hogere reflectie. Het is ook mogelijk hiermee de chemische reactiviteit van de componenten zodanig te verlagen opdat vermenging op het grensvlak wordt tegengegaan. Ook hier geldt het Mo-Si systeem als een belangrijk voorbeeld. Voor de depositie van de componenten is gebruik gemaakt van thermisch verdampen. Door implantatie van Si met waterstof ionen kan voor het golflengtegebied dat wordt gebruikt in de productie van elektronische componenten de reflectie per multilaagsspiegel met 4% worden verhoogd. Dat lijkt niet veel, maar voor een systeem van 10 spiegels betekent dat een toenamen van de transmissie van 2,8 naar 4,9%. Dat betekent dan dar er gebruik gemaakt kan worden van een bron met een 0,6 lagere opbrengst. Implantatie van Si met koolstof heeft de thermische stabiliteit van het Mo-Si systeem verbeterd. Dat gaat helaas wel weer gepaard met een klein verlies aan reflectiviteit. Tenslotte is het waard te vermelden dat onderzoek is gedaan aan het Ni-Si systeem dat toepassing vindt in de biologische microscopie. Dit systeem is dermate chemisch reactief dat vermenging aan het grensvlak niet is te voorkomen. Implantatie van Si met stikstof is hiervoor een bruikbare oplossing gebleken.

Hoofdstuk 6 is gewijd aan implantatie van koolstof gecombineerd met depositie van Si door middel van thermisch verdampen als techniek voor de vorming van een SiC_x-Si multilaag systeem. Reflectieoptieken gebaseerd op deze multilagen zijn ontwikkeld voor de ontwikkeling van lasers in het extreem ultraviolette golflengte gebied (20 – 100 nanometer).

10 Dankwoord.

Dit proefschrift is het resultaat van meer dan 20 jaar onderzoek. Gedurende die tijd hebben zeer velen hun bijdrage geleverd, waarvan een aantal met pensioen is. Teneinde te vermijden dat ik er een aantal zal vergeten, wil mij beperken tot het algemeen noemen van groepen van mensen die hun bijdrage hebben geleverd. Om te beginnen is dit werk tot stand gekomen in samenwerking met verschillende promovendi, post docs, collega's en buitenlandse bezoekers. Binnen deze samenwerking verschoof mijn positie vaak van leraar naar leerling, wat mijn inzicht in het onderwerp ten goede kwam. Als gevolg daarvan heb ik een aantal malen met succes subsidie voor nieuwe projecten kunnen binnen halen.

Uiteraard is al het werk mogelijk gemaakt door de inzet van alle groepstechnici die mij de afgelopen jaren hebben ondersteund. Zij zorgden ervoor dat experimentele opstellingen werden gebouwd, aangepast en operationeel gehouden. Dat alles werd mogelijk gemaakt door de medewerkers van wat vroeger de tekenkamer heette en tegenwoordig het ontwerpbureau, de instumentmakerij en de afdeling electronica en informatica. Ook de bijdrage van de dames die in de loop der jaren verantwoordelijk waren voor de bibliotheek mag niet worden vergeten. Zij zorgden altijd voor het correct afhandelen van ingediende publicaties en het leveren van reprints. Dankzij de boekhoudkundige ondersteuning van de administratie kon ik de projecten uitvoeren die een belangrijke basis hebben gevormd voor het onderzoek.

Ook buiten het instituut heb ik veel medewerking ondervonden van collega's van de universiteiten van Delft, Leiden, Utrecht en Eindhoven, van het FOM Instituut voor Plasmafysica, Philips Natlab en Panalytical. Tenslotte wil ik niet de directeuren vergeten die gedurende de afgelopen jaren leiding hebben gegeven aan AMOLF en mij altijd de gelegenheid hebben gegeven mijn onderzoek naar eigen inzicht te kiezen en te verrichten.

11 Curriculum Vitae

Jan Verhoeven was born in 1942 in The Hague. In 1960 he was admitted to the Department of Applied Physics of Delft University of Technology. He conducted experiments on vibration modes of cyclohexane by inelastic neutron scattering. In 1970 he joined the FOM Institute for Atomic and Molecular Physics in Amsterdam as leader of the vacuum group. At that time all experiments were done in vacuum and the task of this group was to advise other groups about the choice of the proper vacuum components. Therefore much time was spent on testing of vacuum components. During this time Verhoeven also investigated oxidation of a Ni (110) surface by Auger Electron Spectroscopy and Electron Stimulated Desorption. In 1982 the group was transformed into the Thin Film group. The task of the group was to provide other experimental groups with thin films at request. At that moment a collaboration with the group of Prof. Marnix van der Wiel started to investigate the production of multilayers for x-ray reflection. This collaboration continued after Van der Wiel left for the FOM Institute for Plasma Physics. New projects on multilayers were started in collaboration with dr. Fred Bijkerk of the FOM Institute for Plasma Physics and continued up to 2005. In 1994 a project was started on the formation of small metallic islands on insulators (Pd on TiO_2) in collaboration with dr. Onno Gijzeman and prof. John Geus from the University of Utrecht and prof. Joost Frenken from the University of Leiden. This system was especially interesting for application in catalysis. In 1998 the collaboration with Van der Wiel (now at Eindhoven University of Technology) was resumed with a project on the generation of Cherenkov radiation in the wavelength region of several nanometres by relativistic electrons traversing Si, Ti and V foils. In 2003 the group was transformed into the Nanofabrication

group. From that date on, in collaboration with prof. Albert Polman (AMOLF) experiments have been conducted on the formation of silver island structures on indium tin oxide and the interaction with light with these islands. In collaboration with prof. Mark Vrakking a project was started on the sub-surface formation of SiC clusters in Si.